MECHANICAL DESIGN AND ANALYSIS OF A NOVEL FIXATION DEVICE FOR HUMAN BONE FRACTURES

A THESIS SUBMITTED TO
THE GRADUATE SCHOOL OF NATURAL AND APPLIED SCIENCES
OF
MIDDLE EAST TECHNICAL UNIVERSITY

BY

ÇAĞRI YENİGÜN

IN PARTIAL FULFILLMENT OF THE REQUIREMENTS
FOR
THE DEGREE OF MASTER OF SCIENCE
IN
BIOMEDICAL ENGINEERING

FEBRUARY 2016

Approval of the thesis:

MECHANICAL DESIGN AND ANALYSIS OF A NOVEL FIXATION DEVICE FOR HUMAN BONE FRACTURES

submitted by **ÇAĞRI YENİGÜN** in partial fulfillment of the requirements for the degree of **Master of Science in Biomedical Engineering Department, Middle East Technical University** by,

Prof. Dr. Gülbin Dural
Dean, Graduate School of **Natural and Applied Sciences** _____

Prof. Dr. Hakan Işık Tarman
Head of the Department, **Biomedical Engineering** _____

Assist. Prof. Dr. Ergin Tönük
Supervisor, **Mechanical Engineering Dept., METU** _____

Prof. Dr. Erbil Oğuz
Co-Supervisor, **Orthopaedics and Traumatology Dept., GMMA** _____

Examining Committee Members:

Prof. Dr. Nesrin Hasırcı
Chemistry Dept., METU _____

Assist. Prof. Dr. Ergin Tönük
Mechanical Engineering Dept., METU _____

Prof. Dr. Erbil Oğuz, MD
Orthopaedics & Traumatology Dept., GMMA _____

Prof. Dr. R. Orhan Yıldırım
Mechanical Engineering Dept., METU _____

Prof. Dr. F. Suat Kadıoğlu
Mechanical Engineering Dept., METU _____

Date: 03.02.2016

I hereby declare that all information in this document has been obtained and presented in accordance with academic rules and ethical conduct. I also declare that, as required by these rules and conduct, I have fully cited and referenced all material and results that are not original to this work.

Name, Last Name : Çağrı Yenigün

Signature :

ABSTRACT

MECHANICAL DESIGN AND ANALYSIS OF A NOVEL FIXATION DEVICE FOR HUMAN BONE FRACTURES

Yenigün, Çağrı

M.S., Department of Biomedical Engineering

Supervisor: Assist. Prof. Dr. Ergin Tönük

Co-Supervisor: Prof. Dr. Erbil Oğuz

February 2016, 128 pages

Fixation of bone fractures over a desired time period is one of the most important requirement for their healing processes. Fracture fixation devices are designed to satisfy particular requirements for different types of bone fractures. Conventional and locking plates, intramedullary rods and screws of trauma surgery, and polyaxial screws, connectors and rods of spinal surgery are the examples of contemporary implants for varying bones and their fractures. The mentioned fixation system is inspired from spinal implants and contains multi-axial screws, adjustable rod connectors and rods to combine the known advantages and reduce disadvantages of known systems used in shaft fractures of trauma surgery. The aim of this thesis is to design and prototype an internal fixation system that is anatomically suitable for intended area application, minimizing periosteum damage, allowing multi-axial screws and multi-planar application for traumatic and osteotomic applications, as a part of an interdisciplinary project. For this purpose, several preliminary models and resulting final models are designed, and the critical points of conceptual and final models are evaluated by analytical methods. Consequently, mechanical tests are conducted to assess the performance of the final design, and results of these tests

compared with analytical estimations. Finally, suitable areas of application in orthopaedics are concluded based on the assessments.

Keywords: Orthopaedic Implant, Fracture Fixation, Mechanical Testing, Analytical Approach.

ÖZ

İNSAN KEMİĞİ KIRIKLARI İÇİN YENİ BİR KIRIK SABİTLEYİCİSİNİN MEKANİK TASARIMI VE ANALİZİ

Yenigün, Çağrı

Yüksek Lisans, Biyomedikal Mühendisliği Bölümü

Tez Yöneticisi: Yrd. Doç. Dr. Ergin Tönük

Ortak Tez Yöneticisi: Prof. Dr. Erbil Oğuz

Şubat 2016, 128 sayfa

Kemik kırıklarının iyileşmesindeki en önemli noktalardan biri kırığın belirli bir süre boyunca sabitlenmesidir. Kırık sabitleme cihazları bu amaç doğrultusunda çeşitli kemik kırıklarının iyileşme gerekliliklerini sağlaması için tasarlanmıştır. Travmatolojide kullanılan geleneksel ve kilitli plaklar, kemik içi boşluğa yerleştirilen çiviler ve vidalar; omurga cerrahisinde kullanılan çok eksenli vidalar, çubuklar ve bağlantı elemanları, kemik kırıklarının sabitlenmesinde günümüzde kullanılan çeşitli implantlara örnektir. Bahsedilen yeni tasarım, omurga cerrahisinde kullanılan sistemlerden esinlenilmiş olup, bu sistemlerin üstün yanlarını bünyesinde toplayıp, sakıncalı yanlarını ortadan kaldırarak travma cerrahisindeki uzun kemik şaft kırıklarında kullanılacaktır. Bu tez çalışmasının amacı, disiplinler arası proje kapsamında travma sonucu veya doğuştan gelen kemik deformitelerin tedavisinde kullanılabilecek, anatomik olarak uyumlu, periost hasarını en aza indiren, çok eksenli ve çok düzlemli uygulanabilen, içten (internal) kullanıma uygun bir sabitleyici tasarlamak ve ilk örneklerini üretmektir. Bu amaç doğrultusunda, çeşitli kavramsal tasarımlar ve bunların sonucunda ortaya çıkan son tasarımlar modellenmiş, bu modellerin kritik noktaları analitik yollarla değerlendirilmiştir. Devamında,

tasarlanan sistemin performansını değerlendirmek için ilk örnekler üzerinde mekanik testler gerçekleştirilmiş, bu testlerin sonuçları analitik çıkarımlarla karşılaştırılmıştır. Son olarak, analiz ve testlerin sonuçlarından yola çıkarak, bu tasarımın ortopedi içerisindeki kullanım alanları öngörülmüştür.

Anahtar Kelimeler: Ortopedik İmplant, Kırık Fiksasyonu, Mekanik Test, Analitik Yaklaşım.

To My Dear Family and My Beloved Fiancé

ACKNOWLEDGEMENTS

I would like to express my deepest gratitude to my supervisor, Dr. Ergin Tönük, whose profound knowledge, support and encouragement thoroughly guided my study. I appreciate all his contribution and assistance. His support and guidance helped me all the time in writing this thesis.

I would also like to express my sincere gratitude to my co-supervisor Erbil Oğuz, MD for his medical contribution, guidance and technical support. His kind and helpful attitude was definitely meaningful for me.

I would also thank to the members of the Examining Committee, Prof. Dr. Nesrin Hasırcı, Prof. Dr. Orhan Yıldırım, and Prof. Dr. Suat Kadıoğlu for their valuable suggestions, contributions and insightful comments.

I would like to thank to Cemil Yıldız, MD for his medical contributions, and Cihan Keskin and Ömer Pektaş for their support in obtaining the torque gauge and producing some of the prototypes.

I owe my special and innermost thanks to Özge Yersen, my fiancé, for her endless tolerance, patience, sincere help and support during every stage of this thesis. Her ideas, insights and comments have been enlightening, and her emotional support have been priceless. I appreciate her for all of her love and support.

Special appreciation and gratitude are also for my mother and father, for their support and understanding, encouragement and endless love throughout my life. I admire them for all of their achievements in life from nothing, and for all of the knowledge and insight that they have passes on to their only child over the years.

This study was a part of an ongoing project on development of a novel internally and externally applicable bone implant supported by TÜBİTAK (The Scientific and Technological Research Council of Turkey) 1003, under the call TC0101-Diagnosis, Treatment and Support Oriented Novel Medical Devices, with number 113S103.

TABLE OF CONTENTS

LIST OF TABLES

TABLES

LIST OF FIGURES

FIGURES

CHAPTER 1

INTRODUCTION

Anatomy and physiology are two interconnected branches of science which are concerned with the studies of the structure and function of the human body respectively. Anatomy is the study of internal and external structures of body parts and their relationships to each other. Physiology is the study of how body parts work and perform their vital functions. These two branches are interconnected because structure provide information about function, and function can be explained only in terms of the underlying structure. This important concept named as the *principle of complementarity of structure and function* and bones are a good example of this concept: Bones contain hard mineral deposits in their structures, hence they become functional in supporting the body and protecting the vital organs [1], [2].

Since anatomy and physiology are broad fields with their sub-topics, a movement from general to specific is needed to investigate the bone and its fractures. Broadly, anatomy can be classified into two sub-topics as *gross (macroscopic)* and *microscopic* anatomy. Gross anatomy is the study of body structures visible to naked eye (i.e. unassisted by optics) and can have different approaches at surficial, regional and systemic level. Microscopic anatomy deals with body structures that can be seen with optical magnification. Similarly, the sub-divisions of physiology are *cell physiology*, *organ physiology*, *systemic physiology* and *pathological physiology*. These sub-divisions deal with the functions of cells, organs, organ systems and effects of diseases on them respectively. Regarding to definitions and brief classifications of anatomy and physiology, the human body can be organized according to structural levels and their corresponding functions. This organization from the simplest "molecular" level to the most complex "organism" level is summarized in Figure 1.1.

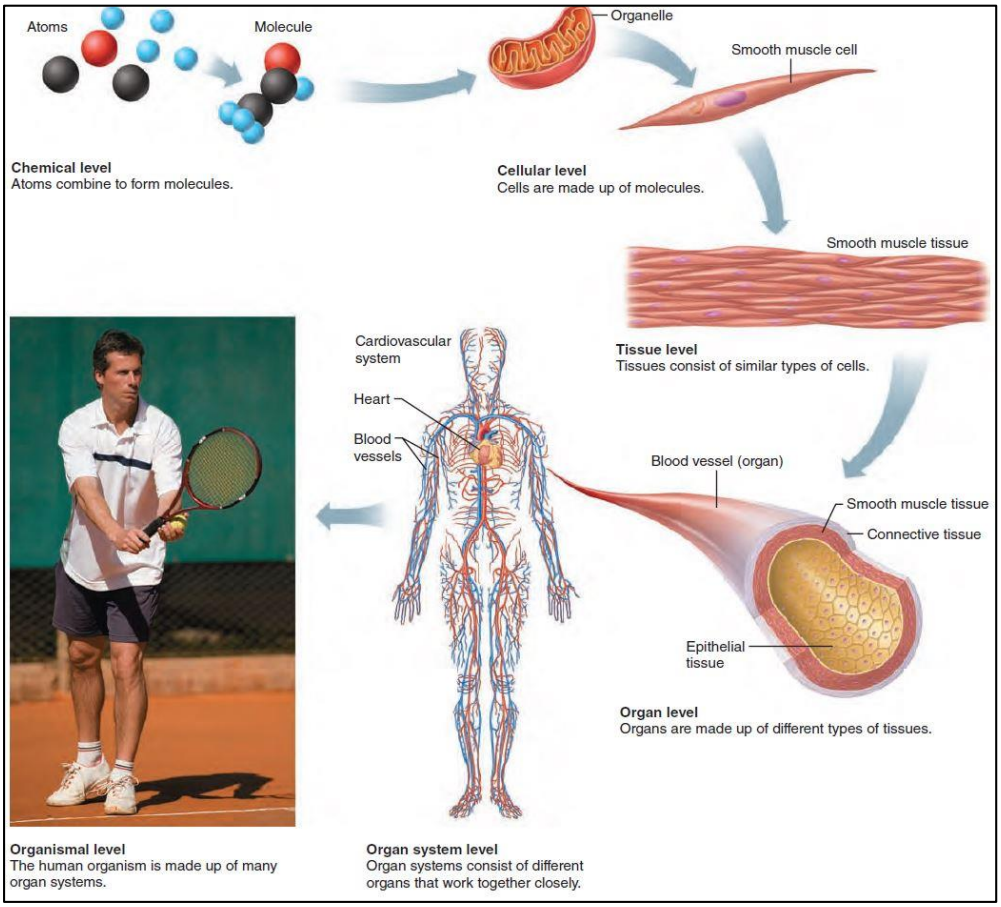

Figure 1.1 Levels of structural organization [2].

The human organism consists of several organ systems such as nervous, skeletal, muscular, cardiovascular, respiratory, endocrine, and digestive systems. These systems work together to maintain internal stability of the human body (termed as homeostasis) under the influence of the environmental conditions. Considering the term “homeostasis”, it can be said that the bone fracture is an example of the change in the environmental conditions which is primarily affecting the skeletal system, and all organ systems work together to recover its impacts. However, this recovery process needs a supporting system for its success, in some cases. To understand these cases, and the reasons why they need support; a very brief introduction to skeletal system will be given in the following section.

1.1. Anatomy and Physiology of the Skeleton: A Brief Summary

The skeleton or skeletal system consist of four major organs including bones, cartilages, ligaments and bone marrow. The bones of the skeleton support the body, enable movement and mobility by acting as a leverage for the muscles, protect critical internal organs and structures, maintain the mineral and acid-base equilibrium of the blood and provide the environment, i.e. bone marrow, for the formation of the cellular components of the blood [4]. Typical adult human skeleton has 206 major bones, which can be divided into two groups as appendicular and axial skeleton. Appendicular skeleton contains the bones in the extremities and the axial skeleton covers the remaining bones including skull, vertebral column and rib cage [1], [2]. Figure 1.2 shows the corresponding bones in each group.

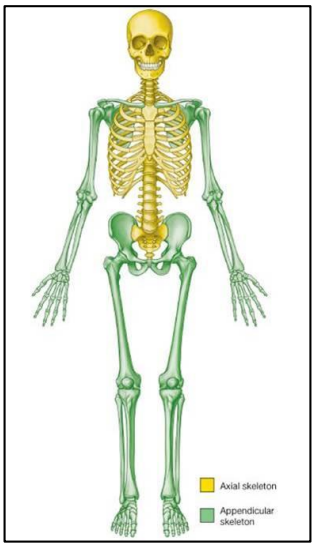

Figure 1.2 The axial skeleton (yellow); the appendicular skeleton (green) [3].

Another classification can be done according to individual shapes of the bones. Figure 1.3, summarizes this classification with the examples of each group. In this thesis, the focus will be on the long bones of the appendicular skeleton including humerus and femur. For more details, the readers are encouraged to refer widely available anatomy and physiology textbooks as [1], [2] or [3].

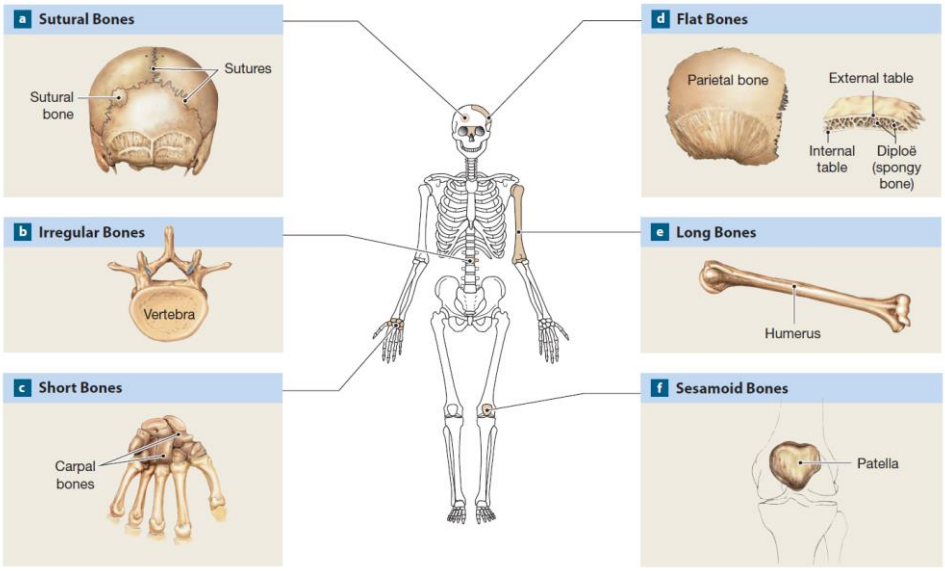

Figure 1.3 Classification of bones by their shape [1].
(a: Sutural, b: Irregular, c: Short, d: Flat, e: Long, f: Sesamoid bones)

A normal human adult long bone is composed of a tubular shaft or diaphysis, metaphysis below growth lines, and broader bone ends called epiphyses. The diaphysis forms a tubular structure with a thick layer of compact bone covering a central medullary cavity, whereas the metaphysis and epiphysis contain spongy bone under relatively thin outer shell of compact bone. External surface of the whole bone is covered with a membrane called the *periosteum*; with the exception of the joint surfaces of the long bones. Similarly, the membrane covering the internal surfaces of the bones (e.g. trabeculae of the spongy bone) is named as the *endosteum*. These two membranes contain mitotically active osteogenic cells that can change into other bone cells. A representative macro anatomy of a long bone (the femur) is given in Figure 1.4.

In micro scale, four main types of cells can be found in the bone tissue: Osteogenic cells, osteoblasts, osteocytes and osteoclasts. Osteogenic cells or osteoprogenitor cells are the stem cells with the capability of changing into bone-forming cells, also called osteoblasts. Osteoblasts are responsible for the production of new bone matrix by ossification.

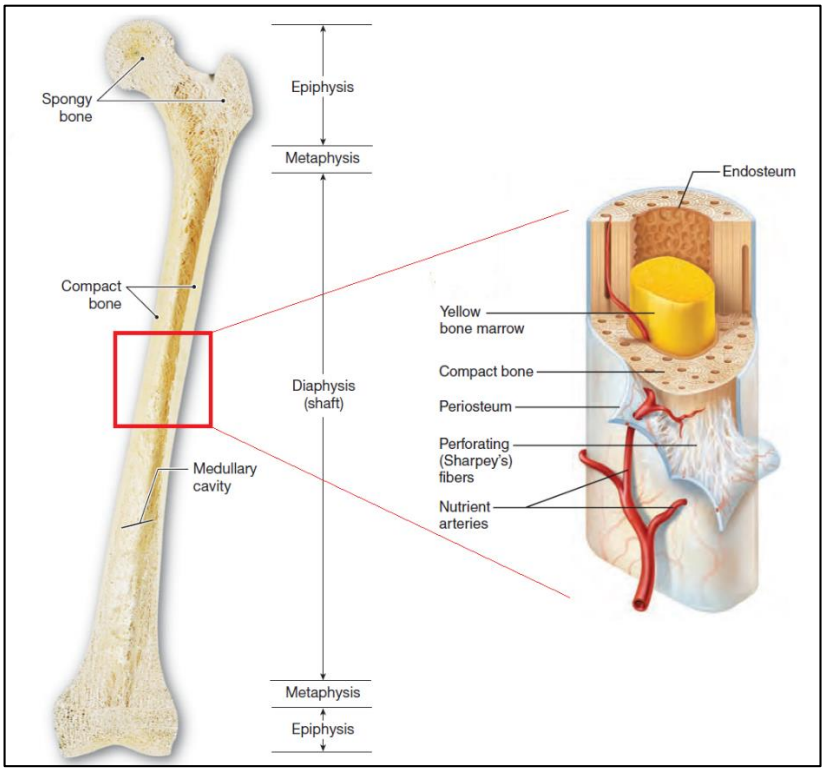

Figure 1.4 The macro structure of a representative long bone, the femur (on left) and cross-sectional view of the diaphysis (reproduced from [1] and [2]).

The ossification process starts with the generation of the organic matrix, *osteoid*, produced by proteins secreted from osteoblasts. After production of osteoid, calcium salts bind in the protein matrix with the help of the osteoblasts resulting the osteoid into the bone. Osteocytes develop after the maturation of the osteoblasts: Protein matrix entirely surrounds osteoblasts and calcium deposition occurs in the matrix. Osteocytes are the most populated cells in the bones. They preserve and monitor their surrounding matrix and also take part in the *repair of the damaged bone*. Osteocytes can also sense and respond to the mechanical stimulus like loading and deformation. They act as mechanic sensors directing osteoblasts and osteoclast in the case of formation and resorption of bone respectively. Osteoclasts differ from other three types of bone cells, because they derive from macrophages and take role into removal and recycle of the bone matrix. Figure 1.5, shows each type of cells with the examples their location on the bone cross-section.

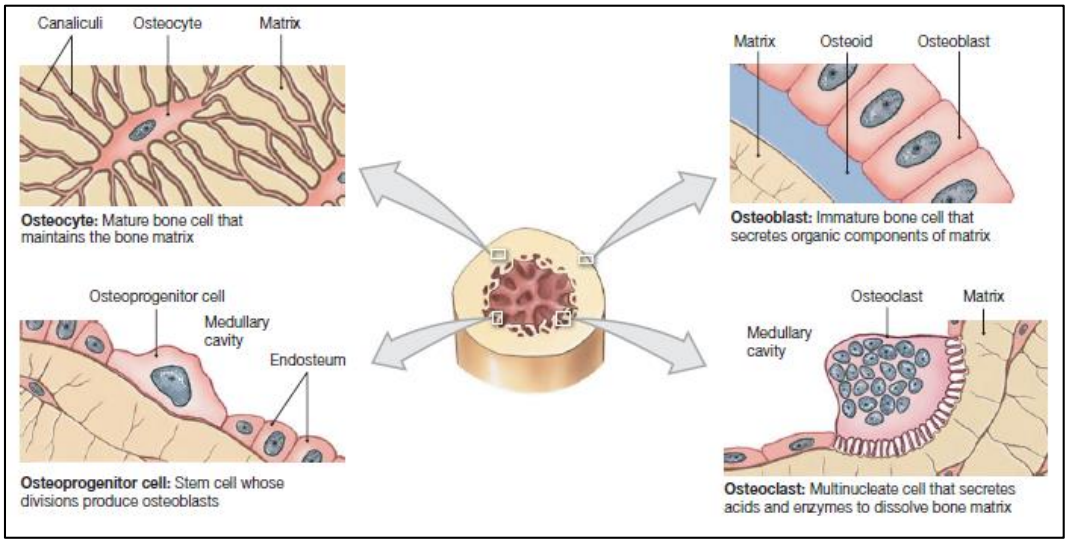

Figure 1.5 Types of bone cells [1].

The bones go through three processes during lifetime: Bone formation (ossification), growth, modeling and remodeling. Normal healthy bone formation is performed by two important means, namely: Intramembranous and endochondral ossification. The former is characterized by the development of flat bones (e.g. skull, mandible) from embryonic tissue called the mesenchyme, and the latter is indicated by the generation of cartilage model acting as a precursor (e.g. femur, humerus). These two ossification processes can also be observed in the healing of the fractures: In compound fractures fixated by metal bone plates and screws with open reduction technique, intramembranous ossification is seen. However, endochondral ossification occurs in the fixation of fractures by cast immobilization technique.

Growth of the bones continues in the childhood and adolescence periods in the both longitudinal and radial directions. For example, cartilage proliferates in growth areas located in the epiphysis and metaphysis parts of the long bones, then calcification process creates new bone, hence longitudinal growth occurs.

Modeling is the process by which bones change entire shape in response to environmental factors like physiological factors or mechanical forces, resulting in progressive adjustment of the skeleton to the encountered forces. In other words,

biomechanical forces can change the thickness and the axis of the bones by addition or removal of the bone to the proper surfaces. Wolff's Law explains the modeling as follows: The normal, healthy bones of human or animal will adapt to the mechanical loads under which they are placed [6].

Different than modeling, bone remodeling starts before birth and continues during all life. Remodeling involves continuous resorption of old bone and formation of new bone to restrict micro-damages of bone matrix. Initiation signal of remodeling comes from osteocyte apoptosis as a result of micro-damages. Osteoclasts and osteoblasts work progressively to carry out resorption of old bone and generation of new bone in this process [4].

1.2. Fractures of Long Bones and Methods of Treatment

A bone fracture is a complete or incomplete break in the continuity of the bone. It corresponds to a structural failure resulting from different factors such as loading conditions and material properties of the bone [7], [8]. There are different classification systems of fractures and they simply serve for naming, describing and comparing, guiding and prediction purposes. Classification systems characterize fractures into three broad categories: Fracture specific (e.g. Garden, Schatzker, Neer), generic or universal (such as Arbeitsgemeinschaft für Osteosynthesefragen (AO) and Orthopaedic Trauma Association (OTA) classification), or soft tissue specific (e.g. Gustilo) [9]. In this section, an overview of long bone fractures, healing process of diaphyseal fractures and treatment methods will be presented.

1.2.1. Fracture Mechanisms of Long Bones

In AO / OTA universal fracture classification system, five questions must be answered for each fractures of long bones [10]:

⇨ Which bone is fractured? (1, 2, 3, 4, ...)

- ⇨ Where is the fracture in the bone? (1, 2 or 3)
- ⇨ Which fracture type? (A, B or C)
- ⇨ Which group do the fractures belong to? (1, 2 or 3)
- ⇨ Which sub-group do the fractures belong to? (.1, .2 or .3)

The numeric answers of the first and the second questions correspond to localization of fracture, and the last three questions define the morphology of the fracture. For example, 32-A1 stands for, femur / diaphyseal segment / simple / spiral type fracture in AO-OTA's alphanumeric classification. For the first question, the first four numbers stand for six long bones namely: 1- Humerus, 2- Radius/Ulna, 3- Femur, 4- Tibia/Fibula. For the second question 1, 2 and 3 stand for proximal, diaphyseal and distal segments of the bone respectively. The answers of the remaining three questions differ for each long bone. Figure 1.6 illustrates the morphological classification of diaphyseal fractures in long bones.

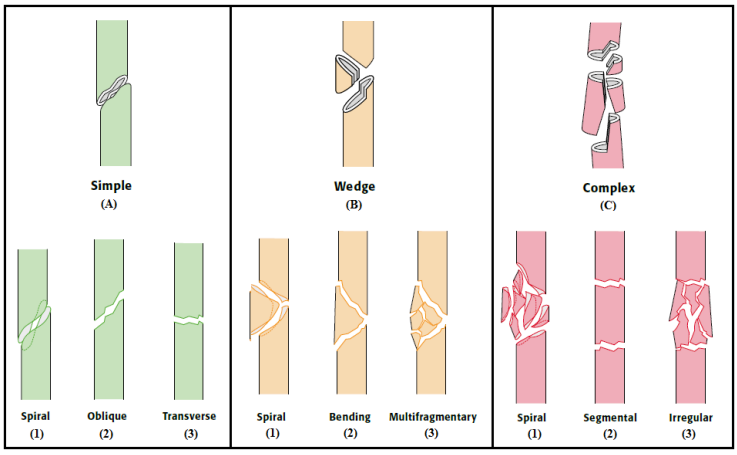

Figure 1.6 Classification of diaphyseal fractures in long bones according to AO-OTA (reproduced from [10]).

According to AO / OTA [10], spiral fractures of simple, wedge and complex types of diaphyseal fractures come from the torsional or twisting forces. Bending forces may result in simple oblique, simple transverse, fragmented wedge, bending wedge or irregular complex fractures. However, AO / OTA's classification does not directly

characterize the forces causing fracture. A more specific categorization in [11] includes indirect and direct injury mechanisms due to the forces acting in fracture. Indirect injury occurs when the force creating the fracture is applied away from the fracture site (see Table 1.1 and Figure 1.7). In similar manner, direct forces causing fractures on their application area, like gunshots, are grouped in direct injury mechanisms (Table 1.2).

Table 1.1 Fractures of indirect forces.

Type of Force	Fracture Type
Tension	Transverse
Compression	Oblique
Torsion	Spiral
Bending	Transverse, Butterfly
Compression and Bending	Transverse oblique

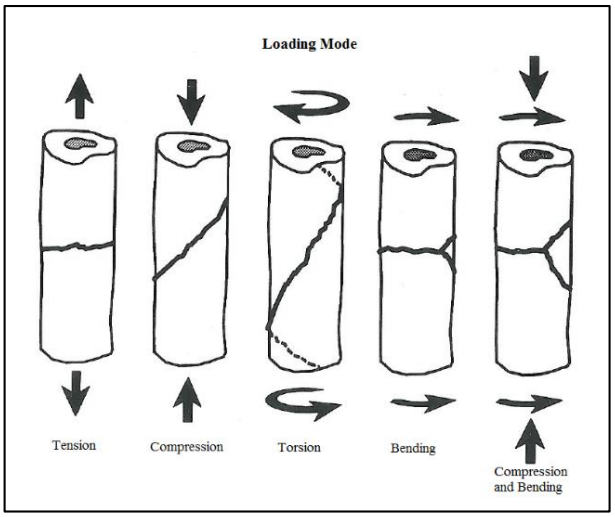

Figure 1.7 Indirect forces and corresponding fracture types in long bone diaphysis.

Table 1.2 Fractures of direct forces.

Type of Force	Description	Fracture Characteristics
Tapping	Small force acting on a small area	Nightstick fracture (ulna)
Crushing	High force acting on a large area	Serious soft tissue injury with irregular shape
Penetrating	High force acting on a small area	Open fracture with minimal to moderate soft tissue disruption
Penetrating and Explosive	High force acting on a small area with a large amount of loading rate	Open fracture with serious soft tissue disruption and bone fragments

In general, loading on a long bone result normal and shear stress on each section. Fracture will happen when these stresses go above the allowable values of the bone. Material properties of the bone, therefore, have influence on the fracture shape. Cortical bone is an anisotropic material, its strength changes in different directions, and it is generally weak in tension and shear, mainly along sagittal or coronal plane. Therefore, under axial loading, the tension (convex) side of the long bone fails first. In some cases, the compression (concave) side of the long bone fails first due to the excessive shear stress generated under compression. Under torsion, a spiral fracture with a 45° theoretical angle appears on the shaft, but under experimental conditions, an average angle of spiral fractures is reported as 30° of the longitudinal axis [12].

Besides these natural causes of the fractures, sometimes artificial cuts or fractures are need to be introduced to the bones to shorten or lengthen them or to change their orientation. These types of surgical operations are called as *osteotomy*, in which the bones are basically cut, reformed or partly removed to realign them into the required structure. These types of surgical interventions of long bones including hip and knee osteotomies are also considered as artificial mechanisms of long bone fractures.

1.2.2. Fracture Healing Process

Fracture healing can be considered as a cascade of biological processes occurring in series but also overlapping at certain level. The overall process can be characterized

by three distinct phases involving inflammation, repair and remodeling. Considering diaphysis of a long bone, a simple transverse fracture results in the splitting of the periosteum, damage to the bone marrow and disruption of the local blood vessels. At tissue level, this trauma causes inflammatory events and the creation of hematoma. In micro level, this trauma breaks the network of osteocytes and it triggers the resorption process of the necrotic cells. After resorption, the constructive cells propagate around the fracture site and generates the fracture callus, a soft granulation tissue supporting the ends of the fragments. The formation of fracture callus signals the start of the repair phase. In the beginning of this phase, cartilage formation occurs within the fracture gap together with the fibrous tissue growth. Simultaneously, mineralization of the cartilage, or ossification, and primary bone deposition starts. Hard (bony) callus formation with the development of the woven bone follows this stage. In the remodeling stage, primary woven bone begins to convert into a mature lamellar bone [13]. In Figure 1.8, four basic stages of the fracture healing involving hematoma formation, fibrocartilage callus formation, hard callus generation and remodeling is illustrated.

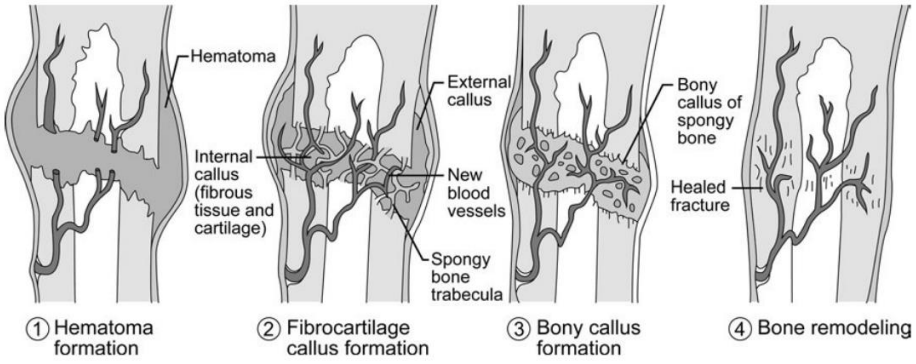

Figure 1.8 Bone healing process [40].

The important feature of healing process is restoration of the original bone structure with mechanical properties equal to those before fracture. Muscle, skin and tendon are incapable to model such a regeneration after wound [11]. The factors affecting

this unique restoration process can be both systemic including age, hormones, functional activity and nutrition or local involving degree of trauma, vascular injury, type of bone fractured, degree of bone loss, infection and other local conditions. However, this unique restoration process sometimes heal unsuccessfully, without treatment. The necessary mechanical and biological environment for the successful healing can be provided by different methods of treatment.

1.2.3. Methods of Treatment

Treatment of the extremity fractures can be categorized into two, namely non-operative and operative treatments. Non-operative treatments include cast immobilization, functional cast or brace and traction. A plaster or fiberglass cast is the most common type of treatment, because the majority of fractures can heal successfully after repositioning and maintaining broken ends in proper position during healing processes. The difference of functional cast from casting comes from its allowance for limited movement of the nearby joint. Unlike castings, tractors align a bone or bones by a steady, light pulling action.

Internal and external fixation methods use surgical means for obtaining and maintaining a reduction for the fracture. Internal fixation may involve open or closed reduction to reposition bone fragments in their original position. Fragments, then held together with using plates and screws or intramedullary nails. Wires and pins can also be used for preserving the reduction in this type of fixation. In external fixation, however, metal pins or screws are placed into proximal and distal fragments of the fracture through the skin and are connected outside the skin by metal bars. The majority of the fixation mechanism stays outside the body in this type of fixation.

Considering the fracture healing process, treatment methods utilize two different healing principles namely, primary and secondary fracture healing. Unlike the healing process explained in previous Section 1.2.2, bone heals without callus formation in primary type of healing. Primary fracture healing can be achieved by applying enough compression over the fragment surfaces facing each other, and as a

result, all forces acting on fracture line get in an equilibrium. The secondary healing, on the other hand, involves the same stages of classical healing process defined in previous chapter.

The strain theory of Perren as cited in [13], gives insight about mechanical factors in a fracture gap, and shows the proper methods of fixation for different fractures. Strain is the response of a material when a stress is generated due to the loading on the material. Engineering strain is the ratio of change in length to the initial length when a force is applied. Intact bone has a 2 % normal strain before the fracture, whereas the granulation tissue has a strain tolerance of 100 % [14]. The strain theory states that, under the same deformation conditions, small fracture gaps (i.e. under 2 mm) may result in disruption of granulation tissue cells, however a wider gap may only deform the tissue and not cause any rupture. For example, a 10 μm-diameter cell may disrupt in 10 μm-gap, but it may deform only in 30 μm-gap if the same displacement is applied. By using this theory, it can be said that the simple fractures with two main fragments tolerate less motion compared to multi-fragmentary fractures because the overall deformation is shared by one or two fracture planes. Therefore, simple shaft fractures require rigid fixation by compression of two main fragments by using screws and plates; multi-fragmentary shaft fractures, on the other hand, need a fixation method that is flexible to some extend such as intramedullary nails or external fixators.

1.3. Fracture Fixation

Fracture fixation is a broad term which includes any system or device used to assist healing of a fractured bone. Devices of the both internal and external methods (e.g. casts, braces, screws and plates) are the components of fracture fixation. Fracture fixation must favor the healing process by creating sufficient stability which determines the type of healing. The diagram in Figure 1.9 explains the effect of mechanical stability on type of healing process.

In fracture fixation field, the introduction of the internal fixation technique is considered to be one of the most important developments, because internal fixation reduces the hospital stay times, the rate of improper healing and allows individuals to return to function earlier [12]. Since this thesis is concentrating on an internal fixation system, the brief history of the internal fixation techniques will be summarized in the following section.

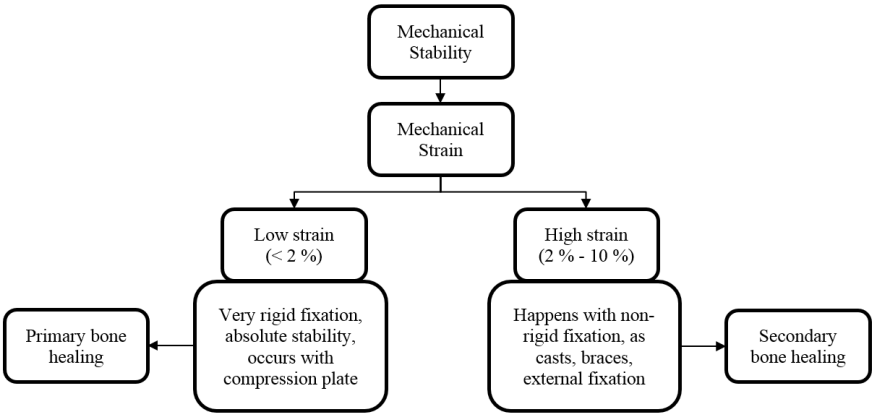

Figure 1.9 Effect of mechanical stability on healing process (The Author, produced from [13]).

1.3.1. Brief History of Internal Fracture Fixation

In the first half of the 19th century, surgeries were primarily dominated by pain and fear of lethal infections. The discoveries of anesthesia (1846), antisepsis (1865), X-rays (1895) and antibiotics (discovery of penicillin in 1928, commercially available antibacterial, Prontosil, in 1932, and purification of penicillin in 1945), made possible operative treatments of fractures [15], [16]. The first attempt at internal fixation of a fracture was made by Kearny Rodgers in 1827, who used iron and silver wires in the fixation of a humeral fracture. Subsequently, Jozef Lister conducted the first sterile operation in which a silver wire used in a patella fracture. The first fracture fixation with a plate had been carried out in 1886 by Carl Hansmann. Albin Lambotte (1866-

1955), who introduced the term of osteosynthesis, described the key points of handling fractures with plates and screws, wire loops and external fixators. In 1908, he published his work of the internal fixation of 35 femur fractures using plates. Besides Lambotte, the great contribution to the field of internal fixation by other surgeons are Robert Danis, William Arbuthnot Lane, Ernest William Hey Grooves and Gerhard Küntscher. Danis introduced the term *primary bone healing* with his observations of fracture reduction using his compression plate. Lane conducted the first interfragmental fixation and he started to use plates in his operations in 1905. Hey Grooves used pins made from cattle bones and horns in fixation of proximal femur fractures. Küntscher developed intramedullary nailing technique, which developed the handling of diaphyseal fractures [12], [13], [17].

The early techniques of internal fixation methods were often suffered from infection, immune system response to the materials used and lack of knowledge about biomechanics of bone repair. These early systems had disadvantages like damaging the periosteum and soft tissue and blocking the blood supply, instead of healing the fracture. However, in the last 60 years there has been a remarkable progress in the understanding of the healing process, resulting in an effective fixation methods with appropriate material choices [12]. The following section is devoted for contemporary devices using in these effective clinical fixation techniques.

1.3.2. Contemporary Devices in Internal Fracture Fixation

The basic components used in internal fixation include plates, screws, pins, wires and rods. The primary materials used in this type of fixation are medical grade 316L stainless steel, titanium alloys (e.g. Ti 6Al 4V, Ti 6Al 4V ELI), and cobalt chrome allows. *Plates* function as internal supports and are attached to the bone with screws to hold fragments in desired positions. Plates may be removed after healing is complete, or left in place depending upon the cases. The most frequently used implants for internal fixation are *screws.* They can be used independently to hold a fracture, as well as in combination with plates, rods or nails. *Pins* are generally used

to fix small fracture fragments that are too small to be attached with screws. Similar to plates, screws and pins can be removed after healing of the fracture or left in place. *Wires* are metal sutures and are commonly used to tie the small pieces of bone like pins. *Rods* or nails are employed to treat the majority of fractures in femur and tibia. After inserting through the hollow center of these long bones, screws at the each end of rod permit any rotation or displacement on the long axis of the bone [12], [18]. Figure 1.10 illustrates different examples of devices using in internal fixation.

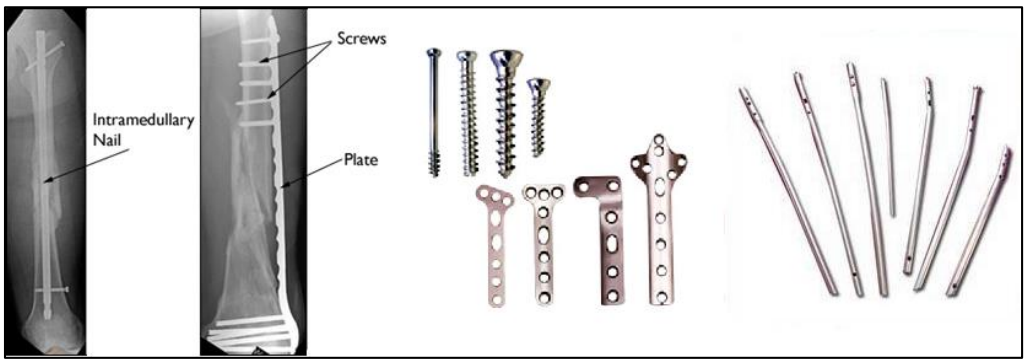

Figure 1.10 Examples of plates and screws (middle), intramedullary nails (right), and their applications on x-ray (left) [18].

1.4. Problems Related with Plate and Screw Systems

There are different implant sets including plates and screws with their corresponding instruments for internal fixation of fractures and osteotomies. These sets are generally called according to the size of fragments in which they are applied (e.g. small fragment set, large fragment set) or the application area (e.g. distal radius set, pelvic and acetabular set). Depending on the surgical objective, the surgeon selects proper plates and screws from the set and apply them with their matching instruments. However, current plate-screw systems used in internal fixation force surgeons to insert screws through fixed holes of the plate. Even though there exist different classifications of fractures, fracture lines differ from person to person like fingerprints. As a consequence of this, the holes over the fracture lines cannot be

used, or there may be no holes over the suitable locations for inserting screws. Therefore, in some cases, different axes of insertion that are not available on the plates are required by surgeons.

Besides this main problem, there are other problems related with plate-screw systems that are not specific for all systems, but considered as major problems namely contact with periosteum, anatomical incompatibility, and improper fixation rigidity. Some of these problems are solved by introducing, for example low contact plates or dynamic locking screws, however, the main problem is stated as a remaining challenge by the medical doctors.

1.5. Motivation and Purpose of the Thesis

Having stated the problems of the contemporary plate-screw systems very briefly, the purpose of this study is to design and prototype an internal fixation system that is anatomically suitable for intended area of application, minimizing periosteum damage, allowing multi-axial screws and multi-planar application for traumatic and osteotomic applications, as a part of an interdisciplinary project.

Specifically, the main points focused in this thesis are:

- Solving the major problems of plate-screw systems by utilizing the idea of using a rod-connector-screw system similar to the ones used in spinal surgery,
- Evaluation of the critical points of conceptual and final models of designed system by using analytical methods,
- Conducting mechanical tests to assess the performance of the final design and to compare with analytical estimations,
- Introducing and prototyping a novel concept that is aimed to be used in combination with the final design,
- Concluding a suitable area of application of the designed system based on the assessments.

1.6. Outline of the Thesis

Chapter 1 is dedicated to provide a brief information about internal fixation of fractures together with the underlying knowledge in the field of anatomy and physiology. Accordingly, the major problems of the contemporary internal plate fixation of fractures are explained.

Chapter 2 provides a summary of recent developments about internal plate fixation systems that are aimed to solve major problems mentioned previously. In addition, different aspects of general considerations about implants of internal fixation which are directly affects their in-vivo performance are explained. Finally, important characteristics of the mutual element of conventional plate fixation systems and designed system are examined.

Chapter 3 presents the design procedure conducted to reach the objectives of the study. In addition, the development and theoretical analyzes of the design are explained in detail. Testing procedure and materials are also provided in this chapter.

Chapter 4 is devoted to present and discuss all the results of the study together with comparison of the analytical results with test results.

Chapter 5 summarizes the overall study and gives the final conclusions drawn from the results. Lastly, suggestions for future work are presented.

Sample calculations, glossary of medical terms, and technical drawings of the finalized designs are also provided in Appendices.

CHAPTER 2

LITERATURE REVIEW

2.1. Introduction

In recent years, there have been several developments about plate-screw systems in order to solve major problems stated in previous chapter. Many of studies in the literature are aimed to evaluate these developments by finding out their contribution and comparing their performance with earlier designs. In the next section, these studies are briefly summarized in terms of their influences on the mentioned design process.

2.2. Previous Studies Related with Plate-Screw Systems

One of the latest improvements on the locking anatomical plates, in which one or two screw holes are designed to enable screw insertion multi-axially, can be an example of a development aimed to insert bone screws somehow in a more favorable or desired angle. In a study related with the fractures of proximal tibia [70], this type of locking plate was designed, and compared with existing application including two plates on medial and lateral planes with mono-axial bone screws. The results of this study showed that, the new design with multi-axial screws have an equivalent fracture stability with the former two-plate solution. Similarly, two different plates of distal femur with poly-axial screws were compared in a study [71], and both plate-screw systems were found stable under pre-defined axial forces. However, different studies on humerus [72]-[79], femur [80], and tibia [81] came up with similar results which suggest that the use of poly-axial screws only remain in metaphyseal region of the plates due to their lack of strength under rotational forces. For this reason, the moving elements of the aimed design should be checked in terms of their movement stability.

In surgical procedures of plate-screw systems, surgeons try to keep periosteum damage at a minimum in order not to disrupt necessary circulatory support of healing fracture. In addition, they avoid not to keep periosteum under pressure, especially for the postoperative period [82]. In this context, closed reduction of fractures with casting treatment provide an excellent fixation for periosteum, and this type of treatment is often called as biological fixation [83], [84]. However, conventional plates cannot offer a biological fixation, since they contact periosteum during fixation. Therefore, low contact plates were introduced to make plate-screw systems advantageous in terms of biological fixation [85], [86]. In this context, a fully biological fixation should not be expected from the intended fixation system, but minimizing periosteum damage should be determined as a design goal.

The initial reduction quality created by reduction clamps can sometimes be lost after fixation with plate and screws during surgery. This problem is generally occurred due to the movement of fracture fragments towards plate instead of each other while inserting screws. Such problems were solved by bending of plates during surgery to conform anatomical shape of the bone [87]. The proposed rod-connector-screw concept, however, need to be formed easily to obtain an anatomically fitting fixation. Usage of rod, therefore, is an advantage regarding to bending stiffness of plates. Even if the diameter of the rod is equal to both thickness and width of the plate, the bending stiffness of rod is smaller than the plate. In addition, the bending stiffness of plate increases with increasing width values.

The Figure 2.1 shows a representative comparison of bending stiffnesses for a rod and plates with varying width. Note that, both rod and plate are assumed to be produced from same material and have same length. For this reason, second moment of area values are illustrated in Figure 2.1.

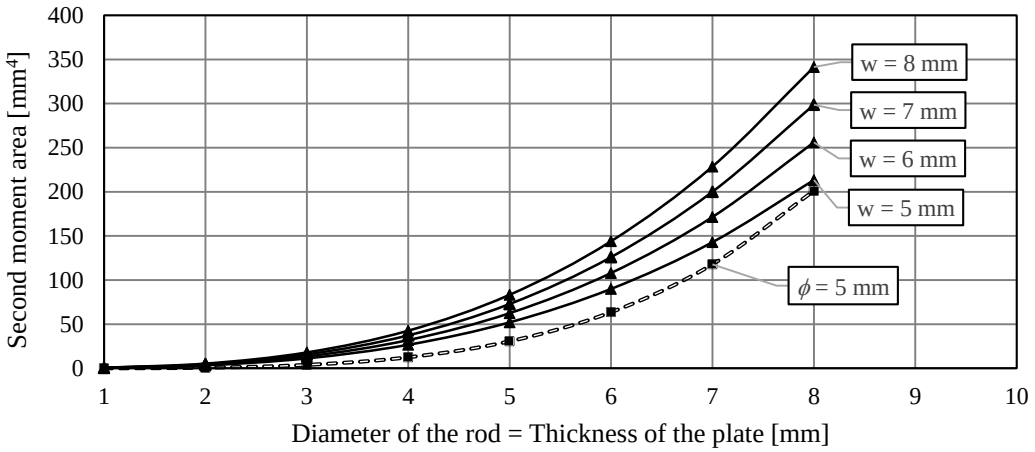

Figure 2.1 Representative comparison of bending stiffness of a rod and a plate (w: Width of the plate, ϕ: Diameter of the rod).

Previous studies showed that, to achieve the purposes of this study one need to take into account the following major points:

- Internal fixation always harms the periosteum owing to the usage of screws, but additional damage caused by the plate should be avoided.
- Reduction stability should not be affected after application of the fixation system.
- If the system has joints (e.g. ball, cylindrical etc.) to create degree of freedom, their mechanical stability after restriction should be investigated.

Besides these major points, there are more general considerations about implant systems of internal fixation which are directly affecting their in-vivo performance. In the next section, different aspects of these consideration will be explained in detail under the *Device Performance* title. In addition, the common element of the both conventional internal plating and proposed system -bone screws- are explored in detail, in Section 2.4; because the most frequently used implants for internal fixation are bone screws, and they can be used independently or in combination with plates, nails and rods.

2.3. Device Performance

2.3.1. Introduction

Any material used to manufacture devices for restoring a function or a section of the body in a biologically compatible manner can be defined as a biomaterial. Biomaterials can differently be classified by considering their properties, clinical application areas or their structures. For example, biomaterials can be synthetic (manmade) or natural: In this classification, collagens used for the replacements would be considered as natural or reconstituted; while polymers, metals, ceramics and composites would be classified as synthetic. Another classification includes the application areas such as orthopaedic (fixation systems, joint replacements, grafts etc.); dentistry (dental implants, stoppings, tempora-mandibular joint (TMJ) replacements etc.); and surgery (sutures, wound dressings). In addition, the previously mentioned class of the synthetic biomaterials (polymers, metals, ceramics and composites) are an example of the classification according to their intrinsic structure [38].

In general, synthetic biomaterials are chosen to manufacture load bearing orthopaedic implants over natural or biological materials because of their advanced mechanical properties. Since these advanced properties of the synthetic biomaterials are engineered, they are also known as “engineering materials”. The selection of an engineering biomaterial for a load bearing orthopaedic implant (e.g. a fracture fixation device) is based on the specific material property requirements such as stiffness, yield strength or toughness to guarantee the reliability of the implant.

In this thesis study, a medical grade titanium alloy has been chosen for all the parts in the fracture fixator assembly (rods, connector and screw). According to previously defined categorizations, this titanium alloy belongs to *metals* under the *synthetic* biomaterials. The designed fixator is intended to be used in the *orthopaedics* clinical application area; specifically in the treatments of the long bone fractures. Typically, the primary aim of the fixator in such an area is to help failed hard tissue (e.g.

fractured bone) heal properly by providing a supportive environment, and thereby the fractured bone restores its structural integrity and functional properties. In line with this aim, the in vivo performance of the device depends not only on the selected material but also on the implant design, processing, clinical issues including biocompatibility, patient factors etc., and regulatory issues such as medical approvals. The Figure 2.2 summarizes these interrelated factors affecting on the implant performance.

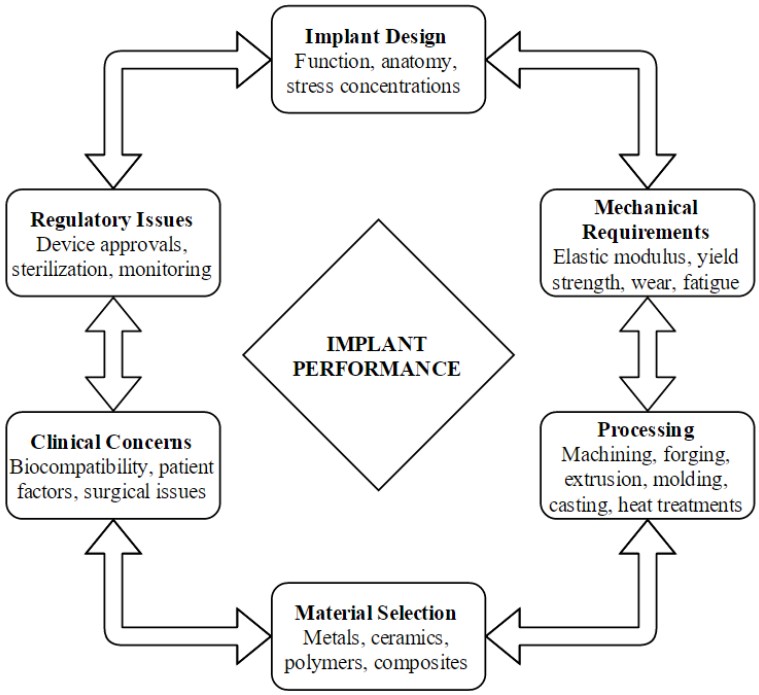

Figure 2.2 The factors affecting the implant performance (adapted from [38]).

The *clinical concerns* are the most important factors which influence both the design process and the implant performance. The biocompatibility, specific immunological response of the patient, in vivo degradation, the role of the surgeon and the patient factors like physical and anatomical conditions are all examples of the major clinical concerns.

Regulatory issues involve device approval stages identified by the authorized institution such as biocompatibility analysis, mechanical testing and clinical

experiments. Among all the factors contributing to implant performance, the regulatory and clinical issues are beyond the scope of this thesis. However, while the mechanical aspects of the fixator are explained in detail, the critical points related with the clinical issues such as biocompatibility, patient and surgeon factors are also addressed in the following text.

2.3.2. Material Selection

Human bone is an anisotropic material, its physical properties differs in direction mainly due to the collagen fiber orientation of this composite structure. The cortical part of a long bone, as an example, has maximum strength in longitudinal axis, and minimum in the transverse axis, therefore it withstands more compressive forces than tensile or torsional forces. If any critical force (compressive, tensile, torsional or combined) above the carrying capacity of the bone is applied, the fracture is inevitable. Due to this load-bearing role of the bones of the skeletal system, metals are suitable for internal fixation devices with their high strength and elastic modulus among other man-made biomaterials. Ceramics also have high compressive strength and hardness, however, their weak tensile strength and low fracture toughness (i.e. brittleness) limit their usage in internal fixation applications. Polymers, on the other hand, have favorable elastic modulus matching with hard tissues, but there are significant problems with polymers regarding load bearing applications, including in-vivo exothermic polymerization (e.g. PMMA bone cement), wear due to fatigue and biological conditions, creep and stress relaxation, and low-strength. To utilize polymers into fracture fixation, composites can be thought with their custom made mechanical properties: Orthopaedic fixation plates produced from polyether ether ketone (PEEK) reinforced with carbon fibers (i.e. a composite with the polymer matrix PEEK and the carbon fibers generally produced synthetically from another polymer) can offer complementary elastic modulus and less stiff fixation to the fracture. By this way, compared to the more stiff bone plates, stress shielding can be reduced and more load can be transmitted to the applied bone. However, due to the

lack of strength between the contacting surfaces of the fibers and the matrix, such composites can be inclined to debris production and this may be problematic in terms of biocompatibility and structural integrity [21], [22], [39].

Considering these main issues about man-made biomaterials, the metallic biomaterials have been determined to be used for the designed fracture fixation plate in the conceptual design stage of this project. The materials used for the contemporary fracture fixation devices in the orthopaedics field have also been taken into account during the general decision of the implant material. In this context, metallic biomaterials have been investigated and compared according to their properties and the final decision on implant material has been made.

Metallic Biomaterials

Typical metallic biomaterials for orthopaedic devices are stainless steels, cobalt-chrome alloys and commercially pure titanium and its alloys (Table 2.1).

Table 2.1 Metals used for medical devices [28].

Clinical Division	**Medical Device**	**Material**
Orthopaedic Surgery	Bone Fixation (bone plate, screw, wire, nail, etc.)	316L, 316LVM Stainless Steels; CP Ti, Ti 6Al 4V, Ti 6Al 7Nb
	Spinal Fixation	316L, 316LVM Stainless Steels; CP Ti, Ti 6Al 4V, Ti 6Al 7Nb
	Artificial Joint, Bone Head	Co-Cr Alloys, Ti 6Al 4V, Ti 6Al 7Nb
	Spinal Spacer	316L, 316LVM Stainless Steels, Ti 6Al 4V, Ti 6Al 7Nb
	Surgical Instruments (scalpels, forceps, etc.)	304, 304L, 316, 316L Stainless Steels, Ti 6Al 4V, Ti 6Al 4V ELI

The development of these materials were based on industrial applications, then they were adapted to medical usage to be suitable with corrosive environment of the living body. As a result of unsuccessful clinical experiences that emerged as biological or mechanical problems, these adapted biomaterials have also been improved by trial-and-error. Table 2.2 shows examples of metallic biomaterial improvements that have been aimed to solve such problems including corrosion and wear resistance, toxicity, high biocompatibility, stress shielding and high strength requirement.

Table 2.2 Development of metallic biomaterials [29].

Materials	**Problems**	**Examples**
Stainless Steel	Corrosion resistance → Reducing C content	18Cr 8Ni 0.03C 18Cr 12Ni 2.5Mo 0.03C
	Skin allergy → Ni free alloy	23Cr 2Mo 1.4N
Co-Cr Alloys	Wear Resistance, high strength, Ni allergy	Co 29Cr 6Mo
Ti Alloys	Cyto-toxicity → Vanadium free	Ti 6Al 7Nb
	High strength & low elasticity → β alloy	Ti 6Al 2Nb 1Ta 0.8Mo Ti 15Mo 5Zr 3Al Ti 12Mo 6Zr 2Fe
	High biocompatibility	Ti 15Zr 4Nb 4Ta Ti 29Nb 13Ta 4.6Zr

Stainless steels are a type of steel alloys containing certain amount of chromium and other elements together with their main content iron (with a maximum of 50 % iron content and a minimum 12-13 % chromium and other elements by mass). Stainless steels do not corrode or stain in an oxygen containing atmosphere, but they are not fully stainless in saline solutions such as liquid environment of the body. They can degrade due to pitting and crevice corrosion in the body fluids, and for that reason certain grades of stainless steels including AISI/SAE Type 304, 304L, 316, 316L, 316LMV (low carbon vacuum melt) steels can be used in surgical or medical applications. Relatively lower cost, high availability, ease of manufacturing and great

strength properties of stainless steels utilize them in a wide range of applications including temporary fracture plates, spinal fixation and surgical instruments. However, they are not suitable for moving parts of the artificial joints due to their poor wear resistance.

Cobalt-chromium-based alloys generally vary as castable and wrought. Their corrosion resistance is good due to the formation of passive oxide layer within the body fluids. Especially, Co-Cr alloys have excellent wear resistance; their ductile behavior make them highly resistant to fatigue and cracking, so they are the best candidates for the material choice of the artificial joints. However, the nickel (Ni) ions, which are released into the body due to corrosion of Ni-containing stainless steels and Co-Ni-Cr-Mo alloys, are very toxic, and allergy problems may occur after implantation of such materials in the body. Thus, nickel free grades of both stainless steels and Co-Cr alloys are developed for in-vivo use (Table 2.2).

Titanium and titanium alloys were actually developed as aerospace materials. Titanium materials have excellent corrosion resistance compared to stainless steel and Co-Cr alloys due to the formation of stable titanium dioxide films on their surfaces. Titanium alloys have the advantage of the combination of excellent characteristics such as having high strength and low density (i.e. high specific strength), complete inertness to body, moderate elastic modulus value (about half of the stainless steel and Co-Cr alloys) and high friction coefficient. However, their usage are limited to the parts of the implants where wear resistance is not essential. They are also not suitable for fixation wires that require twisting, because of their poor torsional strength. [28, 42]. The biocompatibility of the titanium and titanium alloys are exceptional, but there are several concerns about aluminum and vanadium release into the body, particularly in long term use of titanium and titanium alloy implants. For long term treatments, vanadium-free titanium alloys, in which the vanadium content is replaced with niobium (Nb), zirconium (Zr) or tantalum (Ta), make implants more biocompatible and also corrosion resistant [32]. A general comparison of the corrosion resistance, tensile strength and workability of the metallic biomaterials is also summarized in Table 2.3.

Table 2.3 Comparison of the metallic biomaterials [28].

Material	Type	Tensile Strength	Workability			Corrosion Resistance
			Wear Resistance	Plasticity	Machinability	
Stainless Steel	316L	Good	Good	Excellent	Excellent	Fair
Co-Cr Alloy	Cast	Good	Excellent	Poor	Poor	Good
	Annealed	Excellent	Excellent	Good	Good	Fair
Ti; Ti Alloy	CP Ti	Fair	Fair	Fair	Fair	Excellent
	Ti 6Al 4V	Excellent	Fair	Fair	Excellent	Excellent

For many different metallic alloys, various classification systems exist to maintain all the standards organized and correct. In general, *American National Standards Institute (ANSI)* and *International Organization for Standardization (ISO)* manage the other organizations that create standards such as *American Society of Mechanical Engineers (ASME), American Iron and Steel Institute (AISI), Society of Automobile Engineers (SAE), American Society for Testing and Materials (ASTM)* and *Japanese Industrial Standards (JIS)*. Metallic implant materials have also standard specifications developed by these organizations. The most common and well-known example is “Type 316 Stainless Steel” which is often misused to refer to all medical grade stainless steel family. However, the “Type 316” of that stainless steel refers to an AISI/SAE classification of the material.

In this thesis, the material specifications of ASTM are used for material selection purposes; because ASTM is the largest organization in the world for developing and issuing full-consensus standards. The basics of standardization process of ASTM also remained unchanged over a century, and by this way competent and credible standards like material specifications are developed with the input from experts of industry and academia. In addition ASTM standards are continuously reassessed to assure their reliability, while keeping them up-to-date [59]. In the following pages the mechanical properties together with the chemical composition and treatment condition of the metallic implant materials are provided by referring the latest valid

ASTM standards (Table 2.4, 2.5, 2.6). The UNS (*Unified Numbering System for Metals and Alloys)* number, which is a joint specification developed by ASTM and SAE, of each material is also provided in parallel to the title of related ASTM standard in these tables. The ASTM designations for material specifications are classified in an alpha-numeric way, in which the letter indicates the committee responsible for that specification (e.g. A-G), the numbers between the letter and the dash corresponds to the reference number given to the standard (e.g. 67, 136, 1537), and the numbers after the dash show the last technical revision date (e.g. -13 for 2013, etc.). The readers should note that outdated and withdrawn standards such as F55-82, F56-82, and F745-07 are excluded in these tables.

Table 2.4 Stainless Steels [20], [23], [25], [31], [35].

ASTM (UNS)	Chemical Composition	Thermal Treatment Condition	Elastic Modulus [GPa]	Yield Strength [MPa]	Tensile Strength [MPa]
F138-13a F139-12 (S31673)	18Cr 14Ni 2.5Mo	Annealed	190-205	190	490
		Cold-Worked	190-205	690	860
F1314-13a (S20910)	22Cr 13Ni 5Mn 2.5Mo	Annealed	200	380	690
		Cold-Worked	200	862	1035
F1586-13a (S31675)	21Cr 10Ni 3Mn 2.5Mo	Annealed	195-200	430	740
		Medium Hard	195-200	700	1000
		Hard	195-200	1000	1100
F2229-12 (S29108)	23Mn 21Cr 1Mo	Annealed Cond. A	200	517	827
		Annealed Cond. B	200	827	1034
		Annealed Cond. C	200	1241	1379
F2581-12 (S29225)	11Mn 17Cr 3Mo	Annealed	**	482	827
		Cold-Worked	**	827	1103

Table 2.5 Cobalt Chrome Alloys [20], [23], [25], [36].

ASTM (UNS)	Chemical Composition	Thermal Treatment Condition	Elastic Modulus [GPa]	Yield Strength [MPa]	Tensile Strength [MPa]
F75-12 (R30075)	Co 28Cr 6Mo	As-cast	210-250	450	655
		Annealed	210-250	517	890
F90-14 (R30605)	Co 20Cr 15W 10Ni	Annealed (Bar & Wire) [a]	210	310	860
		Cold-Worked (Bar & Wire) [a]	210	760	1250
		Annealed (Sheet & Strip) [b]	210	379	896
F562-13 (R30035)	35Co 35Ni 20Cr 10Mo	Annealed	230	241-586	793-1069
		Cold-Worked	230	655-1586	1000-1793
F688-14 (R30035)	Co 35Ni 20Cr 10Mo	Annealed (Sheet)	230	310	792
		Cold-Worked (48%)	230	1343	1357
F799-11 (R31537-38-39)	Co 28Cr 6Mo	Forgings	210-230	827	1172
F961-14 (R30035)	35Co 35Ni 20Cr 10Mo	Forgings [c]	230	*	*
F1537-11 (R31537-38-39)	Co 28Cr 6Mo	Annealed	210	517	897
		Hot Worked	230	700	1000
		Warm Worked	230	827	1172
F2886-10 (R30075)	Co 28Cr 6Mo	Low Carbon	210-250	450	725
		High Carbon	210-250	480	825

a: bar and wire, b:sheet and strip, c: comply with the minimum mechanical properties as specified in Specification F562

Table 2.6 Titanium and Titanium Alloys [20], [23], [24], [25], [26], [27], [37].

ASTM (UNS)	Chemical Composition	Thermal Treatment Condition	Elastic Modulus [GPa]	Yield Strength [MPa]	Tensile Strength [MPa]
F67-13 (R50250-400-550-700)	Unalloyed Ti (Annealed-bar, billet, forgings and other forms)	Grade 1	105	170	240
		Grade 2	105	275	345
		Grade 3	105	380	450
		Grade 4	108	483	550
	Unalloyed Ti (Annealed-sheet, strip and plate)	Grade 1	105	170-310	240
		Grade 2	105	275-450	345
		Grade 3	105	380-550	450
		Grade 4	108	483-655	550
F136-13 (R56401)	Ti 6Al 4V ELI (Extra Low Interstitial)	Annealed-A	101-110	795	860
		Annealed-B	101-110	760	825
F1108-14 (R56406)	Ti 6Al 4V (Alloy Castings)	Hot isostatic processing (HIP), and annealed	110-114	758	860
F1295-11 (R56700)	Ti 6Al 7Nb (Wrought)	Annealed	105	800	900
		Hot Worked	105	800	900
		Cold Worked	105	800	1100
F1472-14 (R56400)	Ti 6Al 4V (Wrought)	Annealed-A	110-114	860	930
		Annealed-B	110-114	825	895
F1713-08 (R58130)	Ti 13Nb 13Zr (Wrought)	Un-annealed	79-84	345	550
		Solution Treated	79-84	345	550
		Capability Aged	79-84	725	860
F1813-13 (R58120)	Ti 12Mo 6Zr 2Fe (Wrought)	Solution Annealed	74-85	897	931.5
F2063-12	Ni-Ti Shape Memory Alloys	Annealed	28-41	*	551
F2066-12 (R58150)	Ti 15Mo (Wrought)	Annealed	78	483-1050	690-1150
F2885-11 (R56406)	Ti 6Al 4V (Metal Injection Molded)	Type 1 Densified	110-114	830	900
		Type 2 Sintered	110-114	680	780
F3046-13 (R56320)	Ti 3Al 2.5V (Wrought)	Annealed	100	485	620

The tensile and yield strength values of each standard represent the minimum value that the manufacturer of the material should provide to the purchaser. In several standards, the values of yield strength on the basis of 0.2% offset strain and the ultimate tensile strength have different values depending upon the heat treatment types. However, the elastic modulus values of the same alloy grades are identical regardless of thermal treatment condition. It shows that the heat treatments can alter the yield behavior of the alloy, but not the basic chemical composition and configuration of it. The modification of alloy strength through thermal treatments also improve their manufacturability. They can be softened for shape-forming processes and then be hardened in their final shape to obtain a strong part. The processes of material strengthening and shape-forming, which affect the implant performance together with the material selection, will briefly be explained in the following *Processing and Manufacturing* subsection.

The elastic moduli for medical grade metallic alloys lie in the narrow ranges but their yield and tensile properties have wide ranges due to varying degrees of cold working, heat treatment and other hardening mechanisms. According to ASTM material specifications, the elastic moduli for medical stainless steels lie between 190 – 205 GPa, while the yield strengths and tensile strengths of them are in the ranges of 190 – 1300 MPa and 490 – 1400 MPa respectively. Cobalt-chrome alloys have slightly larger elastic moduli (210 – 250 GPa), yield strengths (210 – 1400 MPa), and tensile strengths (655 – 1800 MPa) than stainless steels. Titanium and titanium alloys, on the other hand, present remarkable yield and tensile strengths ranges of 170 – 1100 MPa and 240 – 1200 MPa correspondingly, with an elastic modulus range about half of the Co-Cr and stainless steel alloys (105 – 115 GPa). The typical density value of titanium is also considerably lower than stainless steel and Co-Cr alloys (~4500 kg/m^3 for titanium and ~8000 kg/m^3 for both stainless steel and Co-Cr alloys [43, 44]).

Final Remarks on Material Selection

Different than unchanging and well-known material properties of mentioned engineering materials, intact and healthy bones adapt its mechanical properties such as mass, geometry, and hence strength, according to the daily life usage or needs. A remodeling process occurs in response to loading conditions, where the mechanical signals such as local elastic deformation of bone are changed to biochemical signals, and stimulate bone loss or bone gain [6, 45]. In the case of a fixated bone fracture, however, the loading conditions and the amount of the mechanical signal change temporarily. For example, most of the femoral shaft fractures take four to six months to heal totally. Particularly, open and comminuted fractures take even longer times to heal completely. The patients with such type of fractures may not be able to put weight on their leg until the healing has started. Once the healing has started, the doctors may allow patients to put as much weight as possible on the leg, probably together with the crutches [34]. In some cases, the patients may receive inpatient treatment with a long length of hospital stay that results reduction of bone and muscle density due to the immobilization of the fractured leg. In such cases, the bone adapts itself to new loading conditions by remodeling: There may be compressive normal forces on the fracture line favoring the modeling, but the intact part of the bone loses its mass by remodeling because of the immobilization and hence the removal of mechanical signals (i.e. the normal stress). Once the patient starts walking with the implanted fracture, the normal loads on the bone will be shared with the implant and the bone itself. The stiffness of the bone–fixator structure defines the amount of load sharing, and also gives the clue of whether the stress shielding problem may arise or not. Here, the mechanical properties of the bone and the implant material should be compared, especially their elastic modulus, while deciding the implant material. In this project, Ti 6Al 4V ELI has been selected for all parts of the fixator assembly including the rod, connectors and screws. The main reasons of this choice are as follows: The strength of this alloy is as good as that of stainless steels and cobalt-chromium alloys, however it is only half as stiff. The elastic modulus of Ti 6Al 4V

is still quite a few larger than the cortical bone (E: 101 – 110 GPa for Ti 6Al 4V ELI; 7 – 30 GPa for the cortical bone [40, 41]), but the optimal choice is this alloy in terms of the availability, cost and manufacturability considering the other alloy with low elastic moduli as nickel-titanium alloys. Since, the planned period of usage of the fixator in the body is between 4 – 6 months (short-term application), Ti 6Al 7Nb material is not taken into consideration for the mechanical testing and prototype production purposes, but according to the results of clinical trials and biocompatibility tests, Ti 6Al 7Nb will be reconsidered as the material choice; because the international medical device manufacturers [33], such as Jonhson & Johnson (DePuy Synthes), Zimmer-Biomet and Stryker have already started using Ti 6Al 7Nb for their implants materials in similar orthopaedic applications according to their contemporary catalogs.

2.3.3. Processing and Manufacturing

The structure and properties of the metallic biomaterials can be modified by heat treatments, processing and forming operations similar to other metals and alloys.

Annealing, quenching, and tempering can be included in thermal treatments used in the processes for enhanced material properties. Annealing is the heating of the metal or alloy to an enough temperature below its melting point for the reformation of grains (recrystallization). This method can be used for relieving stresses inside the material and also for controlling the grain size. Quenching is the rapid cooling process to obtain certain material systems such as supersaturated solid solutions and amorphous metals. Tempering is another heat treatment done by heating the metal to a specific temperature for a period of time, then cooling it in still air. Precipitation, grain growth, and removal of the residual stresses can be obtained by this method.

The improved material properties can be achieved by simply introducing a mechanism that prevent the movement of dislocations within the crystal structure of metals. There are mainly three different strengthening methods used in metals such as deformation, lattice substitution and second-phase particles. The deformation

method can work through strain (work) hardening, in which the line dislocations are added via deforming of the material. Reduction of the grain size can also result an increase in the yield strength of the material by creating more grain boundaries in a specified volume. The typical examples of deformation method are cold-working, extrusion, drawing, and (cold) rolling for strain hardening, and hot rolling for reduction in grain size. The solid-solution strengthening method involves the addition of an element which has a geometric difference from the lattice atoms of the crystal structure of a metal. Alloying is the example of this method. The second-phase particle method can be attained either through age-hardening or precipitation hardening. In this method, the alloy should display a decreasing solubility with reducing temperature. By this way, precipitation can be obtained in the matrix with the correct heat treatment. The titanium alloys alloyed with aluminum and vanadium are an example of the decreasing solubility behavior with decreasing temperature: The heating and then quenching of this alloy result a supersaturated solid solution. Annealing can be performed after that, to obtain precipitates which help to improve the yield strength of the alloy. Stainless steel alloys can similarly be strengthened by precipitation of chromium. However, heat treatments are not suitable for stainless steel alloys, because of the high chromium and nickel content of them. The formation of chromium carbide in grain boundaries as a result of the heat treatment may cause corrosion and can overturn the stainless property of the steel. The surface oxide scales are another unwanted effect of the heat treatment of stainless steels, but these scales can be removed by either mechanical (sandblasting) or chemical (pickling) means. For medical grade stainless steels, surface of the component should be polished to a mirror or matte finish; and then should be cleaned, degreased, and passivated in nitric acid after the elimination of the surface scales. The washing and cleaning before the packaging and sterilizing is also a necessity for such a medical stainless steel component [20, 39].

In particular, titanium is very reactive at high temperatures and burns spontaneously if the oxygen exists in the environment. Therefore, an inert environment is required for high-temperature processes of titanium such as vacuum melting. Hot working and

forging processes should also be performed below 925°C to avoid the embrittlement. Titanium also has a tendency to gall or seize the cutting tools, so that the machining at room temperature is not the answer of all problems. These problems can be reduced by using very sharp tools with slow speeds and large feeds, but electrochemical machining seems as a good alternative for similar applications [20].

Besides the processes for altering the material properties, there are four main categories of shape-forming or metalworking processes: Casting, forming, machining, and joining. In *casting*, molten metal is poured into a mold and then allowed to cool to create a specific shape. Investment casting, die casting and sand casting methods are typical examples of this process. The bulk, sheet and tube forming processes are the main *forming* processes, in which the metal or workpiece is modified by deforming, and without removal of material. The bulk deformation processes including rolling, drawing, extrusion, and forging; the sheet and tube forming processes such as bending, coining, and deep drawing are typical examples of forming processes. *Machining* is a collection of processes to finish a component into a needed shape or surface finish. This process involves the removal of the excess material using different types of tooling such as lathe, mills, and drills. Lastly, the *joining* process covers different methods that joins materials such as welding, brazing, soldering and riveting.

Together with this very brief and general information about processing and manufacturing of metals and alloys, an emphasis should be put on the manufacturing of the designed fracture fixation system, which consists of bars, connectors and two different types of screws. The natural form of the titanium is obtained from the ores, and different operations such as extraction, purification, sponge production should be applied before the creation of its alloys. After the production of the alloy as an ingot, forming and shaping processes can be applied for fabricating the desired product. Generally, round titanium ingots can be used for manufacturing titanium bars. Different diameters of titanium bars then be obtained by utilizing a lathe or multi-axis mill. The connector part of the fixator system can be obtained from rectangular-profiled titanium ingots by removing the excess material using mill, drilling for the

holes, and surface finishing. Similar to titanium rods, bar ingots can be used to produce screws using threading process. Different head forms and socket details can be given to the screws by milling and turning as well.

2.4. Bone Screws

Bone screws are critical elements of the internal fracture fixation; they act as links between two objects and hold them together, and any failure of them directly affect both the performance of the fixation device and the healing period of fracture. Although they appear as a simple and subtle device, significant effort of processing and manufacturing has provided to their design. To understand these critical members of internal fixation, many readers may encounter unfamiliar and different features related with the bone screws in the literature (e.g. cortical, poly-axial, mono-axial, self-drilling, cannulated, hex head, etc.). For that reason, a brief review will be given in the following subsections pointing out the principals of bone screws.

2.4.1. Structure of the Bone Screws

The classification of bone screws actually varies depending on the geometry of the bones. Among these different screw types, there are four main, unchanging sections including head, shaft, thread, and tip (see Figure 2.3).

The head: It functions as a hub for the screwdriver, and enables tightening of the screw by transmitting the applied torque. A secure and stable hold is an essential feature during insertion or removal of the screw, because sudden disengagement of screwdriver may result a trauma to surrounding tissue, and also may result stripping of the head.

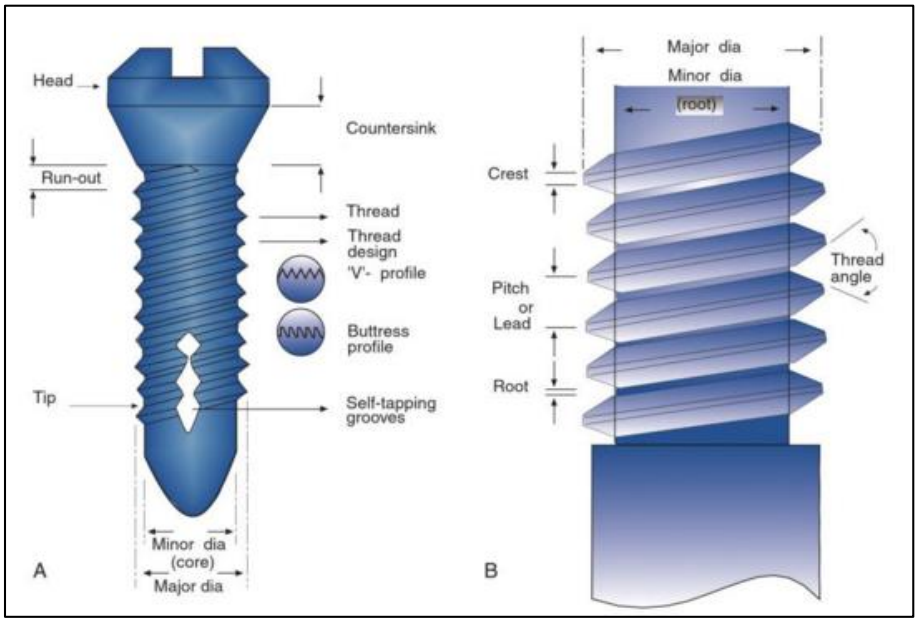

Figure 2.3 Representation of the bone screw details (left), and thread details (right) [62].

There are various drive types of heads with different areas of applications (Figure 2.4), and the common ones used in the bone screws are illustrated in Figure 2.5. In single slot head, only two point transfer the input torque and it can easily be stripped. Cross-head (cruciate) drives more powerful than single slot drives in terms of transmitting torque, but they prone to stripping when the screwdriver is misaligned.

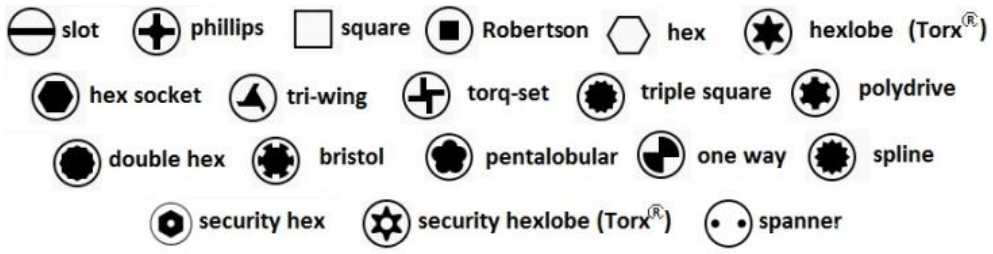

Figure 2.4 Symbolic representation and names of different screw heads from top view [63].

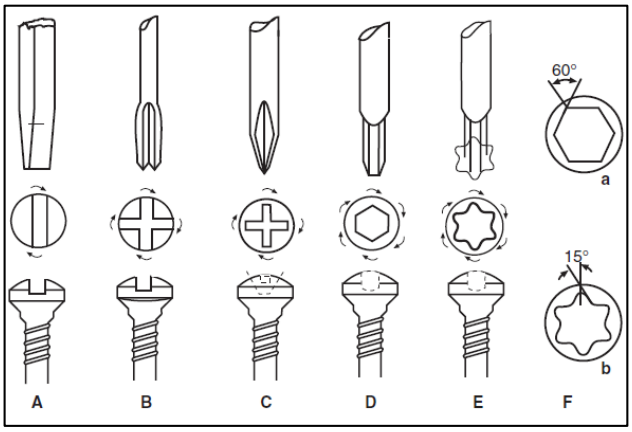

Figure 2.5 Common screw heads and driver tips of bone screws: Single slot (A), cruciate (B), Phillips (C), recessed hexagonal (D), Torx-6 Stardrive™ (E) [62].

The grip characteristics of Phillips head is better than cruciate head because of the recessed cross-slot. However, the same recess creates a dependence between axial thrust and torque transmission. In both of the cruciate and Phillips heads on the other hand, the input torque is transferred from four points. The recessed hexagonal head or hex head is most abundant type of screw head designs, and diminishes the alignment problems of the previous designs. It allows a stable insertion and the transferred torque does not dependent on the axial thrust applied. However, manufacturing of hex head requires creating close tolerance fit, otherwise stripping of the head or driver may occur. Similarly, worn driver bits may also result stripping of the head. Since the flat surfaces of the driver and head are oriented tangentially to the applied torque (Figure 2.5 F-a), excessive amounts of torque can also strip the flats of drive or driver depending on their material properties. To overcome this problem, flats should be aligned at an angle so that they do not become tangential to the applied torque, similar to the hexalobe heads as shown in the Figure 2.5 F-b.

The undersurface of the head of bone screws may also vary depending on the application; and they can be either tapered (conical) or hemispherical. By changing undersurface types of the bone screws various features can be obtained. For example, non-threaded hemispherical surfaces can give bone screws an angular modularity

within a proper hole of bone plate. Likewise, bone screws with threaded and tapered head, which are generally using with locking compression plates, can secure the screw in the plate hole against pull-out and inclination.

The shaft: The shaft is the unthreaded section between the head and the thread. The length of shaft can vary among bone screws. “Fully threaded” of “partially threaded” specifications generally indicates the existence of the shaft on the bone screw.

The thread: It can be defined as a long inclined plane surrounding the shaft or core. The diameter of the core, i.e. root diameter, defines the minimum cross-sectional area of the screw and defines the torsional strength of the screw. Pitch is the distance between the neighboring threads. Pitch and root diameter determines the volume of bone between the threads together with the outer diameter, thus fine threaded screws with small pitch are generally used for the stronger bone, i.e. cortical bone or cortex, and coarse threaded screws with large pitch are used for the weak bones like cancellous bone. Common thread profiles of bone screws, on the other hand, V-type and buttress profiles. The V-type profile generates both compression and shear on the contacting surfaces of bone and thread, however buttress profile mainly produces compression. Since shear forces are likely to result resorption of bone, it is suggested to use buttress threads to avoid loosening for long-term applications of bone screws [62].

The tip: Five main screw tips of the bone screws are illustrated in Figure 2.6. Self-tapping tip opens threads in the bone while advancing, and requires no pre-tapping.

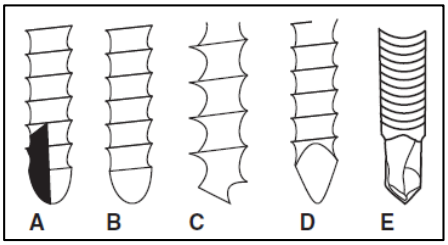

Figure 2.6 Different types of bone screw tips: Blunt and self-tapping (A), blunt and non-self-tapping (B), Corkscrew and cancellous (C), trocar (D), self-drilling and self-tapping (E) [62].

Non-self-tapping screws require pre-tapping, and their rounded tips serve as a guide. Before using non-self-tapping screw, the threads must be cut in the pilot hole. These screws have greater pull out resistance than self-tapping ones, because there may still be bone fragments between the threads of self-tapping screw after inserting, and they lower the pull-out strength of the screw. To remove these fragments, a corkscrew tip can be used; because it clears pre-drilled hole.

2.4.2. Types of Bone Screws

Depending on the application area, the bone screws can mainly be classified as cortical and cancellous. Similarly, they can be grouped as self-tapping, non-self-tapping or self-drilling based on their tip type. According to angular modularity of the screw which is generally created by different head designs, they can be classified as mono-axial, multi-axial or poly-axial bone screws. ASTM F543 specification, on the other hand, classifies bone screws as Type HA, HB, HC and HD [64]. This classification includes bone screws with a solid head and solid core. Type HA refers a bone screw with a shallow, asymmetrical buttress thread with deep screw head, and spherical undersurface of head. Different than type HA, type HB screws are designated with a deep, asymmetrical buttress thread, and a shallow screw head. Type HC refers a symmetrical V-thread with a conical undersurface of head. Finally, Type HD has asymmetrical V-thread different than the Type HC. All four types are presented in Figure 2.7 and 2.8.

2.4.3. Removal of Bone Screws

A removal of bone screw may be necessary in different situations either during or after surgery. The main reason may be the healing of the fracture. In that case, for example, a self-tapping screw is more difficult to remove than non-self-tapping one because bone may develop into the cutting tip of the screw and prevent the rotation.

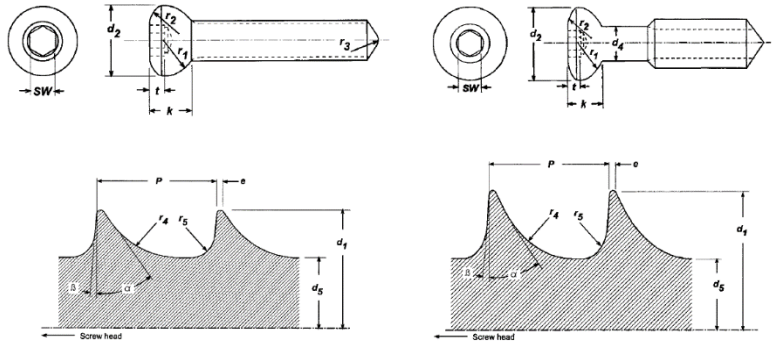

Figure 2.7 Schematic representation of screw types and threads: Type HA (left), Type HB (right) [64].

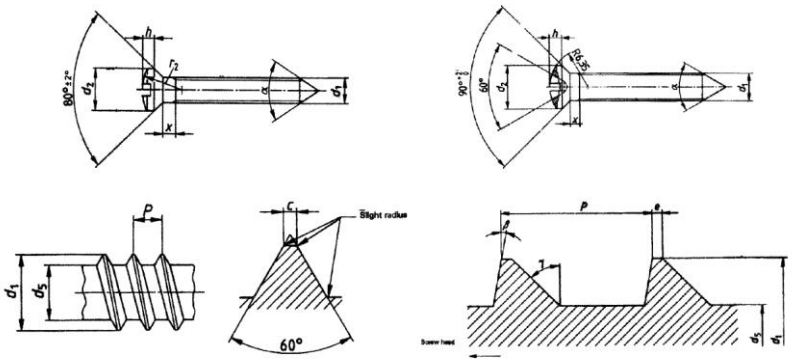

Figure 2.8 Schematic representation of screw types and threads: Type HC (left), Type HD (right) [64].

To handle this situation, it is recommended to tighten one turn to break the bone grow into the tip, and then remove it by rotating screw driver counter-clockwise [62].

In the cases of stripping, different solutions may be used to remove bone screws. In the surgical environment, gauze or foil can be placed between the tip of driver and the head for minimally stripped heads. When the head is totally stripped, conical extractors with left handed threads can be used. The application of these extractors as follows: First a suitable size is selected and it is inserted into the screw head. After purchasing the extractor tip, counter-clockwise turning in line with the screw centerline will result extraction at the same time [65].

In some cases, the distal tip of the screw can be broken. If removal is required in such cases different methods can be followed: The broken tip can be driven out from far cortex by applying some impact and rotating with screwdriver. Vise-grip pliers, and hollow reamers can also be utilized to remove broken screws. For cannulated broken screws, counter-clockwise threaded extraction screws or spade-tipped wires can also be used [62]. All these options are simply illustrated in Figure 2.9.

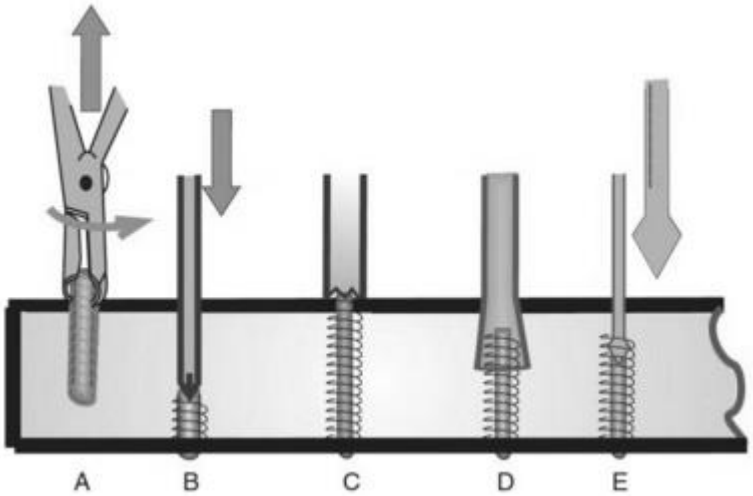

Figure 2.9 Removal options for broken screws (A: Vise-grip pliers, B: Driving-out by screwdriver, C: Hollow reamer, D: Reverse-threaded extractor, E: Spade-tipped wire) [62].

CHAPTER 3

MATERIALS AND METHODS

3.1. Introduction

The borders of design process of an internal fixation device is drawn by different factors from the fields of engineering, biology, medicine and especially orthopaedic surgeons. Besides biocompatibility – the most crucial requirement of all implantable medical devices – the following factors affect the design process: Structural and functional requirements, anatomy of location, surgical methods, material selection, production and processing methods, sterilization and approvals from authorities. The mechanical part of this design process, which is within the scope of this study, primarily depends on the structural and functional requirements of the target fracture.

The current plate-screw systems used in internal fixation force surgeons to send screws through fixed holes of the plate. As a consequence of this, the holes over the fracture lines cannot be used, or there may be no holes over the suitable locations for screwing. However, the proposed system of the project[1], contains rods, screws, cylindrical connectors with multi-axial screw holes and permits independent positioning of the screws from the rod. In this chapter, the mechanical design process[2] of this novel system will be clarified and the contribution of this thesis study to this design process will be explained in detail.

[1] The "*Project"* is the overall design process of the novel fixation system conducted by the GATA under the supervision of the TÜBİTAK. Please refer to the "Acknowledments" for the details.
[2] The "*Mechanical design process"* is a work package of the "*Project"*.

3.2. Mechanical Design of the System

The objective of the project is to design an orthopaedic internal fixator that is fully anatomic, minimizing periosteum damage, allowing multi-axial screws and multi-planar application for surgical applications. The project has been emerged based on the experiences of the orthopaedic surgeons on the currently available systems, and aims to combine all the advantages of the current fixator sets into a single system excluding the weaknesses. Contributions of this thesis to the mechanical design process of such an implant are in the form of literature survey, development and verification of the models, and testing of the prototypes. The outline of the project and the mechanical design process (the first four stages represented with solid-lined bubbles) are illustrated in the Figure 3.1.

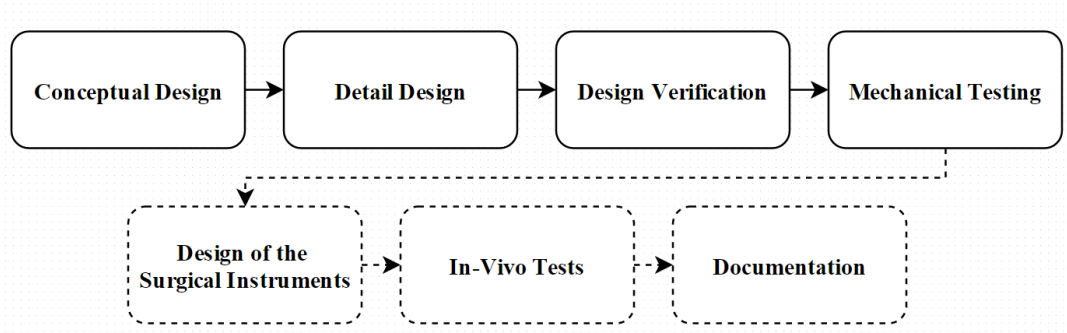

Figure 3.1 The outline of the project.

At the first stage of the design process, the most suitable concept which is inspired from the spinal implants has been selected for the desired fixation system. Instead of the practice of conventional locking plates, the idea of using rod-connector-screw trio as the main parts of the implant system is considered as a solution that can meet the objectives of the project. Four different models of this idea (or the best concept) have been developed consecutively as a result of frequent design verifications throughout the design process. Some features such as two-part connector, use of set screws for clamping, and spherical head of the bone screw were abandoned at some stage in the

development by using different verification methods including demonstrations either in actual or computer environment, inspection of the model prototype in terms of physical properties and ease of application by the surgeons, and mechanical analysis. Different models of the best concept have been generated and modelled in the computer environment using computer-aided design (CAD) programs in the detailed design, together with the evaluation of their geometrical and mechanical properties, and the optimization by reducing the volume of models without restraining the quality of their parts. Based on the evaluation, the models have been compared according to the mechanical design requirements. In the verification stage, the selected type of the best concept has been investigated with analytical methods, and the results of analytical approaches have been compared with the results of the mechanical tests conducted on the prototypes.

3.2.1. Preliminary Models

The rod-connector-screw concept refers an implant assembly, in which a cylindrical-shaped element or *rod* acts as an anchorage and combines the anchor points or *bone screws* through the linking elements or *connectors* (Figure 3.2).

Figure 3.2 An example of rod-connector-screw model in spinal surgery [47].

Actually, this concept is not new for spinal surgery, but the novelty appears in its application of trauma surgery: Since the connectors and rod do not contact the outer surface of the bone in such a system, the periosteum damage will be minimized. The

connector and rod also form a cylindrical joint and it will give multi-planar application option to the system and to the surgeon. In addition, with the different screw head forms, the multi or poly-axial use can be established. Considering the aims of the desired system and limitations of the new application area, the design have been updated four times, and four preliminary models developed as a result. Working prototypes of some revisions have been produced from relatively low-priced material (i.e. using tool steel instead of titanium alloy) to inspect the geometry of the design. The most critical parts of each model have been assessed analytically, and all revisions have resulted a final model.

Geometry of the Preliminary Models

The first CAD model of the rod-connector-screw concept comprised of seven parts, namely two socket set screws, two countersunk connector screws, one poly-axial bone screw, and a two-part connector mounted on the rod. The assembly of model #1 together with the bounding box of the connector is shown in the Figure 3.3. The dimensions of the bounding box gives insight about thickness and volume of the implant, and it has a 1 mm clearance from the extreme surfaces of the connector.

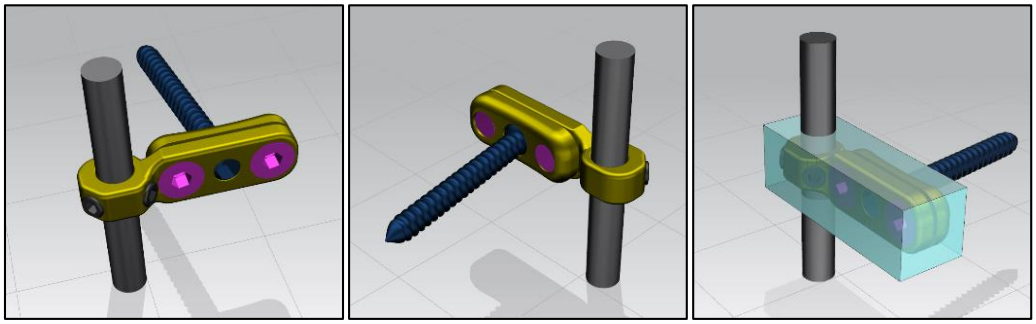

Figure 3.3 Geometry of model #1 from different views (left and middle) and bounding box of the connector (right).

For the model #1, the thickness of bounding box parallel to centerline of the rod is 12 mm and it is assumed as “height” for the sake of consistency. The “width” of this box is the thickness parallel to centerline of the connector screws (magenta-colored screws in Figure 3.3) and it is 12.4 mm. Finally, the “length” of the box is 37.5 mm; and for the remaining preliminary models the dimensions of their bounding box will be given in “*width x length x height*” format. For example, bounding box of model #1 has dimensions of (12.4 mm. x 37.5 mm. x 12 mm).

The first version of the second model contains six main parts, including two socket set screws, one connector screw, one poly-axial bone screw, rod, and connector. Different than the first model, connector of this model is single piece, and its connector screw clamps connector to the rod rather than fixing the poly-axial bone screw. Instead, two socket set screws are used for fixing the spherical head of bone screw in desired position (Figure 3.4).

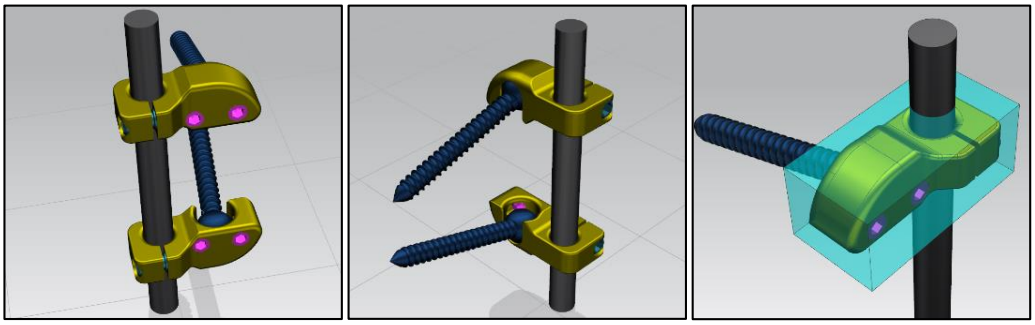

Figure 3.4 Geometry of model #2 (1st version) from different views (left and middle) and bounding box of the connector (right).

To decrease the width of connector, the orientation of connector screw (cyan-colored screw in Figure 3.4) is changed from orthogonal to parallel regarding to centerline of set screws (magenta-colored screws in Figure 3.4) in another version of model #2 (Figure 3.5).

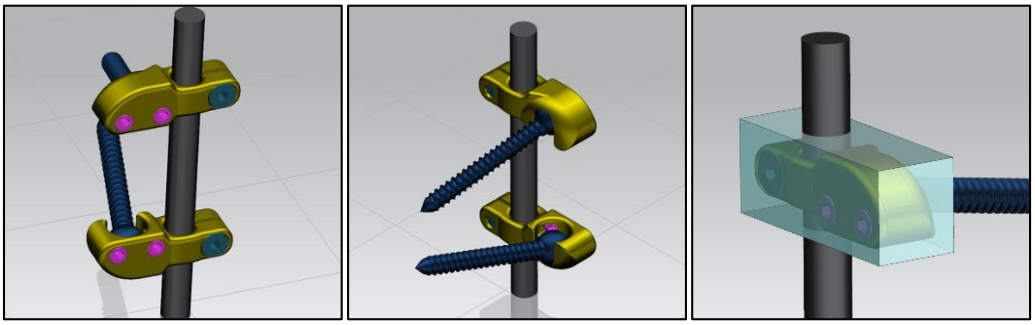

Figure 3.5 Geometry of model #2 (2nd version) from different views (left and middle) and bounding box of the connector (right).

Lastly, in the third version of model #2, two socket set screws are used to join connector to the rod as in model #1 (Figure 3.6). Usage of two set screws for locking the spherical head of poly-axial bone screw is common in three versions of second model. The difference of versions comes from the types of connector screws: Socket head cap, countersunk socket and socket set screws are used in the three versions of model #2 separately.

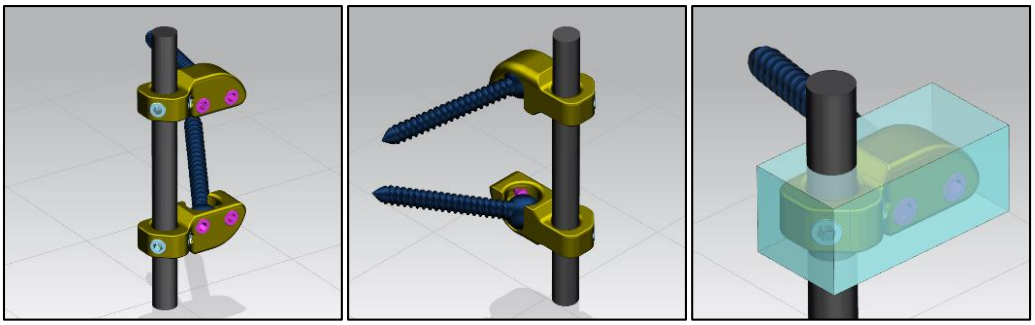

Figure 3.6 Geometry of model #2 (3rd version) from different views (left and middle) and bounding box of the connector (right).

The bounding boxes of these three versions differ in both length and width: The width of the first version (28.2 mm x 14.3 mm x 12 mm) decreased in the second (30.6 mm x 11.0 mm x 12 mm) and the third (28.2 mm x 13.5 mm x 12 mm) version, but the length increase became inevitable for the second version. However, the volume of

the connector is minimum in the second version in which the countersunk socket screw used for clamping purpose.

The third CAD model of the best concept has two versions and they differ each other based on fixing the connector with the rod (Figure 3.7 and 3.8). Unlike the first model, the former version of model #3 use one socket set screw instead of two, and the latter version of the third model utilizes a countersunk socket screw similar to model #2 (2^{nd} version) for clamping of connector to the rod. In both versions of third model, two countersunk socket screws pull the lower part of the connector body and provide housing for a spherical head of poly axial bone screw.

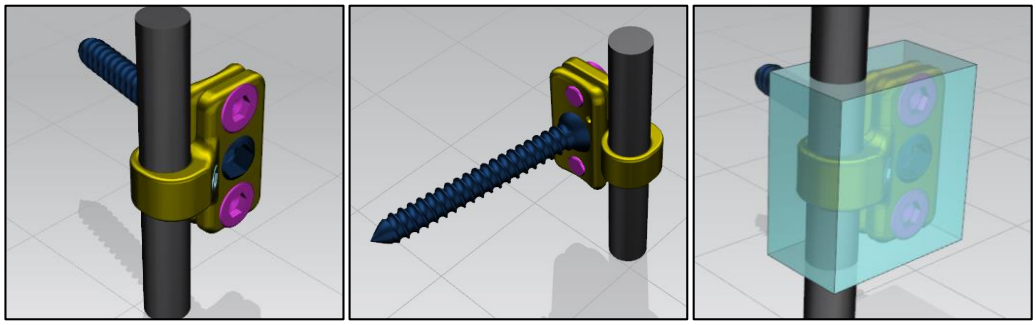

Figure 3.7 Geometry of model #3 (1^{st} version) from different views (left and middle) and bounding box of the connector (right).

The change of the clamping method resulted an increment in the connector volume in the latter version of model #3, and this increase is mainly originated from the change in the length as expected. The dimensions of the first and second version of model #3 are (20.2 mm x 11.35 mm x 22 mm) and (28.3 mm x 10.9 mm x 22 mm) respectively. As seen in Figure 3.8, the second version of model #3 consists of three countersunk socket screws. One of them is used for clamping (cyan colored), and the remaining (magenta colored) are used for locking of poly-axial screw in its spherical housing similar to previous models. In addition to dimensions of bounding boxes, the geometric properties of these connector screws are presented in Table 3.1 to have a better idea about their sizes.

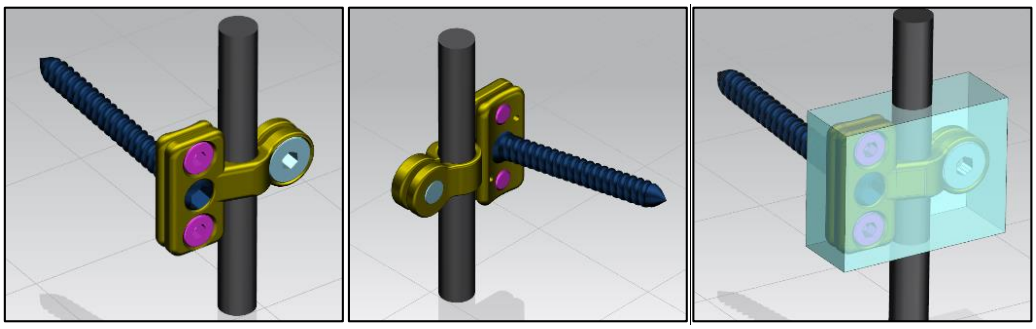

Figure 3.8 Geometry of model #3 (2nd version) from different views (left and middle) and bounding box of the connector (right).

Table 3.1 Geometric Properties of connector screws used in model #3 (2nd version).

Parameters	**Connector Screw** (For clamping the rod)	**Connector Screw** (For fixing the poly-axial screw)
Nominal Diameter [mm]	5	3
Total Length [mm]	5.5	4.75
Threaded Length [mm]	3	2.25
Length of Conical Head [mm]	2.5	1.25
Taper Angle of the Head [deg]	60	75

The final preliminary design (model #4) has only one difference from the first type of model #3, and that is the use of engaging bone screw (Figure 3.9). A poly-axial screw (green colored) can be screwed in another screw (blue colored) that has a suitable threaded hole for this poly-axial screw. By this way, the blue colored screw, which has a socket hexagonal head similar to set screws, can be inserted initially, then the position of the poly-axial screw (green colored) can be arranged by the surgeon. The micro-motion occurred as a result of engagement tolerance of blue and green screws is thought as advantageous for fracture healing according to strain theory of Perren [14]. However, self-locking requirement of inner screw may limit the use of large tolerances (in micrometer scale), and should be considered for similar applications.

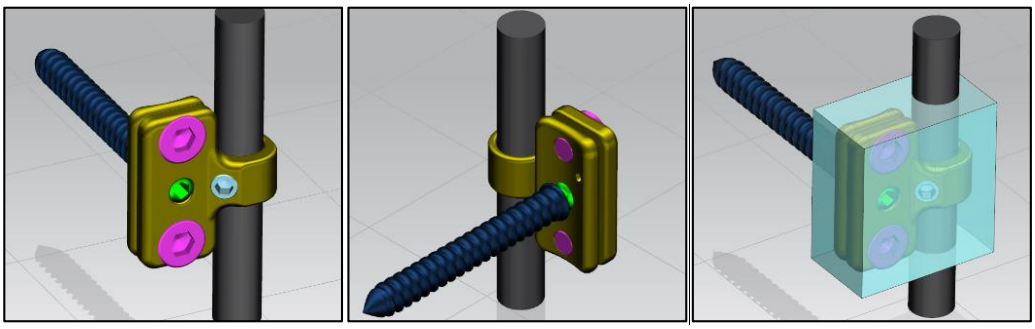

Figure 3.9 Geometry of model #4 from different views (left and middle) and bounding box of the connector (right).

Evaluation of the Preliminary Models

For the models 1, 2.3, 3.1, and 4, compressive force created on the rod by the tip of set screw as a result of tightening must prevent rotation and translation of the cylindrical joint formed by the rod and connector under critical forces. The holding force generated by the set screw against rotation and translation of the rod primarily depends on the compression of the set screw tip, unlike cap screws. As a result of tightening of the set screw, the contact area between the tip of the set screw and the rod creates frictional resistance. In addition, the compression force generated by the set screw results in frictional resistance on contacting surfaces of the rod and the connector.

In general, the tips of the set screws vary for different holding force requirements identified in specific applications. Figure 3.10 shows various types of set screws in terms of their tip geometry. It is recommended that the length of the set screw should be at least half of the diameter of the rod or shaft on which the set screw is used [48]. In this case, the set screws of the models 1, 2.3, 3.1, and 4 should have minimum 3 mm length, since the rod diameter is 6 mm. The current geometry of the set screws are given in Table 3.2. This recommendation also gives the minimum radial thickness of the connector around the rod, and therefore the design of model #1 is modified according to this recommendation by increasing the set screw length to 4.2 mm.

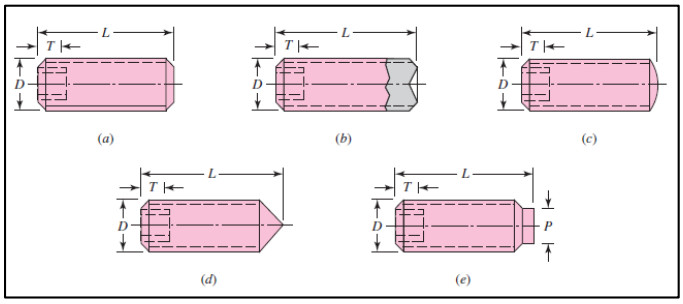

Figure 3.10 Types of the set screws according to their tip geometry: a. Flat point, b. Cup point, c. Oval point, d. Cone Point, e. Half-dog point [48].

Table 3.2 Dimensions of set screws used in preliminary models.

Parameters	Model 1	Model 2.3	Model 3.1	Model 4
Diameter, D [mm]	4	4	4	4
Total length, L [mm]	2.5	4.2	4.2	4.2
Socket depth, T [mm]	2	2	2	2
Tip type	Flat Point	Flat Point	Flat Point	Flat Point
Quantity	2	2	1	1

(Note: The geometrical symbols of the Figure 3.10 is used.)

In the literature, no empirical data relating the thread size and tightening torque of set screw to the axial and torsional holding capacity has been found for titanium grade-5 (Ti 6Al 4V alloy) set screw and rod. Since the holding force is directly proportional to coefficient of friction (CoF) between rod and screw materials, the data for steel set screws with flat point tip are used for calculations. Table 3.3, shows the typical empirical results of axial and torsional holding capacity of socket set screws seated against steel shaft.

According to Table 3.3, 1700 N axial holding capacity can be obtained by M4 steel set screw with 2.20 N.m seating torque. For 6 mm diameter rod, same set screw can create 5.1 N.m torsional holding capacity. However, safety factors of 1.5 – 2 and 4 – 8 are recommended for static and dynamic loading conditions correspondingly by Unbrako [49].

Table 3.3 Torsional and axial holding capacity of socket set screws [49, pp.38]

Thread Size	Seating Torque [N.m]	Axial Holding Capacity [kN]	Torsional Holding Capacity [Nm]		
			Shaft Diameter [mm]		
			2.0	***3.0***	***6.0***
M 1.6	0.10	0.22	0.22	0.33	0.66
M 2.0	0.21	0.29	0.29	0.44	0.87
M 3.0	0.87	0.71	0.71	1.07	2.10
M 4.0	2.20	1.70	1.70	2.60	5.10

(Note: Table shows typical values for alloy steel socket set screws with minimum hardness of Rc 45 and shaft hardness between Rc 15 to Rc 35)

Using sliding coefficient of frictions between steel-steel and titanium-titanium as 0.6 and 0.3 respectively [50], [51] and assuming that the axial and torsional holding capacities are directly proportional with CoF; the holding capacities (axial and torsional) of single socket set screw is valued as 850 N and 2.55 N.m without using a safety factor. Using the highest safety factor, 8, the axial and torsional holding capacities become 106 N and 0.32 N.m respectively. Therefore, these four models with socket set screws (Models 1, 2.3, 3.1 and 4) are considered as incapable against dynamic loads of lower extremity applications for a 700 N weighted-adult. Additionally, the set screw application may result wear and the response of the immune system to micro-particles become problematic in the post-operative stages. For these major reasons, these preliminary (conceptual) designs have been eliminated.

In the remaining three models (2.1, 2.2, and 3.2), countersunk head socket screws secure connector to the rod, however, two of these models (2.1 and 2.2) still utilize set screws for fixing the spherical head of bone screw in its housing. The head of the bone screw has 10 mm diameter, and the geometry of set screws are the same as the ones in model 2.3. In the literature, any empirical data are found for fixing the spherical joint with set screws as expected, and therefore prototypes of selected models are produced from aluminum and tool steel for inspection (Figure 3.11). Since the locking of the spherical head is not form closed, rotation of the bone screw around x-axis could not be restrained successfully by the set screw. In addition, it has been

observed that the bone screw can easily be dislocated from its position by hand-force, even if the set screw is seated. Hence, either for clamping or positioning, the application of set screws are quitted.

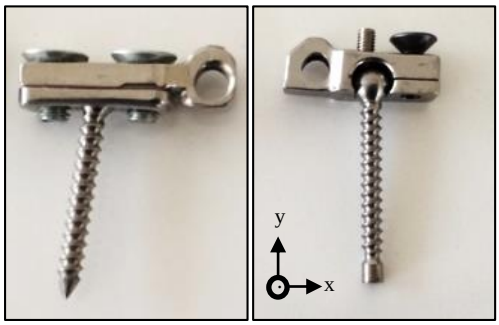

Figure 3.11 Prototypes of the preliminary models #1 (left) and model #2.3 (right).

The remaining preliminary model (#3.2), must restrain spherical head of the bone screw from rotation in its housing by two countersunk screws. In similar manner, the other countersunk screw must create adequate clamping force to maintain rod inside the connector without and rotation or displacement under the critical loads. To assess the holding capacities of these structures, a prototype of the previous model (#3.1) was reviewed firstly (Figure 3.12).

Figure 3.12 Prototype of the preliminary model #3.1.

The medical doctors of the project found two-part-connector design impractical, because the lower part of the connector must remain under the spherical head while

inserting the bone screw. Additionally, two countersunk connector screws that connect the upper and lower parts of the connector were found too small for surgical environment. Therefore, from application point of view, the model #3.2 is also eliminated; and a final model is formed considering the useful and abandoned features of preliminary designs. To sum up, use of two part-connector, set-screws, spherical bone screw head are abandoned and clamping single-part connector with a screw is considered as useful. The production of inner and outer threads of the bone screw in Model 4 is also found problematic, especially when nominal diameter of outer threads of bone screw has small values (i.e. the nominal diameters of current bone screws are around 2 – 5 mm).

3.2.2. Final Model

The radial thickness of the implant according to bone radius is the most significant design criterion that effects the overall geometry of the design. The contemporary and relevant implants (i.e. humeral and femoral bone plates, spinal rod sets) offer various thicknesses from 1.5 mm to 6.5 mm, and this variation is mainly due to the application area: Different plates are designed for different parts of the long bones such as proximal, distal and metaphyseal parts, and these designs are only applicable for intended area. Moreover, the geometries of these plates are based on the average bone shape (or geometry) that is obtained from medical images of a limited number of patients. Since the geometry of bones differ among different populations, the products of both international and domestic manufacturers should be assessed. For this purpose, the catalogs of two domestic firms (Hipokrat and TST) and one international firm (DePuy-Synthes) have been examined and different plate thicknesses have found as follows [52], [53], [55]:

- *Proximal humerus plates*: Hipokrat (3.0 mm), TST (3.9 mm), Synthes (3.7 mm)
- *Distal humerus plates*: Hipokrat (3.0 mm), TST (3.5 mm), Synthes (2.5 mm)
- *Epicondylar plates*: Hipokrat (1.5 mm), TST (4.0 mm, for lateral epicondyle)

- *Metaphyseal humerus plates*: TST (4.0 mm – 2.2 mm), Synthes (3.3 mm)
- *Diaphyseal plates (Narrow)*: Hipokrat (3 – 4 mm), Synthes (4.2 mm)
- *Diaphyseal plates (Broad)*: Hipokrat (5 mm), Synthes (4.2 – 5.2 mm)
- *Proximal and distal femur plates*: Hipokrat (6.0 mm), TST (6.5 mm – 5.0 mm)

The minimum radial thickness of the preliminary models (i.e. widths) was obtained in model #3.2 and it was 8.9 mm (after subtracting 2 mm clearance from width of its bounding box, 10.9 mm). The available rod-connector-screw systems used in spinal surgery generally have 5 mm or 6 mm diameter rods [52], [54]. Considering all these facts, the rod-connector-screw concept for trauma surgery is modelled to its final form.

The final model consisted of four parts including rod, connector, countersunk socket connector screw and bone screw (Figure 3.13). Initially, the rod diameter is selected as 5 mm considering the existing implants of spinal surgery. The reason is as follows: The spinal rod-connector systems are mainly designed for the loading conditions of upper body, and especially of the spine. Therefore, using 5 mm diameter rod for humeral shaft fractures is considered as safe, in which the natural loads during the healing of such fractures is less than the spinal fractures, particularly thoracic and lumbar spine applications [56].

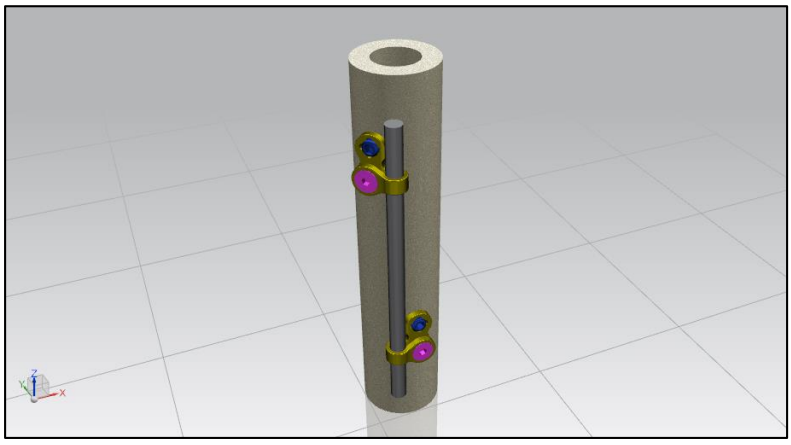

Figure 3.13 Final model applied on a symbolic diaphysis of a long bone.

The selection of rod diameter is actually defined the outer diameter of the cylindrical form of the connector in which rod is passing through, and that is 7.5 mm. The maximum thickness *t* of the connector is the same of this value, 7.5 mm. The maximum length *l* of the connector is 16 mm and the maximum width *w* is 15 mm (Figure 3.14).

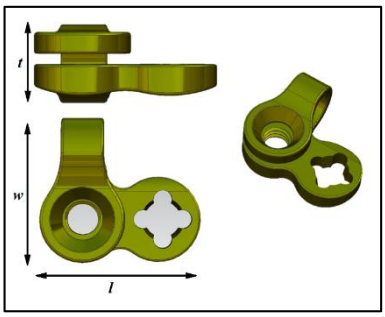

Figure 3.14 Front (upper left), top (lower left), and trimetric (right) views of connector and basic dimensions.

The bone screw is a self-tapping locking cortical screw; its overall length, *L*, is 28 mm and nominal diameter of threads is 3.5 mm (Figure 3.15). The head has 4.5 mm length and 10° taper angle, and 3 mm of this length is also threaded.

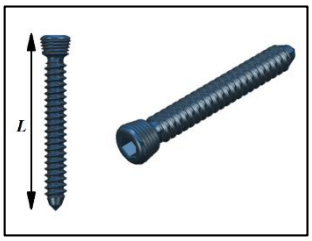

Figure 3.15 Front (left) and trimetric (right) views of self-tapping cortical bone screw.

The connector screw has 4 mm nominal diameter with 2.8 mm threaded length and 5.8 mm total length. Taper angle of the head is 35° from the centerline of the screw. The Figure 3.16 shows the front view (left) and trimetric view (right) of the connector

screw. Additionally, assembly of the connector with both two screws are shown in Figure 3.17. Technical drawings of each element are given in the Appendix C.

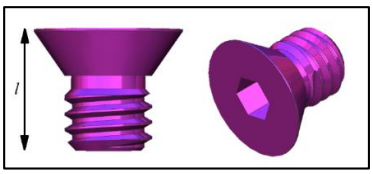

Figure 3.16 Countersunk head, hex socket connector screw.

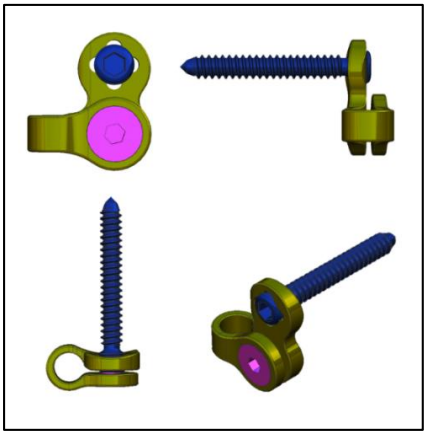

Figure 3.17 Different views of final version of the proposed system (upper-left: top view, upper-right: left view, below -left: front view, below-right: trimetric view).

When an admissible tightening torque is applied to the connector screw, the threads advance inside the threaded hole of the connector. The threads inside the connector hole and on the screw engage with each other and the tapered head of the screw settles into countersunk hole of the connector. The conical surfaces of the connector screw head and the connector connects and a tensile force arises on the screw. As a result of advancing of the connector screw during tightening, the gap in which the connector screw passes through narrows down and finally closes. By this way, the connector clamps the rod and a force closed connection occurs between rod and connector. After

defining and fixing the location of connector on the rod, the bone screw can be tightened to its place.

To analyze and verify this final model, these steps will be followed in the following sections: Based on the briefly introduced elements which are constituting the assembly of the final model, the important geometric parameters and relations will be defined. The force and stress diagrams will be drawn and finally analytic equations will be derived for holding capacity of the final model, depending on the parameters and relations. The reason *why the holding capacity is analyzed first* is as follows: The final model has three main connections (i.e. between bone screw and connector, connector and its screw, and connector and rod), two of them include screws and are form closed connections, and the remaining is a force closed connection. Rather than form closed connections, the friction force between the contacting surfaces of force closed connection primarily defines the axial and rotational stability of the system; because the strength of the asperities on the surfaces of force closed connection is considered lower than the interlocked teeth form connection. Therefore, it is assumed that the most critical feature of the system under any loading condition applied to the bone screw is the axial and rotational stability of the connector (Figure 3.18). After finding the holding capacity of the system, the connection of bone screw (connection 2 in Figure 3.18) will be analyzed. The results of the both analyses will be compared with the corresponding mechanical test results separately, then they will be assessed with each other.

3.2.3. A Novel Concept: Screw within Screw

From medical application point of view, doctors found the final model appropriate, but they underlined the requirement of tightening two separate screws for a single bone screw application as time consuming. Moreover, they emphasized that the connector screw should be delivered as mounted on the connector before the surgery due to its relatively small dimensions.

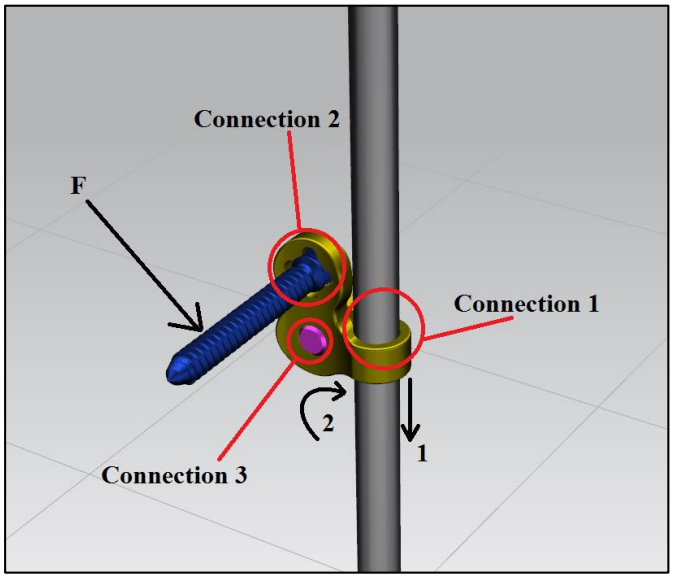

Figure 3.18 Locations of connections, symbolic movement directions (1: axial, 2: rotational) under a three dimensional force, F.

In addition, after assessing the prototype of the final model, a possibility of contact between the bone and connector was observed in the case where the threaded head of bone screw has not been placed correctly into its location. To solve these problems, a novel rod-connector-screw concept is introduced based on the final model (Figure 3.19).

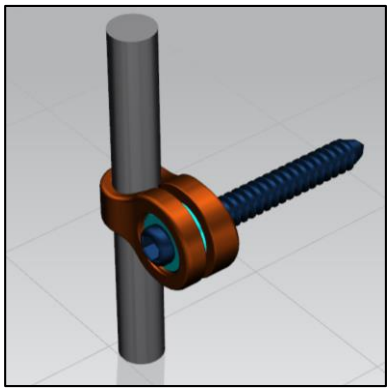

Figure 3.19 A novel concept: Bone screw passes through a threaded hole inside the connector screw.

Similar to the final concept, this new design has three elements excluding the rod. The head of the bone screw is cylindrical and not threaded unlike the previous bone screw design. The connector screw has a threaded hole opened through its centerline and the bone screw can be screwed into this hole. In other words, the bone screw and connector screw act like bolt and nut respectively. The connector screw has left handed threads, and is designed to be seated into bottom section of the connector which is closer to the bone. In this case, the tapered countersunk hole is placed this bottom section of the connector, and a matching left hand threaded hole is placed on the upper section of the connector. The band section of the connector is remained the same as the final model.

The tolerance of the inner threaded connection of the system (between bone screw and threaded hole of connector screw) is assumed finer than the outer left hand threaded connection (between connector screw and connector) so that while tightening the bone screw, the connector also screw rotates and creates a clamping force (see Figure 3.20 for thread details). By this method, a solution is introduced to previously mentioned points of the final design, but the multi-axial feature of bone screw is sacrificed.

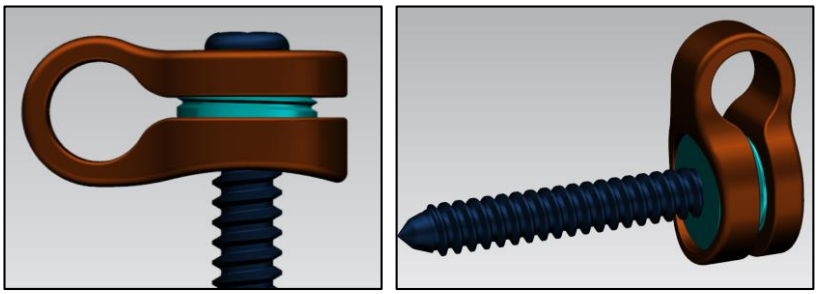

Figure 3.20 Different views of the screw within screw concept.

The prototypes of the novel system was manufactured in the machine shop of Mechanical Engineering Department of METU, however, left hand tapping wrench and guide were not available. To prove the concept, therefore, normal-right hand threaded connector screw is used as in the final model, and a threaded hole is opened

through its centerline of it. Tool steel is used as prototype material and the system is enlarged by a scale of 1:1.6. The features of the connector such as edge blends and chamfers are not processed (Figure 3.21).

Figure 3.21 Pictures of the prototype of screw within screw concept.

Since the prototype is not titanium and it does not represent all the features of the CAD model, no experiments are conducted on the prototype. To assess the performance of the screw within screw model, the theoretical method introduced for the final model in Section 3.3 will be used. Finally, the analytical results of the novel concept will be compared both with analytical and experimental results of the final concept.

3.3. Theoretical Analysis of Holding Capacity of Final Model

In this section, two different theoretical approaches are introduced for finding the holding capacity of the connector and screw arrangement of the final model, introducing the necessary engineering approximations. Before proceeding to these

approaches, important geometric parameters are represented on the cross-section of the connector and its screw which are shown at their initial positions (Figure 3.22). Threaded and interlocked sections of the connector and the screw are denoted as red regions and the threads are shown symbolically. In both approaches, all components are assumed to be rigid and the holding capacity of the connector is obtained by utilizing the theory of band brakes to the section of the connector that is wrapping the rod. Specifically, the working principle of the single-screw, flat section band clamps is applied to the mentioned wrapping section of the connector, and necessary calculations are completed by using principles of band brakes. An example of the flat section band clamps and the working principles of them are shown in the Figure 3.23.

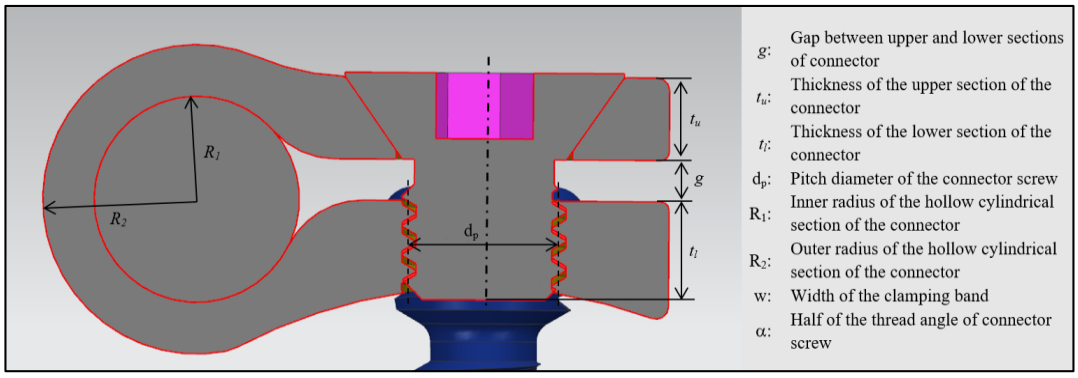

Figure 3.22 The representation of important geometric parameters on the cross-section of the implant.

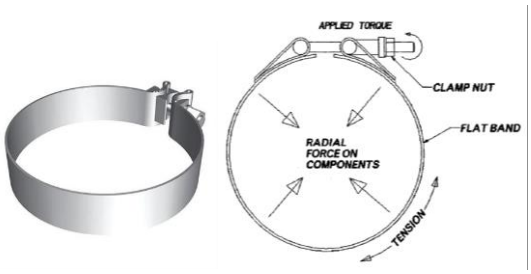

Figure 3.23 An example of a flat band clamp (left) [57], and working principle of a single-screw band clamp [58].

The difference of the approaches comes from the ways of estimation of the clamping force, F. In the first method, the clamping force or the hoop tension, F, is assumed to be equal to the tension in the connector screw, similar to the clamping bolt of the band clamp applications (Figure 3.24). In the second approach, the gap, *g*, between the upper and lower section of the connector is assumed to be only closed as a result of the deflection of the upper section, because the threaded connection between the connector screw and the lower section is fixed, and the screw is rigid. Therefore, the upper section is modelled as a cantilever beam; its deflection is assumed to be equal to the decrease in the gap distance, and the force acting on the centerline of the connector screw, which is causing that deflection, is assumed as clamping force, F. However, in this assumption, the clamping force is only applied to the upper section of the band due to the "fixed" assumption of the lower section of the connector (Figure 3.25).

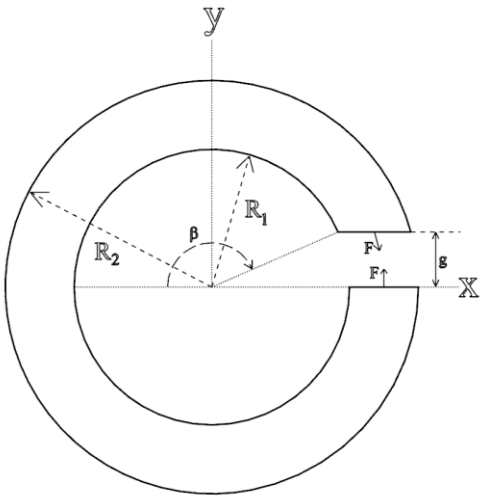

Figure 3.24 The representation of the first approach

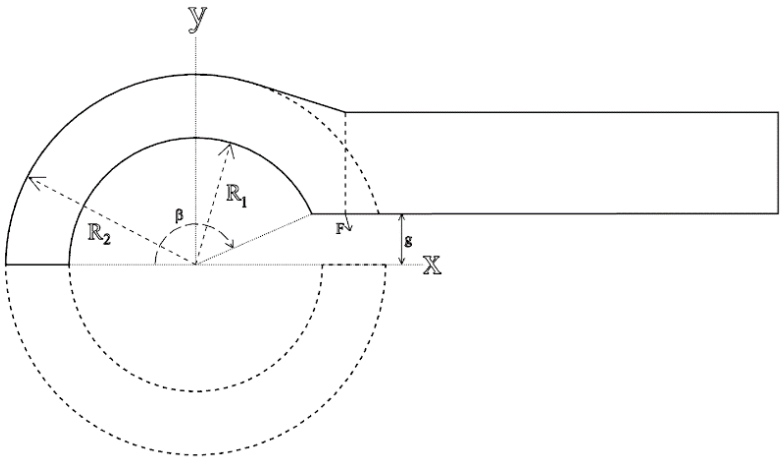

Figure 3.25 The representation of the second approach.

After making the analogy between the clamping section of the connector and the band clamps, an infinitesimal segment of the band section of the connector is considered with an angle dθ and outer length of $R_2 d\theta$ to obtain the normal pressure distribution inside the element in terms of the hoop stress or circumferential stress, σ_θ, (Figure 3.26).

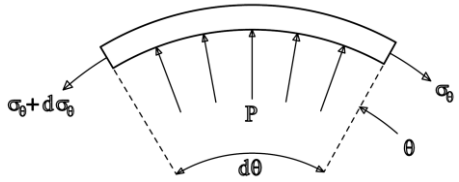

Figure 3.26 Representation of the hoop stress and normal pressure on the infinitesimal band element.

Equating the forces in radial direction

$$PwR_2 d\theta - \sigma_\theta wt \sin(d\theta/2) - (\sigma_\theta + d\sigma_\theta)\, wt \sin(d\theta/2) = 0 \qquad \text{(Eq. 1)}$$

where w is the width of the band. For small angles sin (dθ / 2) is equal to dθ / 2, and the terms dθ / 2, and $d\sigma_\theta$ can be neglected, because of being second order of a small

quantity compared to other terms in Eq 1. These simplifications yield the pressure distribution in terms of the hoop stress as

$$P = \sigma_\theta t / R_2 \qquad \text{(Eq. 2)}$$

The clamping force applied to the end of the band produces an internal hoop tension, F_θ, a normal force dN, and a frictional force, dF_s, on the infinitesimal band element as shown in Figure 3.27. If the band element is in tension, the equilibrium of the forces in the circumferential direction gives

$$F_\theta + dF_\theta = F_\theta + dF_s \qquad \text{(Eq. 3)}$$

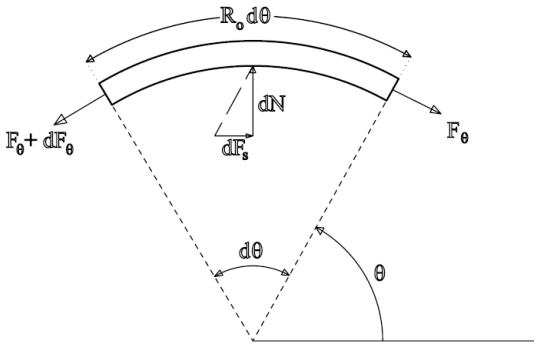

Figure 3.27 Representation of the forces on the infinitesimal band element.

The normal force, dN, is balanced with the normal surface pressure, P. The frictional force, dF_s, is the multiplication of the normal force with the friction coefficient, μ, between the contacting surfaces of rod and band. Hence,

$$dN = PwR_2\, d\theta \qquad \text{(Eq. 4)}$$

$$dF_s = \mu\, dN \qquad \text{(Eq. 5)}$$

Inserting above two equations (Eq. 4 and 5) into the equation of the force equilibrium in the circumferential direction (Eq. 3) gives

$$dF_\theta = dF_s = \mu P w R_2 \, d\theta \qquad \text{(Eq. 6)}$$

The tensile stress inside the band can be found by dividing the hoop tension by the area of the band

$$\sigma_\theta = F_\theta/(wt) \qquad \text{(Eq. 7)}$$

Then, substituting for pressure distribution, P, and the hoop stress, σ_θ, from Eq. 2 and Eq. 7 into Eq. 6 inside the band yields

$$dF_\theta = \mu F_\theta \, d\theta \qquad \text{(Eq. 8)}$$

The tension at any angle α inside the band can then be found by integrating the Eq. 8 over the limits of α to β (see Figures 3.24 and 3.25):

$$F_\beta \Big/ F_\alpha = e^{\mu(\beta-\alpha)} \qquad \text{(Eq. 9)}$$

In the band section of the connector, the angle β represents the limits in which the clamping force is applied. It is an angle lower than π radians for the upper half of the band, and similarly, it is equal to π radians for the lower half of the band (Figures 3.24 and 3.25). Then using the Eq. 9, Eq. 7, and Eq.2 respectively; the tension, the hoop stress, and the pressure distribution inside the band can be written as a function of band angle θ as follows:

$$F(\theta) = \frac{F_\beta}{e^{\mu(\beta-\theta)}} \qquad \text{(Eq. 10)}$$

$$\sigma(\theta) = \frac{F_\beta}{wt\, e^{\mu(\beta-\theta)}} \qquad \text{(Eq. 11)}$$

$$P(\theta) = \frac{F_\beta}{wR_2\, e^{\mu(\beta-\theta)}} \qquad \text{(Eq. 12)}$$

From Eq.12, the friction force, F_s, generated between the connecting surfaces of rod and connector can be found by integrating over the limits of the band section. Note that F_{s_u}, and F_{s_l} correspond to friction forces of the upper-half and lower-half of the band section of connector respectively in the following integrations:

$$F_{s\_u} = \int_0^\beta \mu\, P(\theta)\, wR_2\, d\theta$$

$$F_{s\_u} = \int_0^\beta \mu\, \frac{F_\beta}{e^{\mu(\beta-\theta)}}\, d\theta$$

$$F_{s\_u} = F_\beta\, \mu\left(1 - \frac{1}{e^{\mu\beta}}\right) \qquad \text{(Eq. 13)}$$

Similarly the friction generated on the lower half, and the total friction are

$$F_{s\_l} = F_\beta\, \mu\left(1 - \frac{1}{e^{\mu\pi}}\right) \qquad \text{(Eq. 14)}$$

$$F_s = F_{s\_u} + F_{s\_l} \qquad \text{(Eq. 15)}$$

By inserting Eq. 13 and Eq. 14 into Eq.15, the explicit form of the total friction force becomes

$$F_s = F_\beta\, \mu\left(2 - \frac{1+e^{\mu(\beta-\pi)}}{e^{\mu\beta}}\right) \qquad \text{(Eq. 16)}$$

To obtain the clamping force, F_β (or F as in the Figures 3.20 and 3.21), two different methods are used as mentioned previously. In the first method the input torque applied on the hexagonal socket of the connector is related to the clamping force, F, by utilizing the well-known equations of raising torque and load of the *power screws with angled tooth profile* [48].

$$T_i = F\frac{d_m}{2}\left(\frac{l+\pi\mu d_m \sec(\alpha)}{\pi d_m - \mu l \sec(\alpha)}\right) \qquad \text{(Eq. 17)}$$

Actually, the second approach is arisen from the observations of the prototype during tightening of the screw for locking the connector to the rod: Upper part of the connector elastically deformed under transverse load, F, which is created by the connector screw as illustrated in the Figure 3.28.

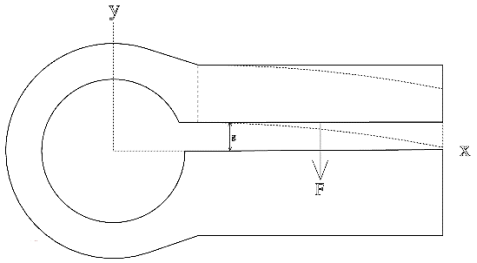

Figure 3.28 Representation of the elastic deformation in the second approach.

Therefore, a relation between decrease in the gap and the clamping force, F, is found based on the cantilever beam assumption as follows [48]:

$$\delta = Fa^2(3l - a)/6EI \qquad \text{(Eq. 18)}$$

Thus, by using Eq. 17, the clamping force can be found in terms of the applied torque on the connector screw. Then, using Eq. 16, the friction force on the band section can be obtained for different values of input torque, T_i. Similarly, by using Eq. 18, the clamping force, F, generated can be obtained when the gap is closed completely (i.e.

$\delta = g$). The friction force between the band surfaces then can be found by putting F, into Eq. 13 as F_β.

To summarize, the proposed analytical method is aimed to find the holding capacity (i.e. axial and torsional holding force) of the connector, clamped on the rod. Since the source of the holding force is the friction force between the connecting cylindrical surfaces of rod and connector, the starting point of the formulations was aimed to define this force in terms of the clamping force. After that, the clamping force have been obtained analytically in terms of two parameters of the system namely the input torque and the gap.

To find the accuracy of the theoretical analysis, mechanical experiments are conducted on the prototypes of the final model, and the results of both are compared. In addition, after validating the accuracy of the analytical method, the holding capacity of the screw-within-screw concept is calculated using the first theoretical approach.

3.4. Theoretical Analysis of the Bone Screw Connection

The bone screw connection is basically the connection existing between the connector and threaded and tapered head of the bone screw (see Figure 3.29).

Figure 3.29 Close up views of the bone screw head and the connector. (Note the four-leaf clover shaped hole of connector)

The threaded hole of the connector screw has a four-leaf clover shape and it is conical. The shape of the hole is same as the screw head, and its threads match those on the screw head. The four quadrants of the hole are removed axially to introduce the feature of multi-axial locking. In surgical environment, locking with plastic deformation and welding of these threads are expected, however the screw head can be aligned in a way that approximately 10° tilt angle can be given without any plastic deformation in both upside, downside, left and right directions (Figure 3.30). One disadvantage of tilting of the screw is the protrusion of the head of the screw. Another disadvantage is the decrease of number of engaged threads in one side of the connection.

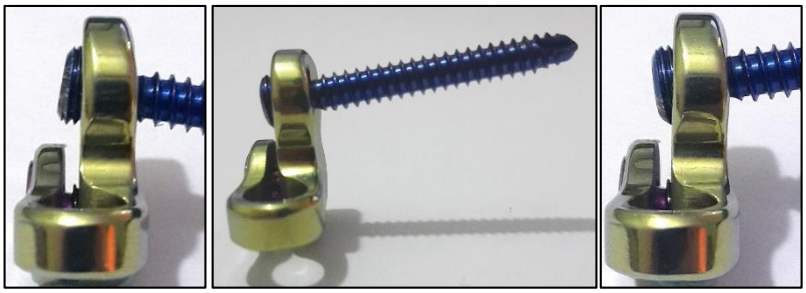

Figure 3.30 Protrusion of the screw head in angled placement (Left: Downside tilt, Right: Upside tilt) and picture of the connector and screw with 10° upside tilt angle.

To find out loading limits of the bone screw connection, two critical sections as shown in Figure 3.31 are investigated by theoretical methods, then their results are compared with experimental findings.

Firstly, the screw is assumed to be inserted horizontal, i.e. with no tilt, then two hypothetical distributed loads representing the reaction forces generated by the cortical bone are placed perpendicular to the bi-cortical bone screw's centerline (Figure 3.31). After, an equivalent force of these two distributed loads are assumed between the application areas of them. Finally, the mechanical limits of the critical locations are found in terms of this equivalent force.

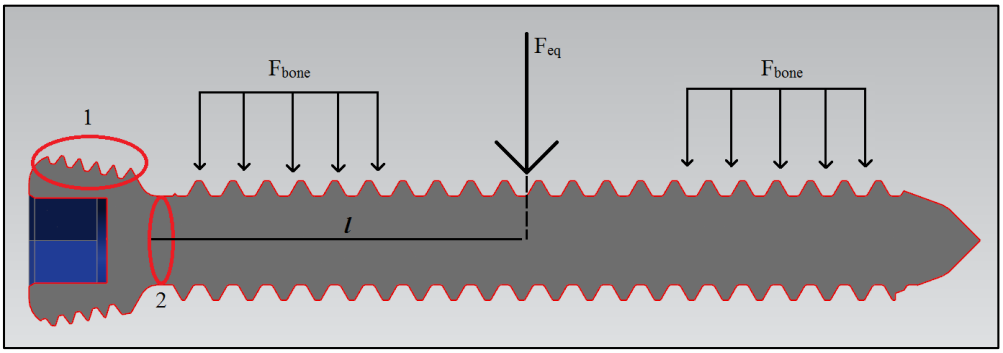

Figure 3.31 Critical locations and hypothetical representation of the forces acting on the bone screw.

Since the bone screw is axisymmetric, two dimensional stresses calculated on the critical locations by using and adapting formulas in [48].

The threads of head has a tooth profile angle of 27.5° different than the V-profiled threads of the bone screw. The taper angle of head is 10° (α in Figure 3.32). When taper head is placed into the connector hole without a tilt, the x and y components of normal force acting on threads of head, F_h, can be found by simply establishing a moment equilibrium with equivalent force F_{eq}. After, nominal thread stresses can be related to thread parameters of head by using standard formulations of normal screws. According to experiments as stated in [48], the first engaged thread takes 0.38 of the load, the second 0.25, the third 0.18, and the seventh is free of load, so that the formulations are based on the first thread of the location 1 in Figure 3.31. (Note: All six threads of the head engage on a horizontal, uninclined application.)

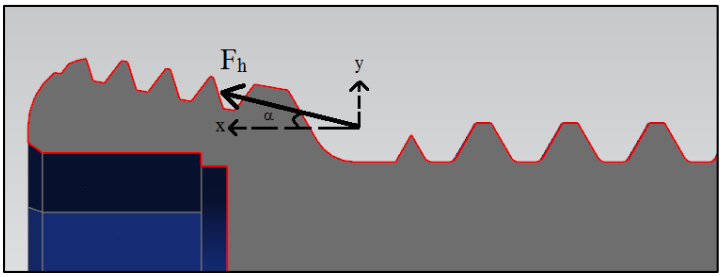

Figure 3.32 Representation of the force generated on the threads of screw head when F_{eq} is applied.

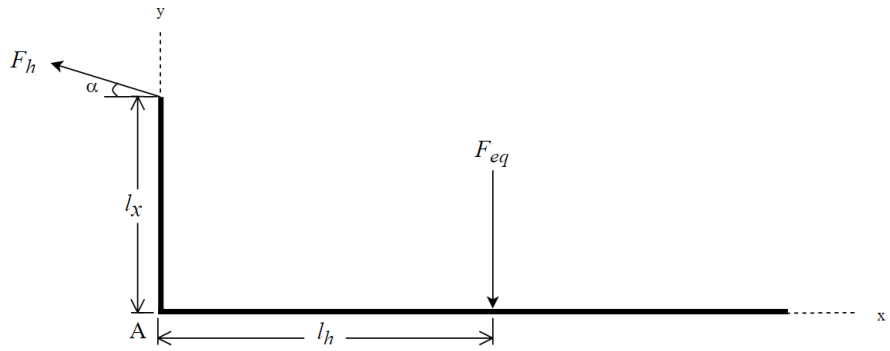

Figure 3.33 Free-body diagram of bone screw in uninclined position.

According to free-body diagram of bone screw (Figure 3.33), when bone screw is fixed horizontally and loaded with F_{eq}, the moment arm of the x component of F_h to the centerline is 1.95 mm (denoted as l_x in Eq.19). Taking moment equilibrium about the intersection point of y component of F_h and the centerline of bone screw (i.e. making the moment of F_{h_y} is zero) yields

$$0 = F_{eq}\, l_h - F_h \cos(\alpha)\, l_x \qquad \text{(Eq. 19)}$$

$$F_h = \frac{F_{eq}\, l_h}{\cos(\alpha) l_x} \cong 0.52\, \frac{1}{mm}\, (F_{eq}\, l_h) \qquad \text{(Eq. 20)}$$

The bearing stress (one thread is carrying 0.38 F_h) is

$$\sigma_B = -\frac{2\,(0.38\, F_h)}{\pi\, d_m\, p} \qquad \text{(Eq. 21)}$$

where, d_m is the mean diameter of first thread and is equal to 2 x 1.95 = 3.9 mm; pitch, p, is 0.5 mm. The thread-root bending stress (one thread carrying 0.38 F_h) is

$$\sigma_b = \frac{6\,(0.38\, F_h)}{\pi\, d_r\, p} \qquad \text{(Eq. 22)}$$

where, dr is the root diameter of first thread and is equal to 3.55 mm. The transverse shear stress at the center of the root of the first thread is

$$\tau = \frac{3V}{2A} = \frac{3\,(0.38\,F_h)}{2\,\pi\,d_r\,p/2} = \frac{3\,(0.38\,F_h)}{\pi\,d_r\,p} \qquad \text{(Eq. 23)}$$

The Ti 6 Al 4V ELI material has 760 MPa yield strength, S_y, according to Table 2.6. Therefore, the factor of safety of the threaded conical head of bone screw can be found by simply introducing an experimental force representing the F_{eq}, and using a yield criteria such as maximum shear stress (MSS). By this way, the factor of safety of depending on the application area (e.g. for humeral or femoral shaft fractures) can be estimated by using reported F_{bone} values in the literature. Inversely, the mechanical compression test can be conducted on the prototypes with a defined l_h distance to the failure, and a recommendation of safety factor can be given based on the failure types. As a final option, the axial holding capacity of the force found in Section 3.3 can be inserted into calculations as F_{eq} to find the first failing connection (screw-connector or connector-rod).

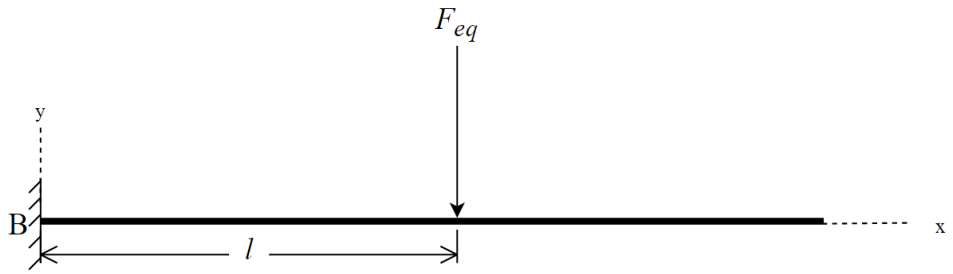

Figure 3.34 Representation of cantilever beam assumption for Location 2.

Besides the critical “Location 1”, the stresses of the “Location 2” can be found by assuming the head of bone screw is fixated rigidly and the threaded part of bone screw is a cantilever beam (i.e. a cylinder with diameter equal to root diameter of thread of bone screw). The formulations are given as follows:

The maximum value of bending stress of “Location 2” is at $d_r/2$, then

$$\sigma_{max} = \frac{Mc}{I} = \frac{(F_{eq}l)(^{d_r}/_2)}{(^{\pi d_r^4}/_{64})} = \frac{32}{\pi d_r^3} F_{eq} l \qquad \text{(Eq. 24)}$$

The maximum shear stresses of “Location 2” is

$$\tau_{max} = \frac{4F_{eq}}{3A_r} = \frac{16}{3\pi d_r^2} F_{eq} \qquad \text{(Eq. 25)}$$

where d_r is the diameter of the run-out section (Location 2), l is perpendicular distance of F_{eq} to Location 2 (Figure 3.34). If $6l >> d_r$, the maximum stress becomes more critical than maximum shear stress and vice versa. Using maximum shear stress theory to be more conservative, the safety factor of the design can be found as

$$\frac{0.5S_y}{\tau_{max}} = \text{n} \quad or \quad \frac{S_y}{\sigma_{max}} = \text{n} \qquad \text{(Eq. 26)}$$

3.5. Mechanical Testing of the Holding Capacity of Final Model

To estimate the holding capacity of final model, two different mechanical experiments are conducted on the prototypes of the final model namely axial gripping and torsional gripping tests. The tests are conducted using Shimadzu AGS-X Series Table-Top Universal Tensile Testing Machine with 5000 N load cell capacity. The input torque applied on the connector screw is measured using Mark-10 Compact Torque Gauge with 135 N.cm capacity. The specifications of the tensile testing machine and the torque gauge can be found in [60] and [61] respectively. The images of the testing devices are also given in the Figure 3.35.

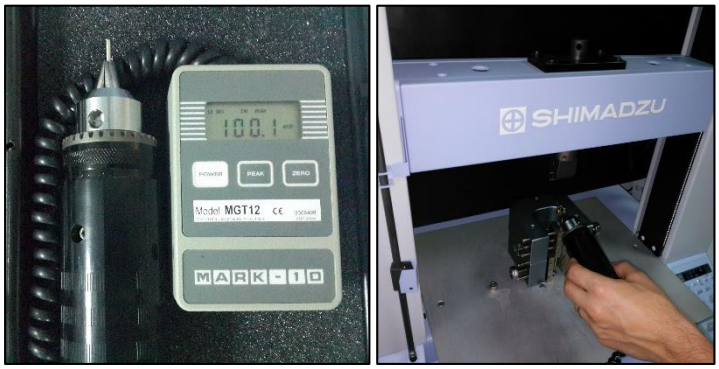

Figure 3.35 The images compact torque gauge (left) and the tensile testing machine (right) during the experiments.

3.5.1. Axial Gripping Tests

In axial gripping tests, ten compression tests are conducted with 1 mm/min constant testing speed. The rod is clamped vertically between the midpoints of two knurled plates with an offset so that the connector is fixed to rod (Figure 3.36).

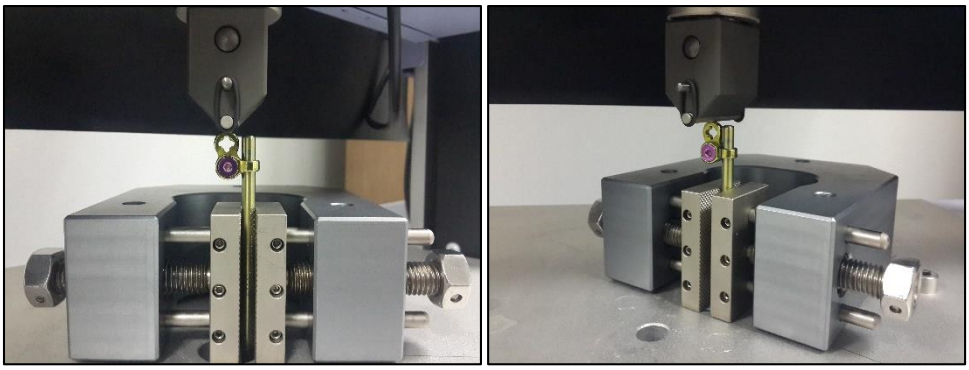

Figure 3.36 Placement of the rod and connector during axial gripping tests.

To avoid fixing the connector on the same place of the rod again, 25 mm offset is given to the rod intentionally: The width of the band section of connector is 4.5 mm, and ten experiments need a 45 mm rod length. If 45 mm offset was given to the rod, bending of the rod could occur possibly during the tests. Therefore, in order to measure only axial holding capacity of the connector due to the friction of junction

surface, the offset is set to its possible minimum value, and five tests are conducted on one side of the rod.

In the first five tests, the input torque is increased starting from a meaningful torque creating a measureable grip. The maximum input torque is selected considering the capacity of the torque gauge, 1350 N.mm. In addition, the typical tightening torque values for countersunk head screws with hexagon socket M4 steel fasteners is taken into account to grasp and anticipate the order of magnitude of tightening torque limits for titanium screws. For property classes 8.8 and 10.9 (ISO 10642), the recommended tightening torques are found as 2600 N.mm, and 3400 N.mm respectively [66], [67]. Consequently, the limits of input torque applied to connector screw is selected as 100 N.mm and 1000 N.mm, and five increasing input torque values (105 N.mm, 205 N.mm, 511 N.mm, 754 N.mm, 1009 N.mm) are given by hand utilizing the torque gauge. To measure the reliability of tests, five tests under constant input torque (1003 N.mm, 1013 N.mm, 1055 N.mm, 1001 N.mm, 1008 N.mm) are also performed.

The effect of the eccentricity of the testing head and the rod on the pressure distribution inside the clamping section is noticed during test, but it is assumed that the pressure increase (due to the moment created by eccentricity) at one side of the band clamp is compensated from the opposite side, and the net change is remained zero. However, the compression is applied through a line contact (see Figure 3.36), i.e. similar to cylinder on cylinder, and obtaining a vertical force, parallel to the centerline of the rod is almost impossible in this experimental conditions, so that a slightly higher holding force than the theoretical analysis are expected in the experiments.

In order to compare the analytical results of the second approach, two axial compression tests are also conducted. The connector screws are tightened until the 1 mm gap is closed. After, the same axial gripping test methodology is applied to the two specimens. Results are tabulated and compared in Section 4.1.

3.5.2. Torsional Gripping Tests

Similar to axial gripping tests, ten experiments are performed to see the torsional gripping capacity of the designed system. In these experiments, different rod specimen is used, because the mid-section surface of the previous one is deformed due to the clamping by claw. Two claws are placed as in Figure 3.37 to maintain rod horizontally. Like in the axial gripping tests, each experiment is performed with different and unused connectors on an unworn surface of the mid-section of the rod. The head of test machine is aligned parallel to the rod and compression is applied on the surface of the connector screw's head, especially on the center of it.

Figure 3.37 Placement of the rod and the connector during torsional gripping tests.

In both axial and torsional tests, the resisting force against translation or rotation of the connector is the total friction force created on the connection surface with rod. Therefore, it is expected that the results of the torsional gripping test is about 36 % of the axial gripping for the same tightening torque values applied on the connector screw. This percentage is obtained by dimensions of the moment arm as illustrated in Figure 3.38. For this reason, the input torque values are selected similar to the axial gripping tests: Increasing input torques (104 N.mm, 203 N.mm, 506 N.mm, 751 N.mm, 1001 N.mm), constant input torques (1002 N.mm, 1001 N.mm, 1003 N.mm, 1003 N.mm, 1002 N.mm).

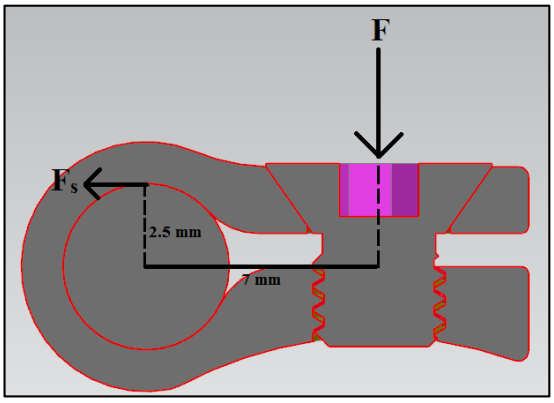

Figure 3.38 Representation of the forces and dimensions moment arms in torsional gripping tests.

3.6. Mechanical Testing of the Bone Screw Connection

Contrary to current bone screws as explained in the literature, the multi-axial characteristic of the bone screw is enabled by a locking and tapered head. In the bone screw tests, five straight, and one angled bone screws are bent with axial compression to the failure. All bone screws are placed on the connector that is fixed to rod, and the rod is clamped by a claw (Figure 3.39, left). As previously mentioned on the Section 3.4, to find out the first failing connection, the connector screws are tightened with the maximum constant torque (~1000 N.mm) that is used in the holding capacity (gripping) tests. Similar to axial gripping tests, five new sets of the connector and screw are used. The input torque values applied on the connector screws are measured as 1011 N.mm, 998 N.mm, 1003 N.mm, 995 N.mm, and 975 N.mm. Correspondingly, the maximum input torque applied on the bone screws are measured as 1206 N.mm, 1224 N.mm, 1203 N.mm, 1221 N.mm, and 1200 N.mm. The testing machine head is placed after 10^{th} crest of the bone screw threads, and together with run-out thickness the perpendicular distance between the machine head and undersurface of bone screw head, i.e. l_h of Eq. 20, is approximately 11.5 mm (see Figure 3.39). With 1 mm/min testing machine head velocity, all connector-bone

screw sets are compressed to the failure. Failure modes and results are represented in the Section 4.2.

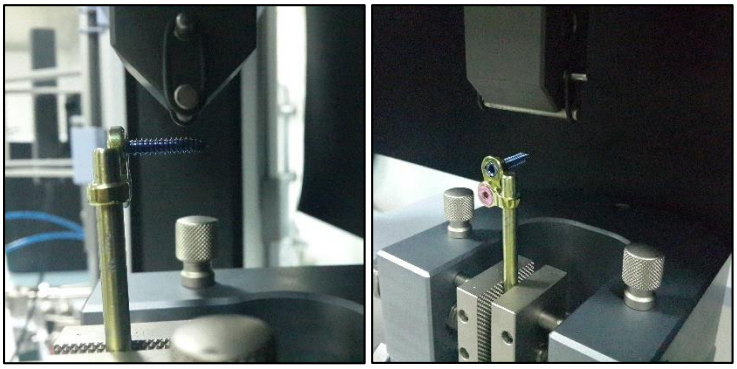

Figure 3.39 Placement of the head (left) and connector (right) during bone screw tests.

3.7. Mechanical Testing of Final Model with an Ovine Tibia

In order to see application performance and typical load bearing capacity of the final model, an artificial segmented fracture with two oblique cuts is created on an ovine tibia (Figure 3.40).

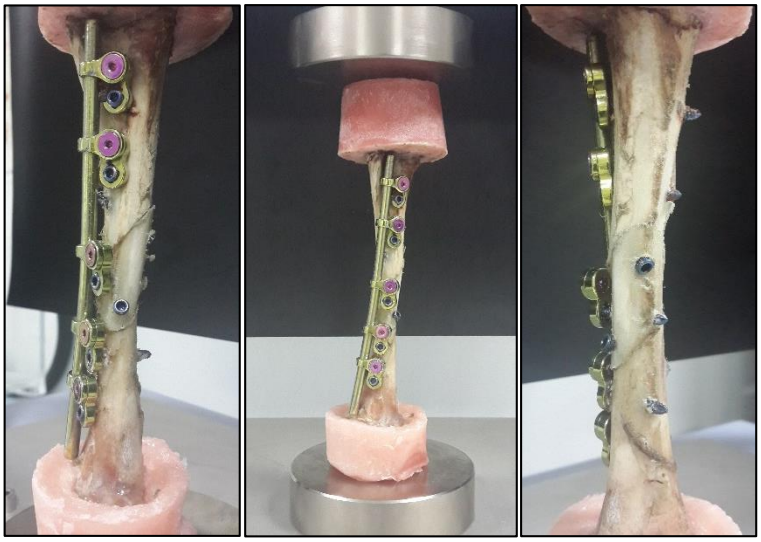

Figure 3.40 Different views of testing specimen.

A denture acrylic powder and acrylic liquid is mixed at a weight ratio of 10 gr. liquid to 24 gr. powder to form poly methyl methacrylate (PMMA) to fix the specimen in the testing machine (Figure 3.40, center).

The application of the fixation system to the bone is completed by an orthopaedic surgeon. The rod is bent to fit the anatomical shape of the bone by using in-situ benders used in surgeries. Five pilot holes are opened before inserting self-tapping cortical bone screws, and two bone screws are inserted perpendicularly to the surface of oblique cuts to stabilize three fragments of bone initially (Figure 3.40, right).

Next, connectors are placed on the rod without tightening, and bone screws are inserted into corresponding pilot holes. Finally, the connector screws are tightened without any input torque measurements intentionally, to observe any possible application failure (e.g. stripping of the screw head) under the optimal torque value felt by surgeon.

CHAPTER 4

RESULTS AND DISCUSSION

4.1. Results Related with the Holding Capacity of the Connector

In order to understand the load bearing capacity of the final design, two different analytical approaches were proposed in the Section 3.2.2. First, application of theory of the band brakes to the flat section band clamps was implemented to define the friction force generated between the surfaces of the connector and the rod in terms of applied clamping force, as explained in the study of Shoghi et al. [58]. Then, the clamping force was obtained separately as a function of two different parameters such as the input torque applied to the connector screw, and the change in the gap thickness during tightening of the screw. To compare the performance of the analytical approaches, mechanical tests were also conducted on the prototypes of the final design. In this subsection, the results of the both theoretical analysis and tests will be presented.

The values of geometric parameters defined in Section 3.3 is tabulated in Table 4.1. The band and connector screw parameters belong to the final model design, and cantilever beam parameters and their values represent the assumed beam geometry according to the upper clamping section of the connector.

Table 4.1 The geometric parameters used in calculations.

Band Parameters		**Connector Screw Parameters**		**Cantilever Beam Parameters**	
β [deg]	156,43	d [mm]	4	*l* [mm]	8,54
w [mm]	4,5	p [mm]	0,7	a [mm]	4,04
t [mm]	1,25	α_t [deg]	30	g [mm]	1
R_1 [mm]	2,5	d_p [mm]	3,545	*w* [mm]	4,5
R_2 [mm]	3,75	*l* [mm]	0,7	*t* [mm]	2

Based on the literature of metallic implant materials, the Young's modulus value of prototype material is selected from Table 2.6. The prototype material is stated as Ti 6Al 4V ELI by the manufacturer (Hipokrat A.Ş, İzmir, Turkey). The static and kinetic friction coefficients of this material selected as in Table 4.2, and are obtained from [68] and compared with [50] and [51] for reliability.

Table 4.2 The material properties used in calculations.

E [GPa]	μ_s	μ_k
101	0,36	0,31

To find the resisting friction force to translation of the connector in terms of the clamping force analytically, Eq. 16 is used. To find the torsional holding capacity against forces acting on the bone screw, the values of frictional resistance at the junction surface (i.e. touching surfaces of rod and connector), is multiplied with the length of its moment arm about the centerline of the rod, then divided to the perpendicular distance between the centerlines of rod and bone screw (see Figure 3.36).

First Analytical Approach

The analytical results of the first approach is expected to be lower than the tests results of both axial and torsional gripping capacity, because while translating the tensile force generated inside the connector screw to neutral axis of the band section as a clamping force, the generated moment is not included into theoretical formulations both for the sake of simplicity and its relatively small value considering its moment arm distance. Also, the effect of taper head of the connector screw to the screw tension is not included, because it is observed that while tightening the bone screw, the conical surface connection between the head and countersunk is reduced to a smaller conical surface due to the deflection of the upper clamping section, and assuming pressure distribution on every point of this conical surface is resulted

unrealistic, and high collar friction values. In addition, since the load is mainly carried on the threads of the connector screw, the relation between input torque and screw tension is defined according to these threads.

Table 4.3 The results of the first analytical approach and corresponding mechanical experiments.

Type of Exp.	#	I.T [N.mm]	Th.R [N]	T.R [N]	Diff. [N]	A.E [N]	Diff %	A.E %
Axial Hold. Increasing Torque	1	105	66,42	72,49	-6,07	6,07	-8,4	8,4
	2	205	129,67	116,70	12,97	12,97	11,1	11,1
	3	511	323,22	303,39	19,83	19,83	6,5	6,5
	4	754	476,92	553,20	-76,28	76,28	13,8	13,8
	5	1009	638,22	701,33	-63,11	63,11	9,0	9,0
Mean		*516,80*	*326,89*	*349,42*	*-22,53*	*35,65*	*-6.5*	*10,2*
Axial Hold. Constant Torque	1	1003	634,42	808,01	-173,59	173,59	-21,5	21,5
	2	1013	640,75	784,34	-143,59	143,59	-18,3	18,3
	3	1055	667,32	695,00	-27,68	27,68	-4,0	4,0
	4	1001	633,16	616,29	16,87	16,87	2,7	2,7
	5	1008	637,59	785,62	-148,03	148,03	-18,8	18,8
Mean		*1016*	*642,65*	*737,85*	*-95,2*	*101,95*	*-12,9*	*13,8*
Tors. Hold. Increasing Torque	1	104	23,49	18,14	5,35	5,35	29,5	29,5
	2	203	45,86	43,57	2,29	2,29	5,3	5,3
	3	506	114,31	129,85	-15,54	15,54	-12,0	12
	4	751	169,65	168,94	0,71	0,71	0,4	0,4
	5	1001	226,13	257,31	-31,18	31,18	-12,1	12,1
Mean		*513*	*115,89*	*123,56*	*-7,67*	*11,01*	*-6,2*	*8,9*
Tors. Hold. Constant Torque	1	1002	226,35	241,54	-15,19	15,19	-6,3	6,3
	2	1001	226,13	184,11	42,02	42,02	22,8	22,9
	3	1003	226,58	213,22	13,36	13,36	6,3	6,3
	4	1003	226,58	305,26	-78,68	78,68	-25,8	25,8
	5	1002	226,35	241,53	-15,18	15,18	-6,3	6,3
Mean		*1002,4*	*226,40*	*237,13*	*-10,73*	*32,89*	*-4,5*	*13,9*

(**I.T**: Input Torque, **Th.R**: Theoretical Results, **T.R**: Test Results, **Difference:** Th.R-T.R, **A.E**: Absolute Error)

The results related with the holding capacity of connector including the calculations of first theoretical approach, values of maximum force before significant movement of the connector and error calculations are tabulated in Table 4.3. As expected, the average percentage of absolute error magnitudes (i.e. difference %), of all four experiment sets are negative (-6.5 %, -12.9 %, -6.2%, and -4.5%). Mean absolute

percentage errors of tests with constant input torque of connector screw is very close to each other (13,8 %, 13,9 %). Likewise the increasing input tests have an average percentage error about 9 % (10,2 % and 8,9 %). Since the constant torque tests are conducted for the highest torque (i.e. ~1000 N.mm), the effects of neglected terms such as the moment of screw tension is appeared as higher absolute errors compared to the increasing torque tests. In other words, the average input torques of increasing torque tests are smaller than the constant ones (former ~500 N.mm, latter ~1000 N.mm), because the neglected moment of tension in the screw after translating it as clamping force is small when the input torque is small.

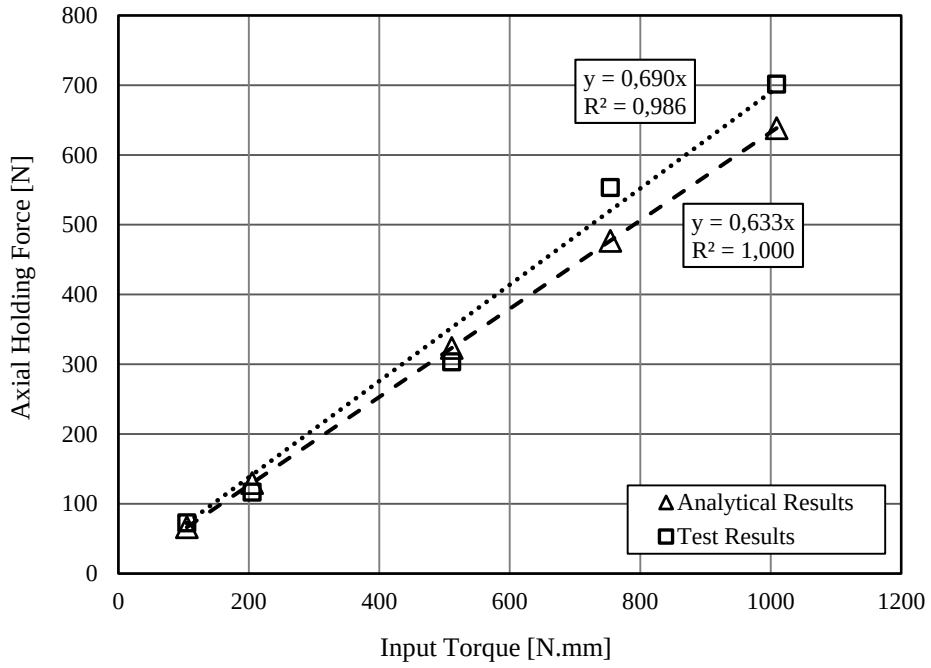

Figure 4.1 Comparison of analytical and test results of axial holding capacity for increasing input torque values.

In Figure 4.1, both analytical and test results of axial gripping capacity of the final model in terms of input torque applied on the connector screw is demonstrated. For small input torques, the analytical results closely match with test results, but the effect of ignored moment of screw tension is observed for higher input torque values. The

average values of five experiments and theoretical results are 326,89 N (SD: 212,69) and 349,42 N (SD: 244,27) respectively. The standard deviations of both results are higher, because of the increasing values of torques, i.e. the results are dispersed.

The second set of experiments, evaluation of torsional gripping capacity with increasing input torque value, give relatively smaller holding forces compared to previous set. The average values of torsional holding capacity for increasing input torques are calculated as 115,89 N (SD: 75,48) and 123,56 N (SD: 86,60) for analytical and test results correspondingly. Since five input torque values are in a wide range (0 – 1000 N.mm), standard deviations are high; the results are scattered around the mean value. The results of torsional gripping test with increasing input torque value with the result of analytical approach are illustrated in Figure 4.2.

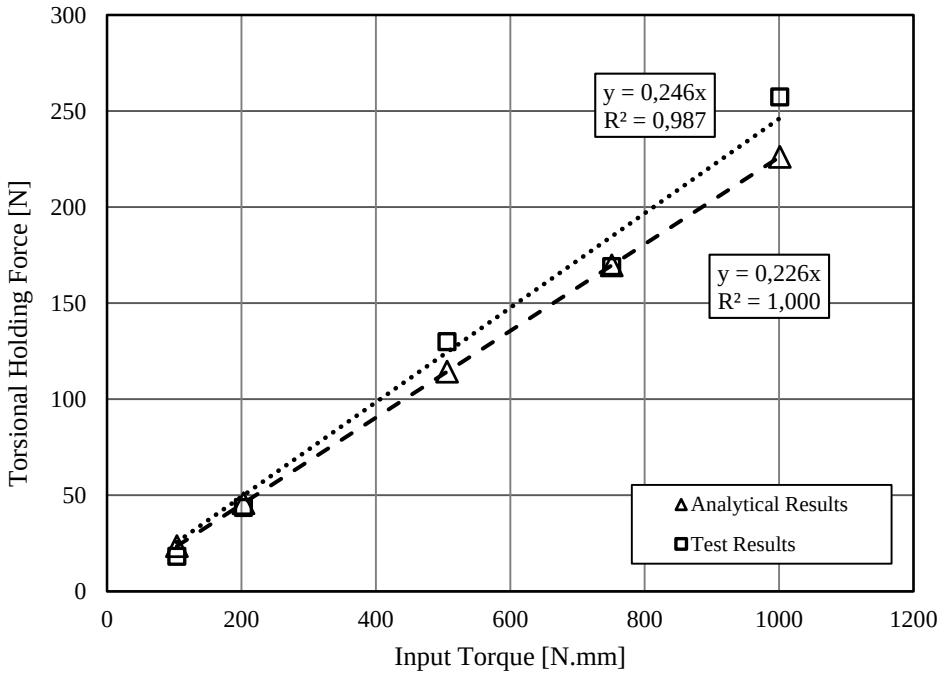

Figure 4.2 Comparison of analytical and test results of torsional holding capacity for increasing input torque values.

It can be said that, the analytical approach agrees closely with the results of torsional tests considering the slopes of their trends. Similar to previous comparison between axial holding tests and analytical results, the absolute error is increased for higher input torques and analytical approach underestimates the experiment results.

The remaining two sets of the experiments give the axial and torsional holding forces when constant input torque about ~1000 N.mm is applied to connector screw. The graph showing the results of the axial gripping tests and corresponding calculations is given in Figure 4.3.

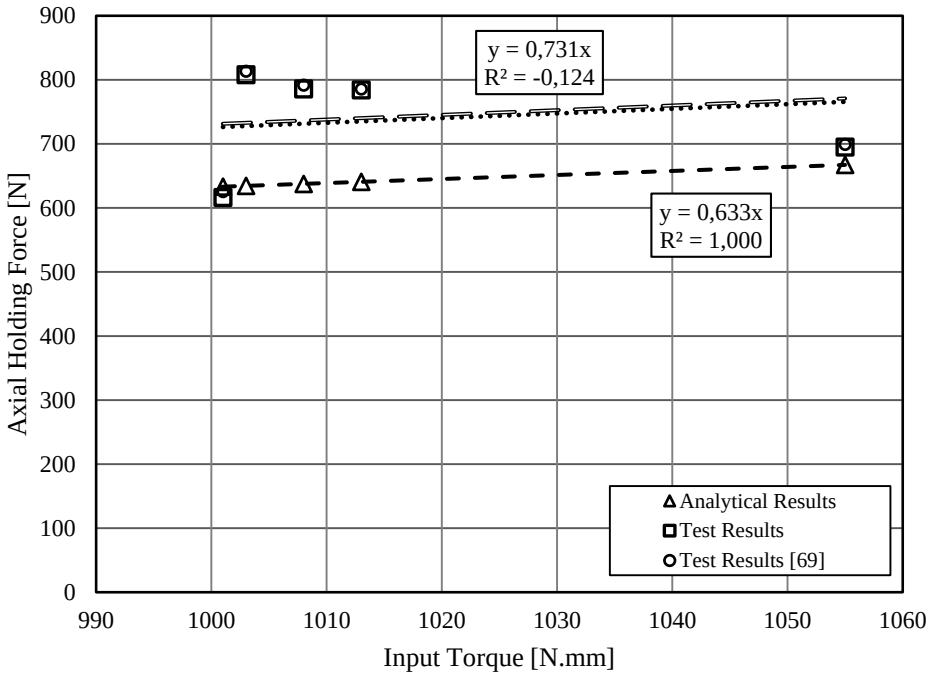

Figure 4.3 Comparison of analytical and test results of axial holding capacity for constant input torque values.

When linear trends of both analytical and test results is plotted in Figure 4.3, a constant error or bias can be seen. This error is almost equal to the difference between the average axial holding forces found from experiment and analytical method (The average axial holding force calculated analytically is 642,65 N (SD: 12,61), and

similarly 737,85 N (SD: 72,08) average holding force is obtained from test results). It should be noted that, the standard deviation of the results are smaller when input torque is constant, compared to previous experiments. However, the coefficient of determination (R^2) value of test result is less than the previous one, since a linear trend cannot explain the variation of results around mean, i.e. the test results cannot be fitted to a linear regression line.

Finally, the results of torsional holding capacity for constant input torque values and their linear trend lines are plotted in Figure 4.4. The analytic results have a mean value of 226,40 N (SD: 0,17), and due to very close input torque values, their standard deviation is almost zero. The experiment results have a slightly higher average value of torsional holding force (237,13 N - SD: 40,16) than analytical results, but the amount of error is smaller than the results of axial holding capacity with constant input torque.

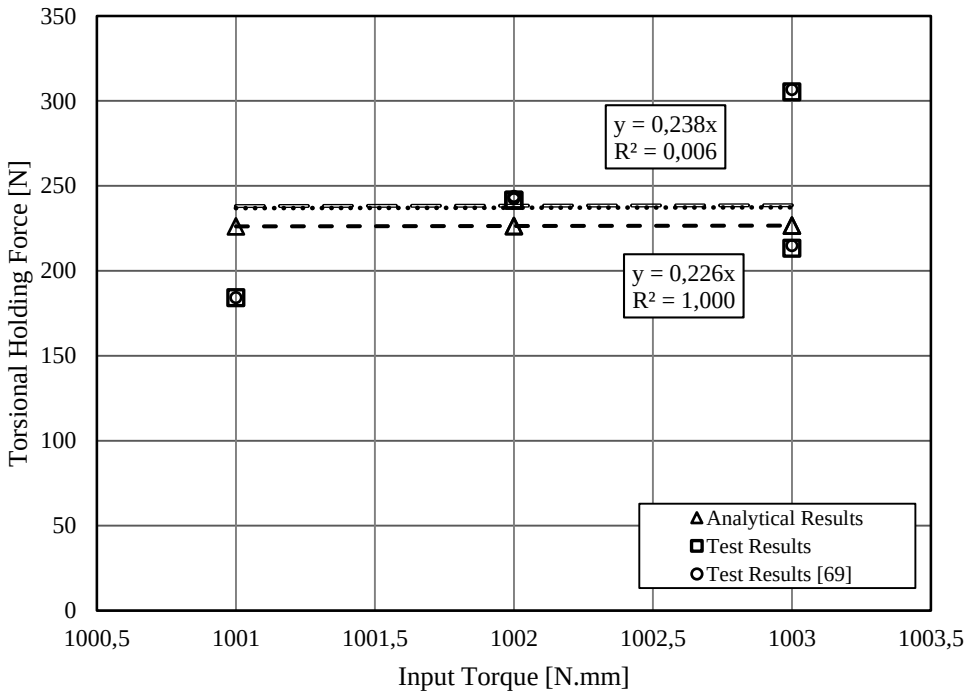

Figure 4.4 Comparison of analytical and test results of torsional holding capacity for constant input torque values.

Although, the analytical approach seems more successful to predict test results of torsional gripping test results, the mean absolute error of both tests are almost equal (13.8 % for axial and 13.9 % for torsional gripping results) for constant input torques. This result also shows that the eccentricity of the test setup in axial gripping test has no significant effect on the holding capacity of the system.

In Figure 4.3 and 4.4, the test results of a previous study [69] are also added into the graphs for comparison and validation purposes, because that study also used the same experimental raw data. According to Figure 4.3 and 4.4, it can be said that the experiment results of both studies are consistent. However, in that study, no attempt has been made to calculate gripping capacity of the system for constant input torque values. In addition, a different approach with some rough assumptions have been used to estimate the axial holding capacity of the connector for increasing input torques, and it has overestimated the test results. Briefly, the following method was followed in that study:

First, the tensile force generated on the screw is calculated analytically by using the Equation 8.27 of the [48]. However, the torque coefficient (K) value of this equation is an implicit form of Equation 8.26 of [48], and it includes a collar friction torque which is not correctly representing the tapered head of the connector screw. After, using finite element analysis (FEA), a contact force has been found on the junction surface of the rod and connector. Consequently, using a force representing the axial force of the experiments, which is acting parallel to the centerline of the rod and passing from the center of major circle of the taper hole of connector, additional contact forces have been added to previous one. Here, these additional forces have been found by static analysis, using the moment created due to the eccentricity of connector, however, these type of force couple can only occur when the rod diameter is smaller than the band diameter of the connector. In real case, clamping of the connector screw results a non-uniform pressure distribution on the intersection surface, and the eccentric force results a pressure distribution which has a maximum positive value at two cross sides while having maximum negative on the other two cross sides. Since the width of the band section and the gap is small, the net change

of the pressure distribution created by eccentric loading can be assumed as negligible. Finally, the reaction force on the rod obtained from the FEA has been multiplied directly with the friction coefficient to find the resisting friction force, meaning that a constant pressure distribution was assumed. Therefore, two harsh assumptions (constant pressure distribution, using implicit form of torque-force relationship) resulted overestimated analytical results for axial holding capacity of the system. The estimated and test results for axial holding capacity of that study [69] are also presented in Figure 4.5 for comparison purposes.

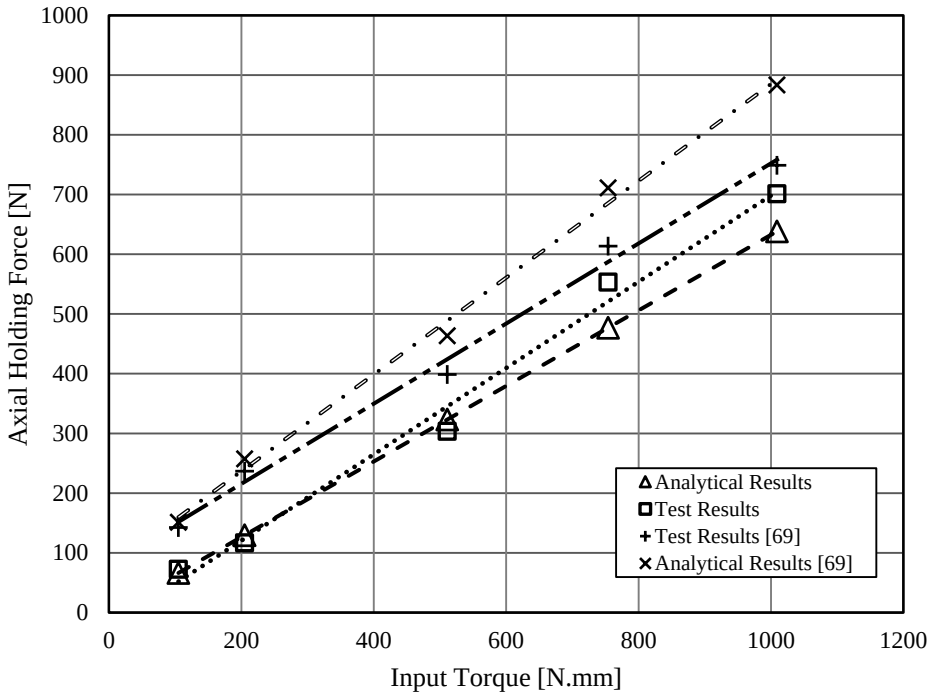

Figure 4.5 Comparison of axial holding capacity and test results.

According to Figure 4.5, it is believed that there is a reading error in the experimental results of [69], because in prior comparisons (Figure 4.3 and 4.4) the experimental data of both studies are almost equal. Interestingly, the analytical results of [69] in Figure 4.5 cannot be fitted exactly by a linear regression line.

For torsional holding capacity calculations, on the other hand, the experimental results comply with the experiment results of [69] (Figure 4.6). Unlike analytical results for axial holding capacity, an exact linear trend is observed for the results of [69] as shown in Figure 4.6. This time, the analytical results of [69] has been underestimated the test results, because it is stated that an average reaction force value obtained from the FEA has been used with uniform pressure distribution assumption, but the non-uniform pressure distribution on the band section junction has been noted.

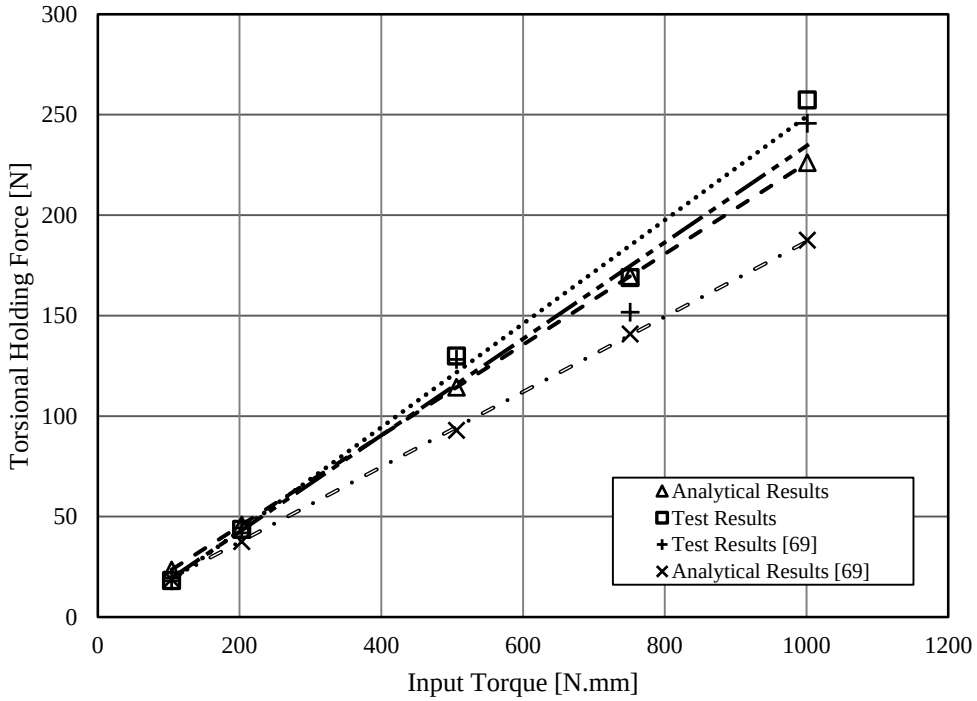

Figure 4.6 Comparison of torsional holding capacity and test results.

To sum up, according to the own results of this thesis which is compared through Figures 4.1 - 4.4, analytical results of the first approach closely agree with the test results. Possible source of error expectations seem correct considering the trends of the both analytical and test results: For small input torques, analytical estimation is more successful; errors between linear trends increase with increasing input torque (Figures 4.1 and 4.2). The constancy of the error between linear trends in the tests

with constant input torque also supports these expectations (Figure 4.3 and 4.4). In addition, comparison of the results with the earlier work [69] reveals both the differences between studies and correctness of the test results.

Second Analytical Approach

According to Table 4.4 the cantilever beam approach overestimates the average axial holding force about 9.2 % in the case where the gap is closed. Actually, this approach estimates a screw tension which is creating a 1 mm deflection when it is applied. However, in the real case, the upper clamping section of the connector have edge bending and its thickness decreases through band section. In other words, the fixed point of the beam has slightly lower thickness and the length of this section is so small compared to overall length of beam; hence the 1 mm deflection can be given with slightly smaller force.

Table 4.4 The results of the second analytical approach and corresponding mechanical experiments.

Type of Exp.	**#**	**Δ g [mm]**	**Calculation Results [N]**	**Test Results [N]**	**Absolute Error (A.E)**	**A.E %**
Closing gap	1	1	1162,77	1069,07	93,70	8,8
	2	1	1162,77	1060,95	101,82	9,6
Mean		*1*	*1162,77*	*1065,01*	*97,76*	*9,2*

Since the linear regression accurately estimates the test results of the axial holding capacity, the equation of linear trend of test results in Figure 4.1 can be used to estimate the required input torque to completely close the gap. Using the test results of second approach in Table 4.4, dividing average axial holding force (1065,01 N) by 0.69 (y = 0.69x, x: Input torque, y: Axial holding force, Figure 4.1), the approximate required torque to close the gap becomes 1543 N.mm. In short, approximately 155 N.cm torque is required to close to gap.

During mechanical tests of the second approach, the connector screw successfully tightened until the gap closes, but the hex recess is stripped when trying to screw off. Therefore, it is not recommended to use tightening torques near or above 1550 N.mm. The stripping of the head also showed that, hexagonal socket of the head is the most critical region for excessive input torques. In addition, the use of 2000 N.mm as assumed input torque to analyze the stresses and calculate the safety factors of each element, as done in [69], seems over-conservative considering mentioned stripping situation and approximated input torque.

4.2. Results Related with the Bone Screw Connection

According to the method defined in Section 3.4, the parameters in Table 4.5 are used in the calculations of bone screw.

Table 4.5 Parameters used in calculations of Location 1 and Location 2.

	Non-Angled Bone Screw				**Angled Bone Screw (~10°)**			
Loc.1	S_y [MPa]	760	l_x [mm]	1,95	S_y [MPa]	760	l_x [mm]	2,27
	d_m [mm]	3,9	l_h [mm]	11,75	d_m [mm]	3,9	l_h [mm]	11,75
	d_r [mm]	3,55	α [deg]	10	d_r [mm]	3,55	β [deg]	10
	p [mm]	0,5	L. Fact.	0,38	p [mm]	0,5	L. Fact.	0,59
Loc. 2	S_y [MPa]	760			S_y [MPa]	760	β [deg]	10
	l [mm]	10,75			l [mm]	10,75		
	d_r [mm]	2,6			d_r [mm]	2,6		

By using maximum shear stress (MSS) yield criterion with yield strength value of the Ti 6Al 4V ELI from Table 2.26, the calculations are intended to find different F_{eq} values considering each of the following stresses as critical separately: For "Location 1", which is the most critical tooth of the tapered head, bearing stress (σ_B), bending stress at the root (σ_b), and transverse shear stress at the center of the root (τ) are assumed to be equal to the yield strength of the material one by one and

corresponding equivalent forces are found using Eq. 21, 22, and 23 respectively. For "Location 2", which is the run-out section under the head (Figure 3.31), maximum bending (σ_{max}) and shear stresses (τ_{max}) are assumed to be equal to yield strength separately, and using Eq. 24 and Eq. 25, related critical F_{eq} values are found. By this way, five different F_{eq} values that are expected to result yielding are found and compared with each other (Table 4.6). Accordingly, the failure mode of the bone screw connection is inferred for the critical stress with the smallest value of F_{eq}.

Table 4.6 Results of theoretical approach for non-angled and angled bone screw

	Location 1			**Location 2**	
Configuration	$\mathbf{F_{eq}}$ [N] ($S_y = \sigma_B$)	$\mathbf{F_{eq}}$ [N] ($S_y = \sigma_b$)	$\mathbf{F_{eq}}$ [N] ($S_y = \tau$)	$\mathbf{F_{eq}}$ [N] ($S_y = \sigma_{max}$)	$\mathbf{F_{eq}}$ [N] ($0{,}5S_y = \tau_{max}$)
Non-Angled	1001,23	303,79	607,58	121,99	1513,15
Angled (10°)	1014,83	234,85	469,70	123,87	1536,49

In a single bone screw, in which a concentrated force perpendicular to screw's centerline is placed l_h mm away to the closest thread of the screw head (or is placed l mm away to the run-out section of the screw head), the maximum critical stress is obtained in the undersurface of the thread. However, the calculated F_{eq} does not represent the actual failure force, instead it gives a smaller critical force due to the use of MSS theory.

Similarly, again according to the theoretical calculations, when this force is applied with a tilt angle, β, (angled positon of the screw) the failure location does not change, although the bending stress on the most critical thread of the taper head increases significantly (i.e. F_{eq} decreases from ~300 N to ~230 N). The reason of this increase of bending stress can be explained as follows: When connector is fixed and not tilted, all six threads bear the load, and the most of this load is carried by the first thread, which is at the minor diameter of the tapered section (about 38 % of the load [48]). However, in a tilted case with 10°, only three threads carry the load because of the

protrusion of the head, and the load share of the first thread increases to 59 % (see load factors in Table 4.5). From this point of view, it can be said that, tightening of the bone screw with an angle higher than 10° can possibly result a failure at the teeth of tapered head, because one or two threads remain in the connection, even if plastic deformation or welding occurs between the threads.

To compare the critical F_{eq} value obtained from the theoretical stress analysis, bending tests with axial compression are applied to the five bone screws assembled on the connector and rod. According to the method of the experiment explained in Section 3.6., the maximum value of the input torques of holding capacity tests (~1000 N.mm) is given to each connector screw, and their exact values are shown in the first results column of Table 4.6. All bone screws are tightened also with the same input torque (~1200 N.mm) to obtain similar results within experiments. Forces just before the start of the yielding are read by eye, however 0.2 % offset can also be used. Instead, the ratio of yield and maximum forces are obtained for each test (Mean: 0,88) and their mean value is compared with the ratios of yield and tensile strength of Ti 6Al 4V ELI and Ti 6Al 4V, which are 0,92 and 0.88 respectively. The comparison showed that, the force at yield readings are acceptable, because the test specimens are identical. However, comparing a force ratio with a stress ratio can yield incorrect results for specimens if their geometry are not identical. Here, it is only used to check the accuracy of the readings from the experimental raw data. All results related with the mechanical experiments of bone screw are summarized in Table 4.6.

Table 4.7 Results of the axial compression tests of bone screws.

Type of Exp.	**#**	**Input Torque (Con.Screw) [N.mm]**	**Input Torque (Bone Screw) [N.mm]**	**Force at Yield [N]**	**Disp. at yield [mm]**	**Maximum Force [N]**	**Ratio of Forces (Yield/ Max.)**
Bone screw Constant Torque	1	1011	1206	343,40	2,93	377,24	0,91
	2	998	1224	269,73	2,53	328,98	0,82
	3	1003	1203	298,00	3,17	339,40	0,88
	4	995	1221	217,15	3,33	226,35	0,96
	5	975	1200	271,91	2,72	337,68	0,81
Mean		*996,40*	*1210,80*	*280,04*	*2,94*	*321,93*	*0,88*

To assess the failure mode in an angled bone screw higher than 10°, the bone screw is tightened with an angle in which the run-out of the bone screw touches to the unthreaded section of the tapered hole of connector (i.e. surface of quadrant after removal of thread). Obviously, plastic deformation occurred during tightening and four threads are appeared at one side of the protrusion. The same procedure is applied to the straight screws and the bone screw failed from the thread region of the tapered head (Figure 4.7). This result showed that the implications made by theoretical calculations for angled insertion of the bone screw are correct. Finally, all specimens after the experiment are illustrated in Figure 4.8. All non-angled specimens (except the fourth one) failed from the undersurface of the head, and angled one is failed from its taper head (the first specimen from the left in Figure 4.8). The fourth non-angled specimen did not tear apart because the testing machine automatically stopped due to the sudden movement in axial direction, but the bending of the undersurface can clearly be seen from Figure 4.8. In addition, one can easily observe the plastic deformation of threads of the angled case from the worn and shiny surfaces of threads (Figure 4.7 and 4.8).

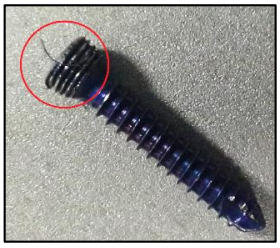

Figure 4.7 Failure of the threads of head in angled configuration.

Figure 4.8 Failure modes of the bone screws after mechanical tests.

The analytical calculations predicted that yielding bone screw (non-angled) starts when approximately 120 N concentrated load applied at previously specified location. However, when a testing force applied to the same location as in the analytical calculations, the screw carried almost an average of 322 N just before the failure, and yielding started at about 280 N. The reason of this difference can be the usage of a conservative yield theory, i.e. MSS theory. The actual yield strength of the material can also be higher than the minimum recommendations of ASTM.

The mechanical tests of bone screws also showed that, a connector input torque higher than 500 N.mm can result a safe axial gripping for the loads that are applied on the bone screw in parallel with centerline of the rod; because in such a case bone screw connection fails first. However, even if the connector is tightened with 1000 N.mm, the connector rotates first when a critical load is applied on the bone screw perpendicular to the centerline of the rod.

Finally, the average stiffness of the experiment setup can be found by simply dividing average values of force (at yield) and displacement (at yield). However, fourth experiment is not included in the calculation of stiffness because of its slightly divergent results. Thus, overall stiffness of the experiment setup is found as 103.74 N/mm. To compare this value, theoretical equivalent stiffness of the system is found by using Eq. 27 and Eq. 28.

$$k_{b.screw} = 6EI/[(3l - a)a^2] \quad \text{(Eq. 27)}$$

$$k_{rod} = EA/L \quad \text{(Eq. 28)}$$

Eq. 27 considers bone screw as a cantilever cylindrical beam under transverse loading shown as in Figure 4.9. Similarly, Eq. 28 assumes the rod is under compression and fixed at point O. It should be noted that, the rod is also in bending, and due to its small angular deflection (i.e. around 0.01 degrees) bending stiffness did not considered in calculations. Assuming bone screw and rod as springs in series, the equivalent

stiffness of the test system is found analytically as 109,34 N/mm. In these calculations, the bone screw is assumed as rod, and "*a"* is considered as the distance between the point of application of the testing force and centerline of the rod (*a* = 14 mm). Total length of bone screw, *l*, and the length of the rod over the clamping claws, *L*, are both measured as 20 mm. A good agreement between test and analytical results are also found in bone screw experiments.

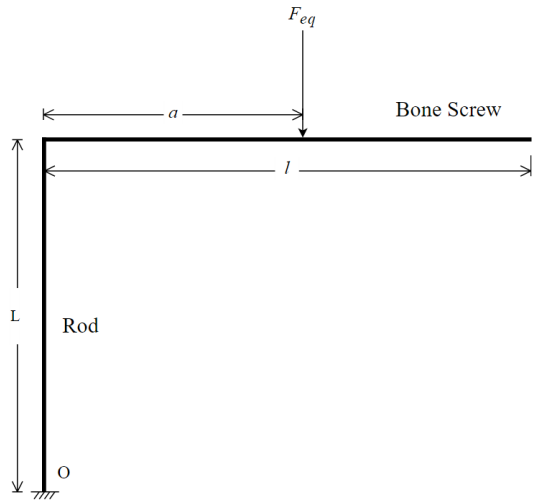

Figure 4.9 Simplified free-body diagram of test setup.

Beside stiffness calculations, length of the rod is also checked against buckling. Since the round cross sections have radius of gyration value of d/4 [48, pp 178], the slenderness ratio is found as 16. Therefore, the rod length in testing conditions is assumed as a short compression member. Using the equation 4-53 of [48], the limiting compressive force against buckling is found approximately 616 N.

As a conclusion, it can be said that the bone screw fails from its undercut region and possibly breaks under increasing transverse loading. However, when bone screw is placed with an inclination, the failure is expected from the threaded head section. The buckling of the rod is also not expected under mentioned loading conditions, but when loads applied on bone screw is not parallel to the centerline of the rod, assembly may fail due to the rotation of connector around rod.

4.3. Results Related with Screw within Screw Concept

The geometric properties of the screw within screw (SwS) concept are obtained from its CAD model and tabulated in Table 4.8.

Table 4.8 Geometric parameters of the screw within screw concept.

Band Parameters		**Connector Screw Parameters**		**Cantilever Beam**	
β1 [deg]	143,13	d [mm]	7	*l* [mm]	8,65
β2 [deg]	149,26	p [mm]	0,5	a [mm]	3,65
w [mm]	4,5	α_t [deg]	30	g [mm]	1
t [mm]	1,25	d_p [mm]	6,68	*w* [mm]	4,5
R_1 [mm]	2,5	*l* [mm]	0,5	*t* [mm]	3,25
R_2 [mm]	3,75				

The holding capacity of this novel system is estimated theoretically for the input torque values used in the calculations of the final model. The results of this estimation are given in Table 4.9 together with the results of the final model for comparison purposes.

Table 4.9 Axial holding capacity of the SwS concept.

Input Torque [N.mm]	**Final Model [N]**	**SwS Concept [N]**	**Test Results [N]**
105	66,42	36,45	72,49
205	129,67	71,17	116,70
511	323,22	177,40	303,39
754	476,92	261,77	553,20
1009	638,22	350,30	701,33

According to Eq. 17, which is relating the input torque to the screw tension, when the nominal diameter of the connector screw is increased (i.e. in the case of SwS concept compared to the final model), more input torque is required to obtain the same tension in the screw. Since the band geometry of final design and SwS concept are the same,

the same analytical approach used in the final model yields smaller axial holding force for the SwS concept. For example, the connector screw of SwS concept requires approximately 1680 N.mm input torque to generate the same screw tension when the connector screw of final model is tightened with 1000 N.mm. Considering the increase in the input torque requirement, the SwS concept still can be used as an alternative connector together with the final model. Since the diameter of connector screw is increased, the stripping problem possibly will not be observed. Still, hexalobe sockets can also be used to avoid stripping of the screw drive.

4.4. Results of Mechanical Testing of Final Model with Ovine Tibia

According to the method explained in Section 3.7, the results of the axial compression test is conducted on a bone-implant structure are illustrated in Figure 4.10. The test is manually terminated when 1000 N is reached, and linear trend of force vs. displacement curve yielded 384.15 N/mm stiffness value.

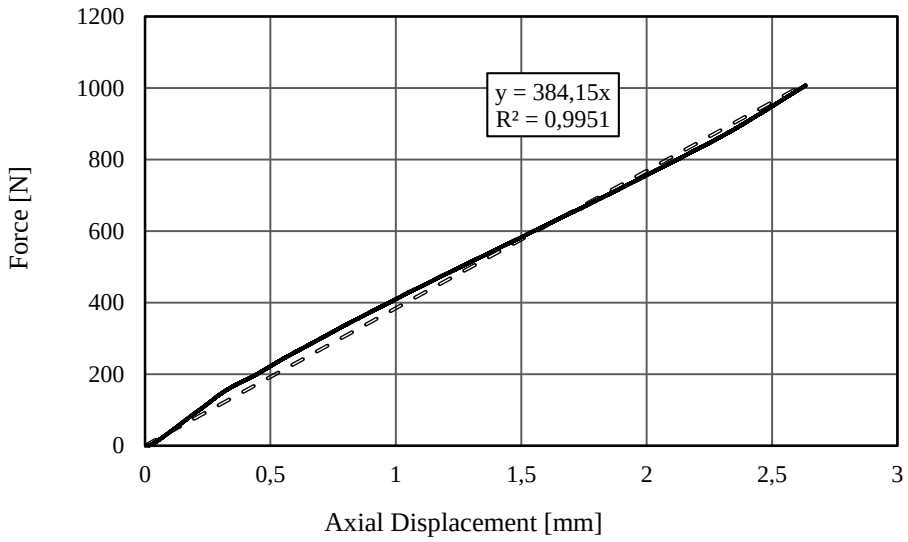

Figure 4.10 Result of the axial compression test applied on bone-implant structure.

The overall stiffness value of the bone-implant structure can also tried to be estimated by using analytical methods, however, no significant results are obtained due to the following reasons:

- The material properties of the ovine tibia used in the experiment is unknown. The material properties in the literature are also tried, but changes in the geometry affected significantly the results owing to the hollow cylinder assumption.
- Two interference screws are used to connect fracture fragments with each other. Unfortunately, the tip of the upper interference screw fractured the facing cortex of the upper segment during insertion. For this reason, the increase in the axial displacement is directly converted to the sliding of the upper fracture line.

Still, considering the stiffness of the bone screw experiment setup (~103 N/mm), its analytical verification (~109 N/mm), and the stiffness of the application (~384 N/mm), it can be said that, the designed system does not bear all the applied load by itself, and shares with the bone. From this point of view, the system provides less rigid fixation, which favors against stress shielding.

Besides, based on Figure 4.10, the fixation still can carry loads up to 200 N, considering the forces of small axial displacement values. Since the final model is applied on a complex fracture (segmented and oblique), it can be said that the final model can be applied to the simple diaphysial long bone fractures of upper extremity, in which the body weights are smaller than 200 N, and also relatively smaller compared to lower extremity. However, there are still question marks about the performance of the final model on upper extremity applications (e.g. humerus), if unexpected external forces other than body weights are applied.

Finally, it is recommended that, rotation and bending tests should also be conducted on a bone-implant structure with a representative simple diaphyseal fracture. These tests are not included on this thesis study, due to the lack of required experimental setup.

CHAPTER 5

CONCLUSION

In this thesis study, it was aimed to design and prototype an orthopaedic internal fixation system that is anatomically suitable for intended area application, minimizing the periosteum damage, allowing multi-axial screws and multi-planar application for traumatic and osteotomic applications.

The design process carried out was part of a project which is emerged based on the experiences of the orthopaedic surgeons on the currently available systems, and aimed to solve the major problems of the current plate-screw fixator sets.

Firstly, a novel idea of using rod-connector-screw systems into trauma was introduced by medical doctors. This idea was accepted as the best concept because it was considered as a solution that can meet the objectives of the project. Next, four different preliminary models were generated consecutively as a result of the design verifications throughout the design process. Since, the geometric design criteria were not specific, some design features (e.g. two-part connector, use of set screws for clamping, and spherical screw head) were abandoned at some stage in the development by using different verification methods including demonstrations either in actual or computer environment, inspection of the model prototype in terms of physical properties and ease of application by the surgeons, and mechanical analysis. After assessment of the preliminary models, the final design was formed and it was followed by mechanical analysis via different analytical approaches.

The mechanical analyzes were mainly concentrated on the connections of the proposed system instead of finding the strength of the elements under hypothetical loading condition, in order to obtain more realistic limits of the proposed fixation device.

Both holding capacity of the connector, and the connection between bone screw and connector were examined analytically, and the results of these approaches were compared with the results of the mechanical tests conducted on the prototypes. The comparison of theoretical analyzes showed good agreement with the test results, especially for the holding capacity of the system.

After investigation of the final model, a novel concept (screw within screw) was introduced based on the comments of the medical doctors on the designed system. First, they underlined the requirement of tightening two separate screws for a single bone screw application as time consuming. Second, they complain about the relatively small geometry of the connector screw. After assessing the prototype of the final model, they also noticed the possibility of contact between the bone and connector in the case where the threaded head of bone screw has not been placed correctly into its location. The novel concept was actually based on the final model, and the clamping section was remained the same; only the multi-axial property of bone screw was sacrificed. The same analytical calculation were used to find holding capacity of the novel concept and its prototypes were manufactured. As a result, this novel concept is suggested to be used in combination with the final system designed.

Finally, the overall performance of the proposed final design was evaluated by applying it to an ovine tibia. To see the mechanical behavior of the bone-implant structure, axial compression test was conducted. A simple stiffness comparison between the bone-implant structure and bone screw showed that the designed system favors the less stiff fixation, and hence load sharing with bone.

The main objectives of this thesis was completed by following means:

- Multi-axial and multi-planar application was introduced by utilizing a lockable cylindrical joint and partially threaded taper hole-screw connection.
- Only connection between the implant system and bone was occurred through screw and no contact observed with lower surface of connector and periosteum. By this way, periosteum damage is minimized.

- More easily bendable rod was introduced instead of prismatic bone plates, by which fully anatomical application can be obtained.
- Accurate analytical methods were generated to analyze the performance of the designed system. The usefulness of these methods were proven by utilizing them in a similar novel concept.

The further investigation can be done by conducting different mechanical test assessing the rotation and bending characteristics of the bone-implant structure with a representative simple diaphyseal fracture. In addition, the overall stiffness of this structure should be examined more accurately by either analytical methods or finite element analysis. Finally, the resistance of the designed fixator to fatigue needs to be assessed in an environment representing the in-vivo conditions.

REFERENCES

[1] E. F. B. Frederic, H. Martini, Judi L. Nath, *Fundamentals of Anatomy & Physiology*, 9th ed. Pearson, 2012.

[2] K. H. Elaine N. Marieb, *Human Anatomy & Physiology*, 9th ed. Pearson, 2013.

[3] R. L. Drake, A.W. Vogl, A. W. M. Mitchell, *Gray's Anatomy for Students*, 2nd ed. Churchill Livingstone, 2010.

[4] B. Clarke, "Normal bone anatomy and physiology", *Clinical Journal of American Society of Nephrology*, 2008-3 Suppl. 3, pp. 131–139, 2008.

[5] U. Kini and B. Nandesh, "Physiology of Bone Formation, Remodeling, and Metabolism", in *Radionuclide and Hybrid Bone Imaging*, I. Fogelman, G. Gnanasegaran and H. van der Wall, Ed. Springer-Verlag, 2012.

[6] J. Wolff, "The Law of Bone Remodeling", Berlin Heidelberg New York, Springer, 1986 (translation of the German 1892 edition).

[7] S. T. Marshall, B. D. Browner, " Chapter 20: Emergency Care of Muscoskeletal Injuries" in *Sabiston Textbook of Surgery: The Biological Basis of Modern Surgical Practice*, C. M. Townsend Jr., Elsevier, pp. 480-520, 2012.

[8] TheFreeDictionary.com, "Fractures", 2015. [Online]. Available: http://medical-dictionary.thefreedictionary.com/Fractures. [Accessed: 08- Jul- 2015].

[9] D. R. Dirschl and L. K. Cannada, "Classification of Fractures", in *Rockwood and Green's Fractures in Adults*, 7th Ed., R. B. Bucholz, J.D. Heckman, C. M. Court-Brown, and P. Tornetta, Ed. Lippincott Williams & Wilkins, 2010.

[10] AO Foundation, *AO/OTA Fracture and Dislocation Classification*, Switzerland, 2014. [Online] Available : https://aotrauma.aofoundation.org/Structure/education/self-directed-learning/reference-materials [Accessed: 08- Jul- 2015].

[11] E. Y. S. Chao and H. T. Aro, "Biomechanics of Fracture Fixation", *in Basic Orthopaedic Biomechanics*, V. C. Mow and W. C. Hayes, Ed. Raven Press, Ltd., New York, 1991.

[12] L.A. Pruitt and A. M. Chakravartula, *Mechanics of Biomaterials – Fundamental Principles for Implant Design* – 13. Orthopedics, Cambridge University Press, 2011.

[13] M. Schütz and T. P. Rüedi, "Principles of Internal Fixation", in *Rockwood and Green's Fractures in Adults*, 7th Ed., R. B. Bucholz, J. D. Heckman, C. M. Court-Brown, and P. Tornetta, Ed. Lippincott Williams & Wilkins, 2010.

[14] K. Ito and S. M. Perren, "Mechanobiology of Indirect or Secondary Fracture Healing", in *AO Principles of Fracture Management*, T. P. Rüedi, R. E. Buckley, and C. G. Morgan, Ed. AO Foundation Publishing, 2007.

[15] J. Bartonicek, "Early history of operative treatment of fractures", *Archives of Orthopaedic and Trauma Surgery*, 130(11), pp. 1385-1396, 2010.

[16] R. M. Greenhagen, A. R. Johnson, and A. Joseph, "Internal fixation: a historical review", *Clinics in Podiatric Medicine and Surgery*, 28(4), pp. 607-618, 2011.

[17] A. R. Lešić, S. Zagorac, V. Bumbaširević, and M. Ž. Bumbaširević, "The development of internal fixation – historical overview", *Acta Chirurgica Iugoslavica*, 59(3), pp. 9-13, 2012.

[18] Orthoinfo.aaos.org, "Internal fixation for fractures", 2014. [Online]. Available: http://orthoinfo.aaos.org/topic.cfm?topic=A00196. [Accessed: 29- Jul- 2015].

[19] A. F. Tencer, "Biomechanics of Fractures and Fracture Fixation", in *Rockwood and Green's Fractures in Adults*, 7th Ed., R. B. Bucholz, J.D. Heckman, C. M. Court-Brown, and P. Tornetta, Ed. Lippincott Williams & Wilkins, 2010.

[20] J. Park and R. S Martini, *Biomaterials: An Introduction*, 3th ed. Springer-Verlag New York, 2007.

[21] D. G. Poitout, "Biomaterials Used in Orthopedics", in *Biomechanics and Biomaterials in Orthopedics*, D. G. Poitout, Ed. Springer-Verlag London, 2004.

[22] M. J. Grimm, "Orthopedic Biomaterials", in *Biomedical Engineering and Design Handbook-Volume 1: Fundamentals*, 2th Ed., M. Kutz, Ed. McGraw-Hill, 2009.

[23] R. M. Pilliar, "Metallic Biomaterials", in *Biomedical Materials*, 2th Ed., R. Narayan, Ed. Springer-Verlag US, 2009.

[24] M. A. Imam and A. C. Fraker, "Titanium Alloys as Implant Materials", in *Medical Applications of Titanium and Its Alloys: The Material and Biological Issues*, S. A. Brown, J. E. Lemons, Eds. ASTM Publication, 1996.

[25] H. Hermawan, D. Ramdan and J. R. P. Djuansjah, "Metals for Biomedical Applications", in *Biomedical Engineering-From Theory to Applications*, R. Fazel, Ed. InTech, 2011.

[26] D. Kuroda, M. Niinomi, M. Morinaga, Y. Kato, and T. Yashiro, "Design and mechanical properties of new β type titanium alloys for implant materials", *Materials Science and Engineering*, A243, pp. 244-249, 1998.

[27] M. Niinomi, "Mechanical properties of biomedical titanium alloys", *Materials Science and Engineering*, A243, pp. 231-236, 1998.

[28] T. Hanawa, "Overview of metals and applications", in *Metals for Biomedical Devices*, M. Niinomi, Ed. Woodhead Publishing Limited, 2010.

[29] T. Matsushita, "Orthopaedic applications of metallic biomaterials", in *Metals for Biomedical Devices*, M. Niinomi, Ed. Woodhead Publishing Limited, 2010.

[30] T. Narushima, "New-generation metallic biomaterials", in *Metals for Biomedical Devices*, M. Niinomi, Ed. Woodhead Publishing Limited, 2010.

[31] C. Haraldsson and S. Cowen, "Characterization of Sandvik Bioline High-N: A Comparison of Standard Grades F1314 and F1586", in *Stainless Steels for Medical and Surgical Applications*, G. L. Winters, M. J. Nutt, Eds. ASTM Publication, 2002.

[32] M. Palanuwech, "The fatigue resistance of commercially pure titanium (grade II), titanium alloy (Ti6Al7Nb) and conventional cobalt-chromium cast clasps", Ph.D. dissertation, the Faculty of Medicine, Eberhard-Karls Univ., Tübingen, 2003.

[33] Qmed.com, "Top Orthopedic Firms and Trends from 2014 to 2020", 2015. [Online]. Available: http://www.qmed.com/mpmn/medtechpulse/top-orthopedic-firms-and-trends-2014-2020. [Accessed: 05- Dec- 2015].

[34] Orthoinfo.aaos.org, "Femur Shaft Fractures (Broken Thighbone)", 2015. [Online]. Available: http://orthoinfo.aaos.org/topic.cfm?topic=A00521. [Accessed: 05- Dec- 2015].

[35] *ASTM Standard Specifications for Surgical Implants (Stainless steels)*, Designations: F138-13a, F139-12, F1314-13a, F1586-13, F2229-12, F2581-12.

[36] *ASTM Standard Specifications for Surgical Implants (Co-Cr alloys)*, Designations: F75-12, F90-14, F562-13, F688-14, F799-11, F961-14, F1537-11, F2886-10.

[37] *ASTM Standard Specifications for Surgical Implants (Titanium and its alloys)*, Designations: F67-13, F136-13, F1108-14, F1295-11, F1472-14, F1713-08, F1813-13, F2063-12, F2066-13, F2885-11, F3046-13.

[38] L.A. Pruitt and A. M. Chakravartula, *Mechanics of Biomaterials – Fundamental Principles for Implant Design* –1. Biocompatibility, sterilization, and materials selection for implant design, Cambridge University Press, 2011.

[39] L.A. Pruitt and A. M. Chakravartula, *Mechanics of Biomaterials – Fundamental Principles for Implant Design* –2. Metals for medical implants, Cambridge University Press, 2011.

[40] L.A. Pruitt and A. M. Chakravartula, *Mechanics of Biomaterials – Fundamental Principles for Implant Design* –5. Mechanical behavior of structural tissues, Cambridge University Press, 2011.

[41] R. De Santis and L. Ambrosio, "Mechanical Properties of Human Mineralized Connective Tissues", in *Modeling of Biological Materials*, F. Mollica, L. Preziosi, and K. R. Rajagopal, Eds. Birkhäuser Boston, 2007.

[42] M. B. Nasab, M. R. Hassan, and B. Sahari, "Metallic Biomaterials of Knee and Hip", *Trends Biomater. Artif. Organs*, Vol 24(2), pp. 69-82, 2010.

[43] Matweb.com, "Material Property Data: Titanium, Ti", 2015. [Online]. Available: www.matweb.com (by searching the keyword *titanium*). [Accessed: 05- Dec- 2015].

[44] Matweb.com, "Material Property Data: Medical Grade Stainless Steel 316LVM", 2015. [Online]. Available: www.matweb.com (by searching the keyword *medical grade stainless steel)*. [Accessed: 05- Dec- 2015].

[45] H. M. Frost, "Bone's mechanostat: A 2003 update", *Anat. Rec.*, 275A, pp. 1081-1102, 2003.

[46] MadeHow.com, "Titanium", 2015. [Online]. Available: http://www.madehow.com/Volume-7/Titanium.html. [Accessed: 07- Dec- 2015].

[47] IntelligentImplantSystems.com, "Products: Maraduer Spinal System, Maraduer ™-Lumbar", 2015. [Online]. Available:http://www.intelligentimplant-systems.com/products_marauder.php. [Accessed: 07- Dec- 2015].

[48] R. G. Budynas and J. K. Nisbett, *Shigley's Mechanical Engineering Design*, 8th Ed. McGraw-Hill, 2008.

[49] *Unbrako Engineering Guide: Socket Products*, Unbrako LLC, Los Angeles, CA, USA, 2015.

[50] Roymech.co.uk, "Coefficient of Frictions Table", 2015. [Online]. Available: http://www.roymech.co.uk/Useful_Tables/Tribology/co_of_frict.htm. [Accessed: 27- Dec- 2015].

[51] M. Fellah, M. Labaiz, O. Assala, et al., "Tribological behavior of Ti-6Al-4V and Ti-6Al-7Nb alloys for total hip prosthesis", *Advances in Tribology*, vol. 2014, Article ID 451387, 13 pages, 2014.

[52] *Hipokrat General Catalog: Section B: Bone Plates*, Hipokrat A.Ş., Pınarbaşı, İzmir, Turkey, 2015.

[53] *Synthes Catalog – Trauma 2011: Plates and Screws*, DePuy Synthes, West Chester, PA, USA, 2015.

[54] *Synthes Universal Spinal System (USS): Technique Guide*, DePuy Synthes, West Chester, PA, USA, 2015.

[55] *TST Trauma Plate & Screws Catalog*, TST Ltd. Şti. , Pendik, İstanbul, Turkey, 2015.

[56] A. Whitten, and J. Carter, "Literature discrepancies in biomechanical loading of orthopedic trauma devices intended for lower extremities", *Fatigue and Fracture of Medical Metallic Materials and Devices*, ASTM Int. STP 1559, pp. 68-84, 2013.

[57] JayRacing.com, "Magnaflow Lap Joint Band Clamp", 2015. [Online]. Available: http://www.jayracing.com/index.php?main_page=popup_image&pID= 21110 [Accessed: 7- Jan- 2016].

[58] K. Shoghi, H. V. Rao, and S. M. Barrans, "Stress in a flat section band clamp", *Proc. Instn. Mech. Engrs.*, Vol. 217 Part C, pp. 821-830, 2003.

[59] *The Advantages of ASTM International to the Materials Engineer*, ASTM International, 2015. [Online] Available: http://www.astm.org/COMMIT/G01_ Materials.pdf [Accessed: 13- Jan- 2016].

[60] Shimadzu.com, "AGS-X Series", 2016. [Online]. Available: http://www.shimadzu.com/an/test/universal/ags-x/ags-x_6.html. [Accessed: 14- Jan- 2016].

[61] ColeParmer.com, "Compact Torque Gauge Item # EW-59847-07", 2016. [Online]. Available: http://www.coleparmer.com/Product/Compact_Torque _Gauge

_12 _lbin_140_kgmm_135_Ncm_capacity_220V/EW-59847-07. [Accessed: 14- Jan- 2015].

[62] A. J. Thakur, *Elements of Fracture Fixation* – 3. Bone Screws, 3rd Ed., Elsevier Health Sciences APAC, 2015.

[63] Wikipedia.org, "List of screw drives", 2016. [Online]. Available: https://en.wikipedia.org/wiki/List_of_screw_drives. [Accessed: 14- Jan- 2016].

[64] *ASTM Standard Specification and Test Methods for Metallic Medical Bone Screw*, Designation: F543-13.

[65] *Stryker Implant Extraction Guide – Module One & Two*, Stryker, Kalamazoo, MI, USA, 2015.

[66] Engineersedge.com, "Countersunk Screws Torque Table Metric, ISO", 2016. [Online]. Available: http://www.engineersedge.com/hardware/countersunk_ screws _torque_table_13477.htm. [Accessed: 14- Jan- 2016].

[67] Mdmetric.com, "Preloads and tightening torque for fasteners from steel", 2016. [Online]. Available: http://mdmetric.com/fastindx/TI-170.pdf. [Accessed: 14- Jan- 2016].

[68] K. G. Budinski, "Tribological properties of titanium alloys", *Wear*, 151, pp. 203-217, 1991.

[69] O. M. Erkan, "Design of an orthopedic modular implant", *Unpublished Master Thesis*, Middle East Technical University, 2015.

[70] A. B. Cullen, S. Curtiss, and M. A. Lee, "Biomechanical comparison of polyaxial and uniaxial locking plate fixation in a proximal tibial gap model", *Journal of Orthopaedic Trauma*, 27-7, pp. 507-513, 2009.

[71] R. J. Otto, B. R. Moed, and J. G. Bledsoe, "Biomechanical comparison of polyaxial-type locking plates and a fixed-angle locking plate for internal fixation of distal femur fractures", *Journal of Orthopaedic Trauma*, 23-9, pp. 645-652, 2009.

[72] H. H. Handoll, B. J. Ollivere, and K. E. Rollins, "Interventions for treating proximal humeral fractures in adults", *Cochrane Database Syst. Rev.*, Dec.12, pp. 12, 2012.

[73] J. B. Erhardt, K. Stoffel, J. Kampshoff, N. Badur, P. Yates, and M. S. Kuster, "The position and number of screws influence screw perforation of the humeral head in modern locking plates: a cadaver study", *Journal of Orthopaedic Trauma*, 26-10, pp. 188-192, 2012.

[74] M. Königshausen, L. Kübler, H. Godry, M. Citak, and T. A. Schildhauer, "Clinical outcome and complications using a polyaxial locking plate in the treatment of displaced proximal humerus fractures. A reliable system? ", *Injury*, 43-2, pp. 223-231, 2012.

[75] S. Ruchholtz, C. Hauk, U. Lewan, D. Franz, C. Kühne, and R. R. Zettl, "Minimally invasive polyaxial locking plate fixation of proximal humeral fractures: a prospective study", *Journal of Trauma*, 71-6, pp. 1737-1744, 2011.

[76] R. Zettl, T. Müller, T. Topp, U. Lewan, A. Krüger, C. Kühne, S. Ruchholtz, "Monoaxial versus polyaxial locking systems: a biomechanical analysis of different locking systems for the fixation of proximal humeral fractures", *Int. Orthop.*, 35-8, pp. 1245-1250, 2011.

[77] H.F. Shi, J. Xiong, Y. X. Chen, J. F. Wang, S. F. Wang, Z. J. Chen, and Y. Qiu, "Management of proximal humeral fractures in elderly patients with uni- or polyaxial locking osteosynthesis system", *Arch. Orthop. Trauma Surg..*, 131-4, pp. 541-547, 2011.

[78] G. Röderer, J. Erhardt, M. Graf, L. Kinzl, and F. J. Gebhard, "Clinical results for minimally invasive locked plating of proximal humerus fractures", *J. Orthop. Trauma*, 24-7, pp. 400-406, 2010.

[79] B. Ockert, V. Braunstein, C. Kirchhoff, M. Körner, S. Kirchhoff, K. Kehr, W. Mutschler, and P. Biberthaler, "Monoaxial versus polyaxial screw insertion in angular stable plate fixation of proximal humeral fractures: radiographic analysis of a prospective randomized study", *J. Trauma*, 69-6, pp. 1545-1551, 2010.

[80] K. J. Wilkens, S. Curtiss, and M. A. Lee, "Polyaxial locking plate fixation in distal femur fractures: a biomechanical comparison", *J. Orthop. Trauma*, 22-9, pp. 624-628, 2008.

[81] H. Gao, C. Q. Zhang, C. F. Luo, Z. B. Zhou, and B. F. Zeng, "Fractures of the distal tibia treated with polyaxial locking plating", *Clin. Orthop. Relat. Res.*, 467-3, pp. 831-837, 2009.

[82] M. Ronga, C. Shanmugam, U. G. Longo, F. Oliva, and N. Maffulli, "Minimally invasive osteosynthesis of distal tibial fractures using locking plates", *Orthop. Clin. North. Am.*, 40-4, pp. 499-504, 2009.

[83] P. Kolar, K. Schmidt-Bleek, H. Schell, T. Gaber, D. Toben, G. Schmidmaier, C. Perka, F. Buttgereit, and G. N. Duda, "The early fracture hematoma and its potential role in fracture healing", *Tissue Eng. Part B Rev.*, 16-4, pp. 427-434, 2010.

[84] S. H. Park, K. O'Connor, R. Sung, H. McKellop, and A. Sarmiento, "Comparison of healing process in open osteotomy model and closed fracture mode", *J. Orthop. Trauma*, 13-2, pp. 114-120, 1999.

[85] R. Will, R. Englund, J. Lubahn, and T. E. Cooney, "Locking plates have increased torsional stiffness compared to standard plates in a segmental defect model of clavicle fracture", *Arch. Orthop. Trauma Surg.*, 131-6, pp. 841-847, 2011.

[86] S. O. Dietz, L. P. Müller, E. Gercek, F. Hartmann, and P. M. Rommens, "Volar and dorsal mid-shaft forearm plating using DCP and LC-DCP: interference with the interosseous membrane and forearm-kinematics", *Acta. Chir. Belg.*, 110-1, pp. 60-65, 2010.

[87] T. Apivatthakakul, S. Anuraklekha, G. Babikian, F. Castelli, A.Pace, V. Phiphobmongkol, R. White, K. Kojima, and M. Camuso, "Tibial shaft 42-A2 ORIF", in AO Surgery Reference, P. Trafton, Ed., AO Foundation, 2013.

APPENDIX A

SAMPLE CALCULATIONS

Holding Capacity Calculations

First Analytical Approach

F_t: Tension generated the screw

T_{in}: Torque applied to the screw

$F_t = T_{in} / K$ according to Eq.17 then, K only depends on the geometric properties of the connector screw:

$$K = \frac{[0{,}7\ mm + \pi * 0{,}3 * 3{,}545339\ mm * \sec(30°)]}{[\pi * 3{,}545339\ mm - 0.3 * 0{,}7mm * \sec(30°)]} * \frac{3{,}545339\ mm}{2}$$

$$K = 0{,}741625\ mm$$

If $T_{in} = 1009\ N.mm$ then $F_t = 1009\ N.mm / 0{,}741625\ mm = 1360{,}5\ N$

Second Analytic Approach

According to Eq. 18,

$$F_t = \frac{1\ mm * 6 * 101000\ MPa * 3\ mm^4}{(4{,}04\ mm^2 * (3 * 8{,}54\ mm - 4{,}04\ mm)} = 5161{,}5\ N$$

Holding Capacity of the System According to First Approach

According to Eq.16, if 1009 N.mm is applied axial holding force is,

$$F_s = 1360{,}526\ N * 0{,}36 * \left(2 - \frac{1 + \exp(0{,}36 * 2{,}73\ rad - \pi)}{\exp(0{,}36 * 2{,}73\ rad)}\right) = 638{,}2\ N$$

Then, torsional holding force becomes,

$$638{,}219\ N * \frac{2{,}5\ mm}{7\ mm} = 227{,}9\ N$$

Holding Capacity of the System According to First Approach

According to Eq.14, if 1 mm gap is closed,

$$F_s = 0{,}36 * 5161{,}515\ N * \frac{\exp(0{,}36 * 2{,}73\ rad - 1)}{\exp(0{,}36 * 2{,}73\ rad)} = 1162{,}7\ N$$

APPENDIX B

GLOSSARY OF MEDICAL TERMS

The medical terms were adapted from Cambridge Dictionaries Online and Merriam-Webster Medical Dictionary.

apoptosis: a genetically determined process of cell self-destruction —called also programmed cell death.

appendicular: relating to the arms or legs or a part of the body that is joined to another part, such as the appendix.

bio-compatibility: compatibility with living tissue or a living system by not being toxic, injurious, or physiologically reactive and not causing immunological rejection

callus: a mass of exudate and connective tissue that forms around a break in a bone and is converted into bone in the healing of the break.

diaphysis: the shaft of a long bone.

distal: situated away from the point of attachment or origin or a central point: as

located away from the center of the body (e.g. the distal end of a bone)

endosteum: the layer of vascular connective tissue lining the medullary cavities of bone.

epiphysis: a part or process of a bone that ossifies separately and later becomes ankylosed to the main part of the bone; especially: an end of a long bone.

granulation tissue: tissue made up of granulations that temporarily replaces lost tissue in a wound.

homeostasis: the ability or tendency of a living organism, cell, or group to keep the conditions inside it the same despite any changes in the conditions around it, or this state of internal balance.

inflammation: a local response to cellular injury that is marked by capillary dilatation, leukocytic infiltration, redness, heat, pain, swelling, and often loss of function and that serves as a mechanism initiating the elimination of noxious agents and of damaged tissue.

inpatient treatment: a patient who stays for one or more nights in a hospital for treatment.

in-vitro: outside the living body and in an artificial environment.

in-vivo: in the living body of a plant or animal.

lateral: of or relating to the side; especially of a body part: lying at or extending toward the right or left side: lying away from the median axis of the body (e.g. the lungs are lateral to the heart, the lateral branch of the axillary artery)

medial: lying or extending in the middle; especially of a body part: lying or extending toward the median axis of the body (e.g. the medial surface of the tibia)

metaphysis: the transitional zone at which the diaphysis and epiphysis of a bone come together.

ossification: the process of becoming hard and changing into bone.

osteogenesis: development and formation of bone.

osteogenic: of, relating to, or functioning in osteogenesis; especially: producing bone (e.g. the osteogenic layer of the periosteum)

osteotomy: a surgical operation in which a bone is divided or a piece of bone is excised (as to correct a deformity).

periosteum: the membrane of connective tissue that closely invests all bones except at the articular surfaces.

post-operative: relating to, occurring in, or being the period following a surgical operation.

pre-operative: occurring, performed, or administered before and usually close to a surgical operation.

proximal: situated next to or near the point of attachment or origin or a central point; especially: located toward the center of the body (e.g. the proximal end of a bone)

APPENDIX C

TECHNICAL DRAWINGS

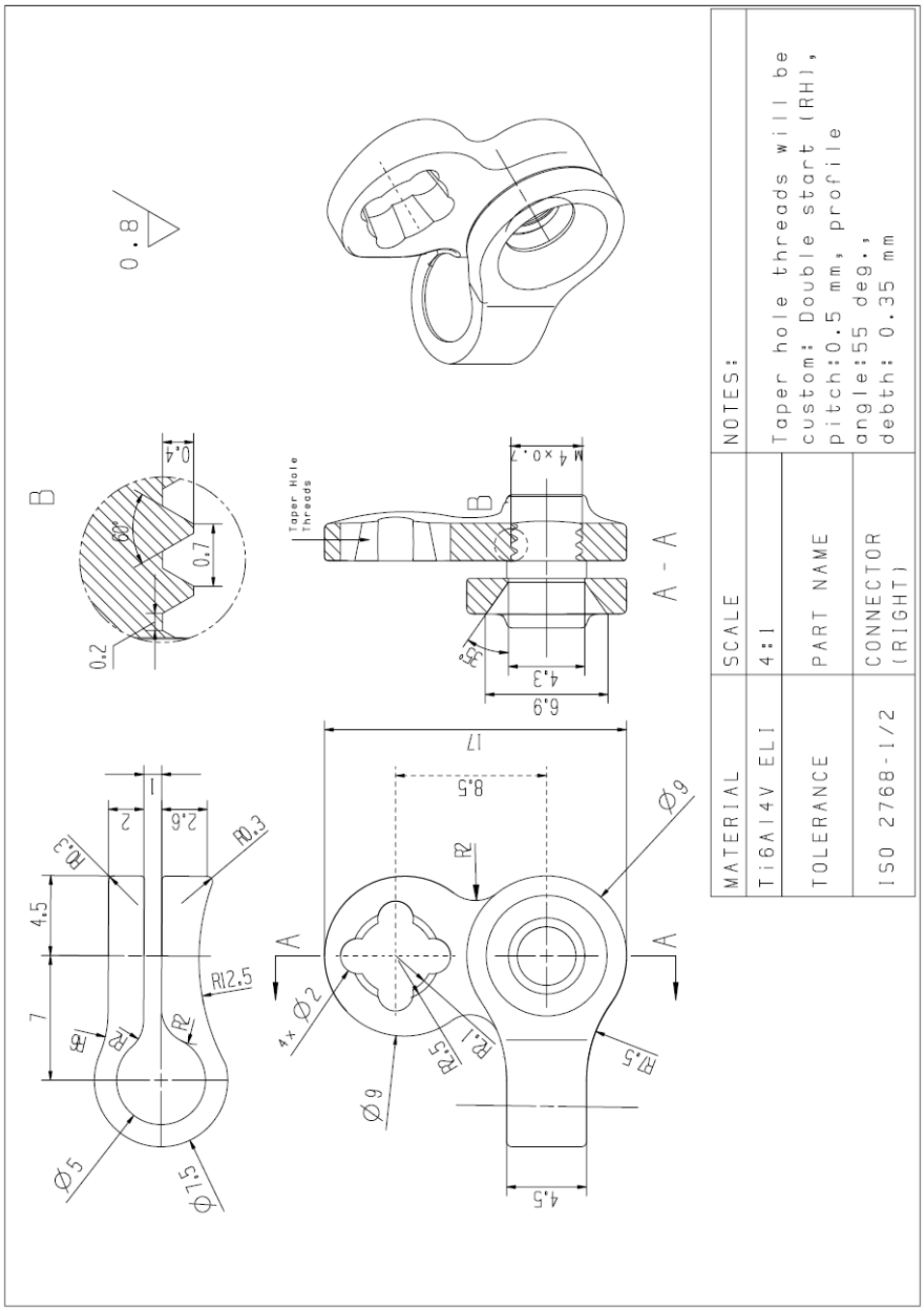

Figure C.1 Technical drawing of the connector.

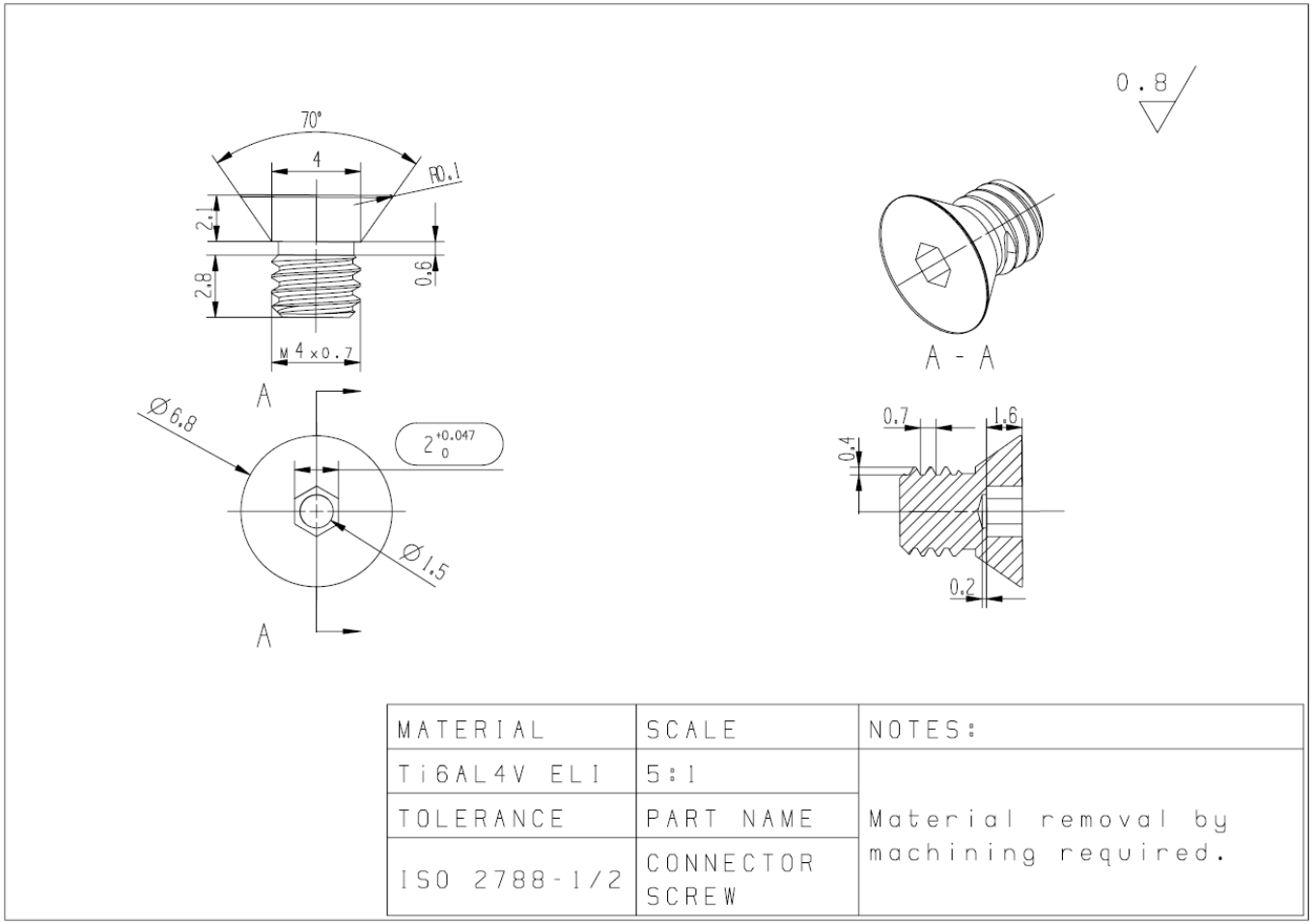

Figure C.2 Technical drawing of the connector screw.

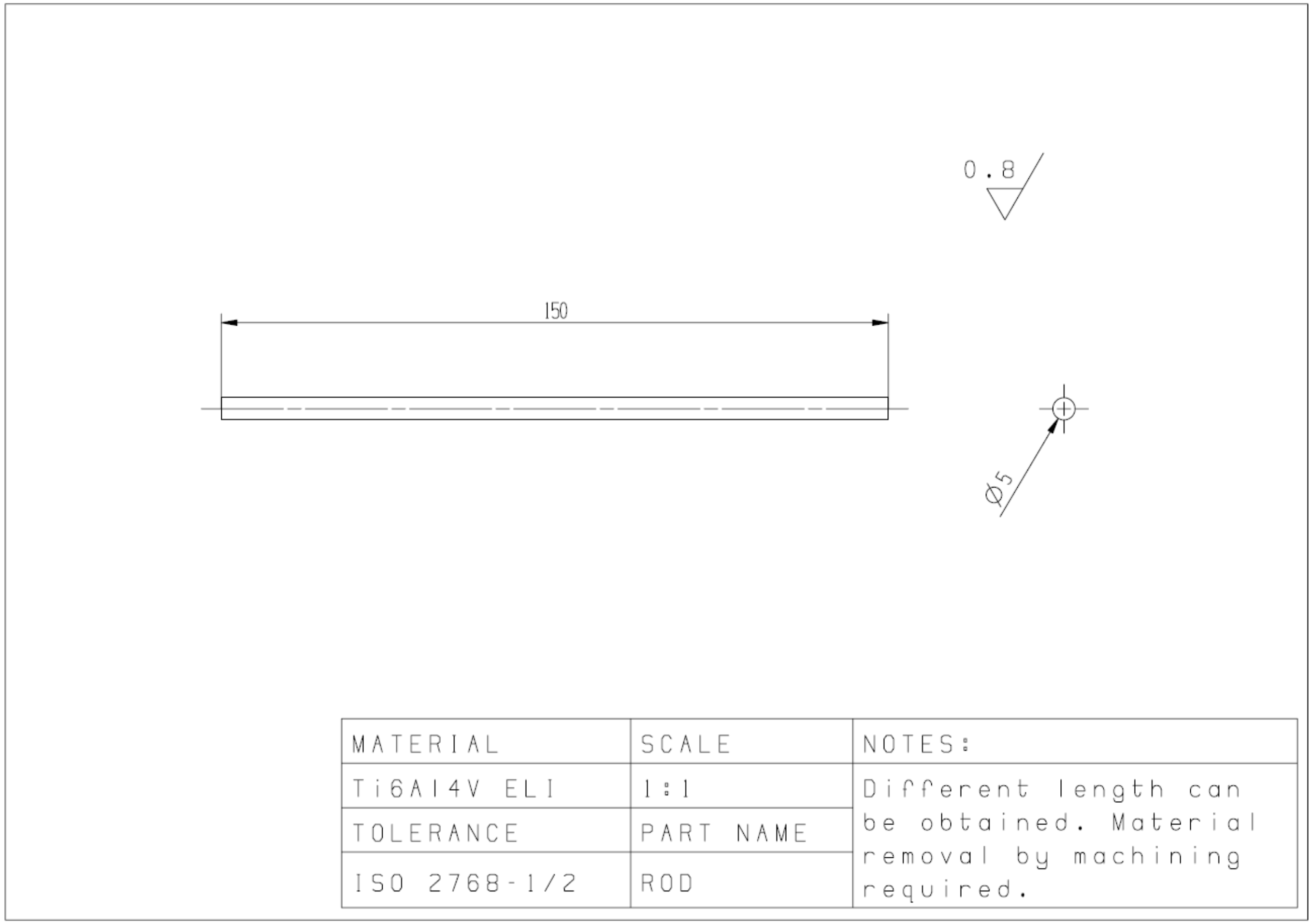

Figure C.3 Technical drawing of the rod.

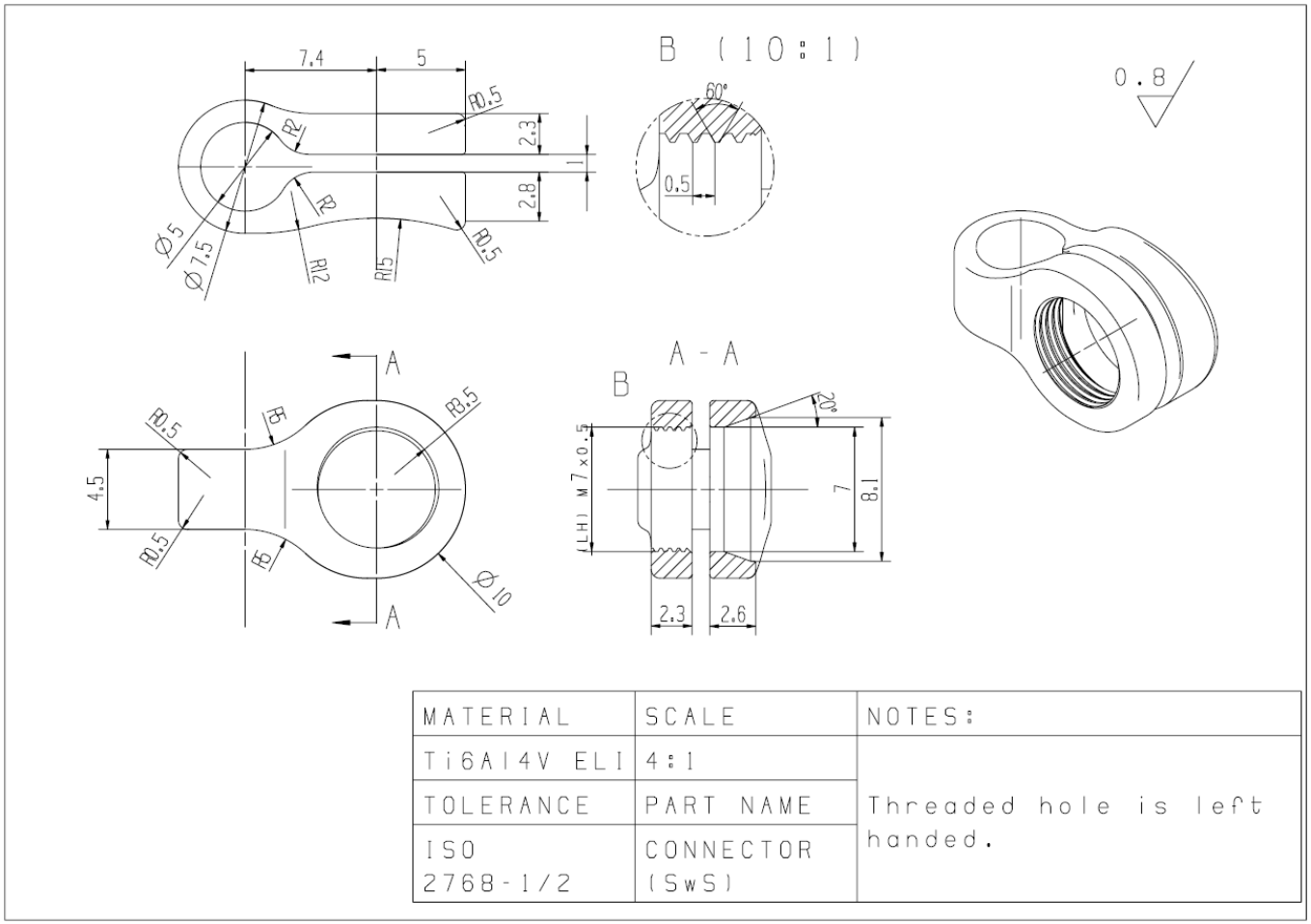

MATERIAL	SCALE	NOTES:
Ti6Al4V ELI	4:1	Threaded hole is left handed.
TOLERANCE	PART NAME	
ISO 2768-1/2	CONNECTOR (SwS)	

Figure C.4 Technical drawing of the connector of SwS concept.

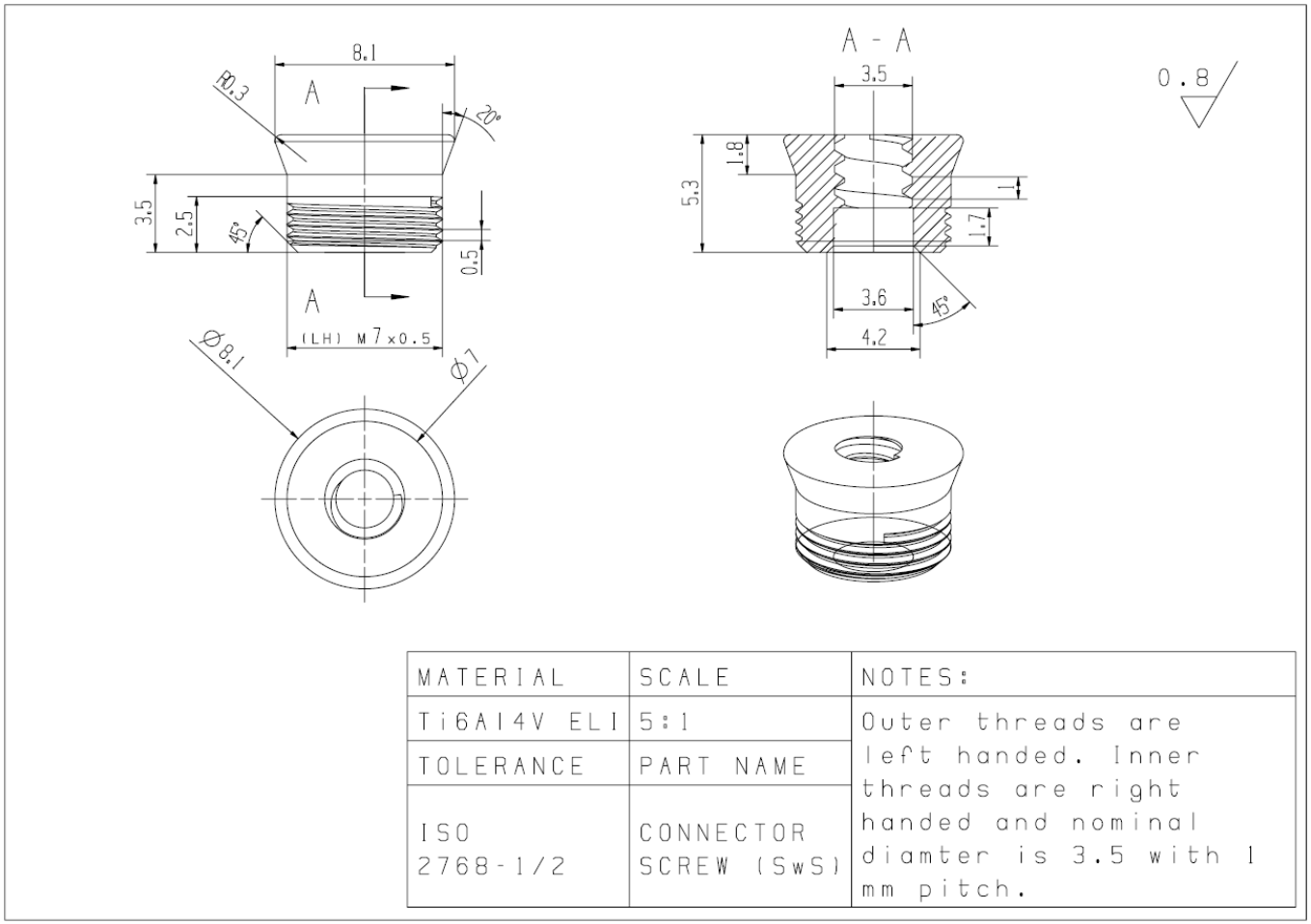

Figure C.5 Technical drawing of the connector screw of SwS concept.

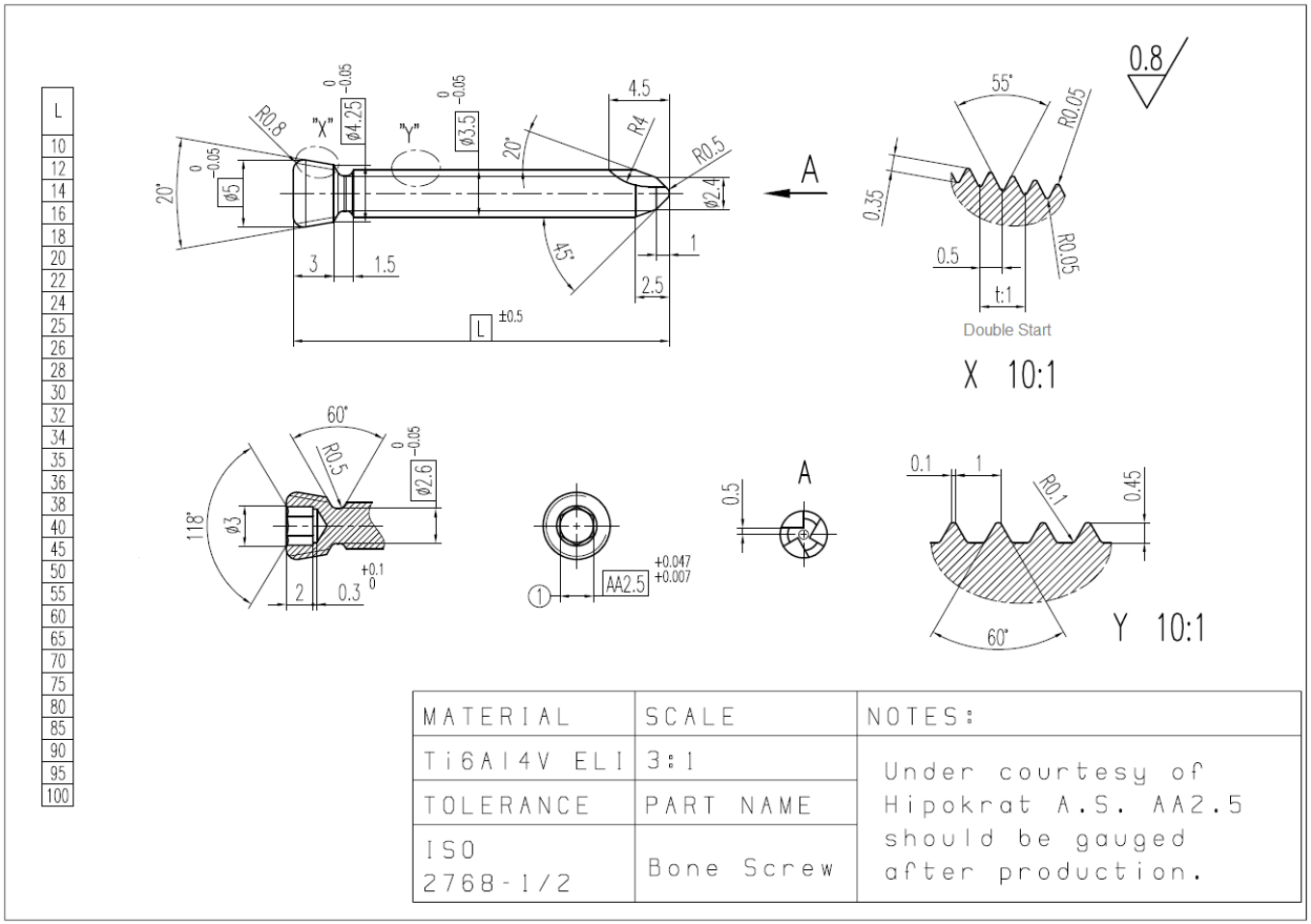

Figure C.6 Technical drawing of the bone screw.